CONSTRUCTION MATERIALS CONSULTANTS, INC.

Laboratory Investigation of A Masonry Mortar From A Historic Masonry Tower

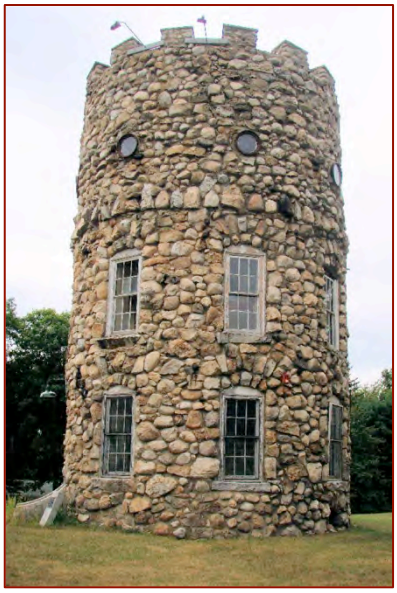

Smyth Tower
VA Medical Center
718 Smyth Road
Manchester, New Hampshire

Prepared for:
ABC Contractors, Inc.

Date
CMC Project#

Construction Materials Consultants, Inc.

Berkshire Center, Suite 104
4727 Route 30
Greensburg, PA 15601 USA
Phone: 724-834-3551
Fax: 724-834-3556
www.cmc-concrete.com

Date

ABC Contractors, Inc.
Address

RE: SMYTH TOWER, 718 SMYTH ROAD, MANCHESTER, NEW HAMPSHIRE

Dear Mr. McEntee:

Construction Materials Consultants, Inc. (CMC) is pleased to provide the enclosed comprehensive report on 'Laboratory Investigation of A Masonry Mortar From A Historic Masonry Tower," located in Manchester, New Hampshire.

Results, opinions, and conclusions presented herein are based on the information and sample provided at the time of this investigation. We reserve the right to modify the report as additional information becomes available. Neither CMC nor its employees assume any obligation or liability for damages, including, but not limited to, consequential damages arising out of, or in conjunction with the use, or inability to use this resulting information.

All reports are the confidential property of clients, and information contained herein may not be published or reproduced pending our written approval.

Please feel free to contact us with any additional questions. We look forward to providing our service again for your future projects.

Sincerely Yours,

CONSTRUCTION MATERIALS CONSULTANTS, INC.

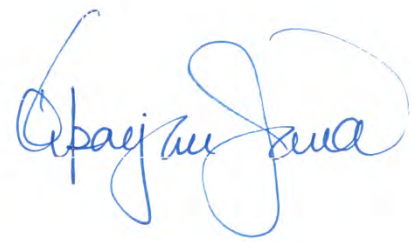

Dipayan Jana, PG
President, Petrographer

DJ:jlh

TABLE OF CONTENTS

Abbreviations:
PPL: Observations in plane polarized light mode in a petrographic microscope;
XPL: Observations in crossed polarized light mode in a petrographic microscope; most thin-section photomicrographs are taken in both PPL and corresponding XPL modes in a Nikon Eclipse 600 POL petrographic microscope.
XRD: X-ray diffraction.

EXECUTIVE SUMMARY

Smyth Tower, after Frederick Smyth, was constructed in 1888 on the current grounds of the VA Medical Center by following an exact replica of a famous Scottish lookout that Smyth saw while visiting Scotland. The tower is 40 feet (12 m) high, with walls 2 feet (0.61 m) thick. Its outside diameter is 28 feet (8.5 m). It has a basement level 8 feet (2.4 m) high, and three floors topped by a parapet. Building materials used in the tower were locally gathered. Smyth's widow gave the tower to the city in 1939, and it was used to house radio facilities during World War II. The tower was listed on the National Register of Historic Places in 1978.

A single piece of mortar, measuring 70.6 mm × 49.1 mm and 14.5 mm in respective lateral dimensions and maximum thickness (weighing 63 grams), was retrieved from the tower and provided for detailed compositional analyses. The sample was examined by following the methods of ASTM C 1324 to determine the composition of the mortar, and, subsequently, suggest an appropriate tuck-pointing mortar for renovation.

The mortar was examined by using the methods of ASTM C 1324 including detailed petrographic examinations (optical and scanning electron microscopy and X-ray microanalyses), X-ray diffraction, and various chemical analyses, including determination of acid-insoluble residue contents (by hydrochloric acid digestion), bulk oxide compositions of mortar by ED-XRF, soluble silica content to determine the proportions of cement component, if any, in the binder, free and combined water contents and degree of carbonation (from losses on ignitions at 110°C, 550°C, and 950°C, respectively). Petrography and chemistry have not only provided detailed composition, mineralogy, and microstructure of the mortar but also compositions, mineralogies, and proportions of various ingredients used in formulation of this historic mortar.

Initial examinations of a saw-cut section of the sample revealed two different mortars types having different colors, densities, and compositions: (a) a *host mortar*, which is tan-colored, dense and hard, and (b) a *recycled mortar* which is noticeably lighter gray-colored than the host, 1 mm to 10 mm in size, scattered as isolated fragments throughout the host. The recycled mortar was probably added as a coarse fraction of sand in the host, representing one of the earliest uses of recycled construction materials in a masonry dating back to 1888.

Two different populations of sands are, therefore, detected in the mortar (a) a 'coarse sand' population where majority of the particles are 1 to 3 mm in nominal size (some as much as 10 mm), which is judged to be the recycled mortar fragments (including its finer sand fractions), and, (b) a 'fine sand' population of nominal 2 mm or less, which is present both in the recycled and in the host mortar. Sand in the recycled mortar consists of: (i) quartzite, (ii) biotite granitic gneiss, and (iii) fine angular siliceous sand. Sand in the main mortar consists of siliceous angular fine sand similar in composition to those in the recycled mortar, containing major amounts of quartz, along with minor feldspar (microcline, orthoclase). The fine angular quartz-feldspar sand in the recycled and main mortars are compositionally similar, probably locally obtained and crushed, clean, well-graded, well-distributed, and are present in sound condition with no evidence of any deleterious alkali-aggregate reaction. It is, therefore, suggested that both the recycled mortar and the fine sand population in it and in the host mortar are locally obtained, as was reported in the history of this tower.

Paste in the host mortar shows the typical mineralogy and microstructure produced from the use of (i) natural cement and (ii) lime as the two essential binders. By contrast, recycled mortar is judged to have been prepared by using natural hydraulic lime binder without any natural cement or any other binder. As a result, pastes from corresponding mortars have differed in color, appearance, density, and compositions from respective hydration and carbonation products of their binders.

Overwhelming composition of paste in the host mortar showed an intimate mixture of: (i) hydration and carbonation products of natural cement, (ii) fine-grained carbonation products of lime, (iii) residual calcined raw feed argillaceous limestone/dolomite particles of natural cement, and (iv) some lime lumps from use of lime probably as lime putty. SEM-EDS studies of paste from various areas across the host mortar have detected: (a) a calcium-rich Mg-Al-Fe-silicate from lime and natural cement, (b) a calcium-poor to intermediate-calcium Mg-Al-Fe-silicate from natural cement, and, (c) a few miscellaneous minor components. Oxide compositional variations clearly showed a trend between the two end member (lime-rich and lime-poor) components, indicating use of lime and natural cement as two separate binders.

Recycled mortar showed a very different binder chemistry than the host at least in the following ways: (i) binder in the recycled mortar is noticeably lighter gray colored, softer and porous for its lime-based composition than the tan to medium brown stained and far denser paste in the host from its natural cement-based composition, (ii) natural cement is not detected in the recycled mortar, indicating a different hydraulic binder was used in the recycled mortar; (iii) lime is the only binder detected in the recycled mortar as opposed to natural cement and lime in the host, and occurred as porous, fine-grained, cryptocrystalline carbonated lime matrix in the recycled mortar; and (iv) a few residual calcium silicate particles are detected in the lime-based binder of recycled mortar indicating perhaps a hydraulic lime was used in the recycled mortar, e.g., a natural hydraulic lime. SEM-EDS analyses of binders have detected: (i) a calcium-rich Al-K-Fe-silicate composition, which was inherited from lime, (ii) a calcium-poor Al-K-Fe-silicate composition inherited from silica-rich (hydraulic) phases of lime, and, (iii) an intermediate calcium Al-K-Fe-silicate, which is probably the mixture of two end members of lime-rich and lime-poor (silica-rich) components of the binder, similar in composition to a *natural (high-calcium) hydraulic lime* the raw feed of which had contained limestone as the source of lime and clay as the source of silica, alumina, potassium, and iron.

Therefore, based on detailed laboratory studies, the host mortar is determined to be a natural cement – lime – siliceous sand mortar, whereas the recycled mortar is determined to be a natural hydraulic lime mortar containing crushed biotite granite as coarse sand and fine, angular, siliceous (quartz-feldspar) sand similar to the fine sand in the main mortar.

Due to this incorporation of a *natural hydraulic lime recycled mortar* into the *host natural cement-lime mortar*, compositional analyses of this 'composite mortar' to get a mix proportion is not only difficult but also meaningless, unless the new pointing mortar is to be made using a natural cement-lime mortar with a natural hydraulic lime mortar added as sand at similar proportion to the host as the examined mortar. Nevertheless, the bulk composition of this composite mortar was analyzed, and used to determine all chemical parameters, e.g., soluble silica content to get corresponding natural cement content, major oxide compositions, losses on ignitions to determine free, combined water contents and carbonation, and insoluble silica contents to get sand proportions. Chemical data, thus obtained, were then processed in the mix calculations with an underlying assumption that the bulk mortar contains less than 10 percent recycled mortar (at least in the sample examined), and, hence did not contribute a major share of the bulk chemistry of this composite mortar. With that assumption, mix proportions calculated from chemical data showed use of 1-part natural cement to $3^1/_2$-part lime to $7^1/_2$-part sand. It is, therefore, important to remember the influence of recycled mortar in this mix calculation. For example, the high lime-content of the calculated mix could have a contribution from the natural hydraulic lime of the recycled mortar, and so is the calculated sand proportion. Sand content, however, is 1.6 times the sum of separate volumes of natural cement and lime, as opposed to commonly recommended $2^1/_4$ to 3 times, thus indicating an under-sanded nature of the mortar.

Based on: (a) the determined natural cement and lime-based composition of the host mortar, (b) natural siliceous sand composition of aggregate, and (c) calculated volumetric proportions of 1-part natural cement to $3^1/_2$-part lime to $7^1/_2$-part sand, a possible tuck-pointing mortar could be a natural cement-lime-sand mortar made using Rosendale natural cement, hydrated lime, and natural sand, conforming to the respective ASTM specifications of C 10, C 207, and C 144.

Therefore, to repoint the existing mortar in the Tower, perhaps it will be better to stay away from the modern masonry mortars, e.g., the ones confirming to the ASTM C 270 cement-lime or masonry (or mortar) cement mortars. Modern mortars are not always a suitable substitute for the historic mortars unless such substitution can be confirmed appropriate from small test locations. Fortunately, natural cement, lime, and natural hydraulic lime – all these binder components are available today, which can be used. Clean, crushed silica sand confirming to the ASTM C 144 specification of modern crushed masonry sand would be appropriate. The cement-to-lime-to-sand mix proportions, however, gave to be tested by trial and error, perhaps starting with the calculated one provided here, which by no means is clamed to the one to use, let alone for the interference of recycled mortar in this calculation.

For example, a Rosendale natural cement conforming to the specification of ASTM C 10 (e.g., Rosendale 10C from Edison Coatings, Inc.), perhaps mixed with a subordinate amount of a natural hydraulic lime (e.g., Biolime NHL 2 from Edison Coatings, Inc.), and a masonry sand, or, perhaps a pre-mixed natural cement mortar (e.g., Rosendale 12M from Edison Coatings, Inc.) could be some appropriate first choices to try. The final choice of binder and sand ingredients, and mix proportion would depend on the match in appearance, compositions, and properties with this existing mortar. Design and formulation of an appropriate tuck-pointing mortar should be based on trial and error on small test areas by the project engineer/architect.

INTRODUCTION

Reported herein are the results of detailed laboratory studies of a masonry mortar sample, collected from a historic masonry tower at 718 Smyth Road in Manchester, New Hampshire. ABC Contractors, Inc. provided the sample. The subject building was reportedly constructed in 1888.

The purposes of the laboratory investigation are to determine:

a) The overall composition of the mortar, including type and composition of sand used in the mortar;
b) The type of the binder(s) used;
c) Evidence of any physical and/or chemical deterioration of the mortar;
d) Detailed chemical and mineralogical compositions of mortar, including the sand and the binder;
e) Based on determined composition, an estimation of volumetric proportions of various binder and sand components used in the original mortar mix; and,
f) Based on the determined composition and mix proportions, suggestions for suitable tuck-pointing mortar that can be used during renovation.

SMYTH TOWER, MANCHESTER, NEW HAMPSHIRE

Figure 1 shows the subject *Symth Tower* (at the top left), its location on the grounds of the VA Medical Center (at the top right), and a brief history of the tower from Wikipedia (at the bottom).

The fieldstone tower, a granite and stone landmark, was reportedly built in 1888 by Frederick Smyth, who owned an extensive estate, part of which became the VA Medical facility. Mr. Smyth, reportedly, built the tower as an exact replica of a famous Scottish lookout that he saw while visiting Scotland. The tower is 40 feet (12 m) high, with walls 2 feet (0.61 m) thick. Its outside diameter is 28 feet (8.5 m). It has a basement level 8 feet (2.4 m) high, and three floors topped by a parapet. Building materials used in the tower were locally gathered. The tower was given to the city by Smyth's widow in 1939, and it was used to house radio facilities during World War II. The tower was listed on the National Register of Historic Places in 1978.

MORTAR SAMPLE

Figure 2 shows the two opposite sides of a solid intact fragment of the mortar as received in a plastic bag. The overall condition of the sample is dense, hard, intact, dry, and cannot be disintegrated by finger pressures.

The total mass of the sample is 63.0 grams, and the dimensions are 70.6 mm × 49.1 mm × 14.5 mm. Table 1 summarizes information obtained from preliminary visual examinations, e.g., overall weight (in grams), dimensions of largest fragment, appearance, and integrity of mortar.

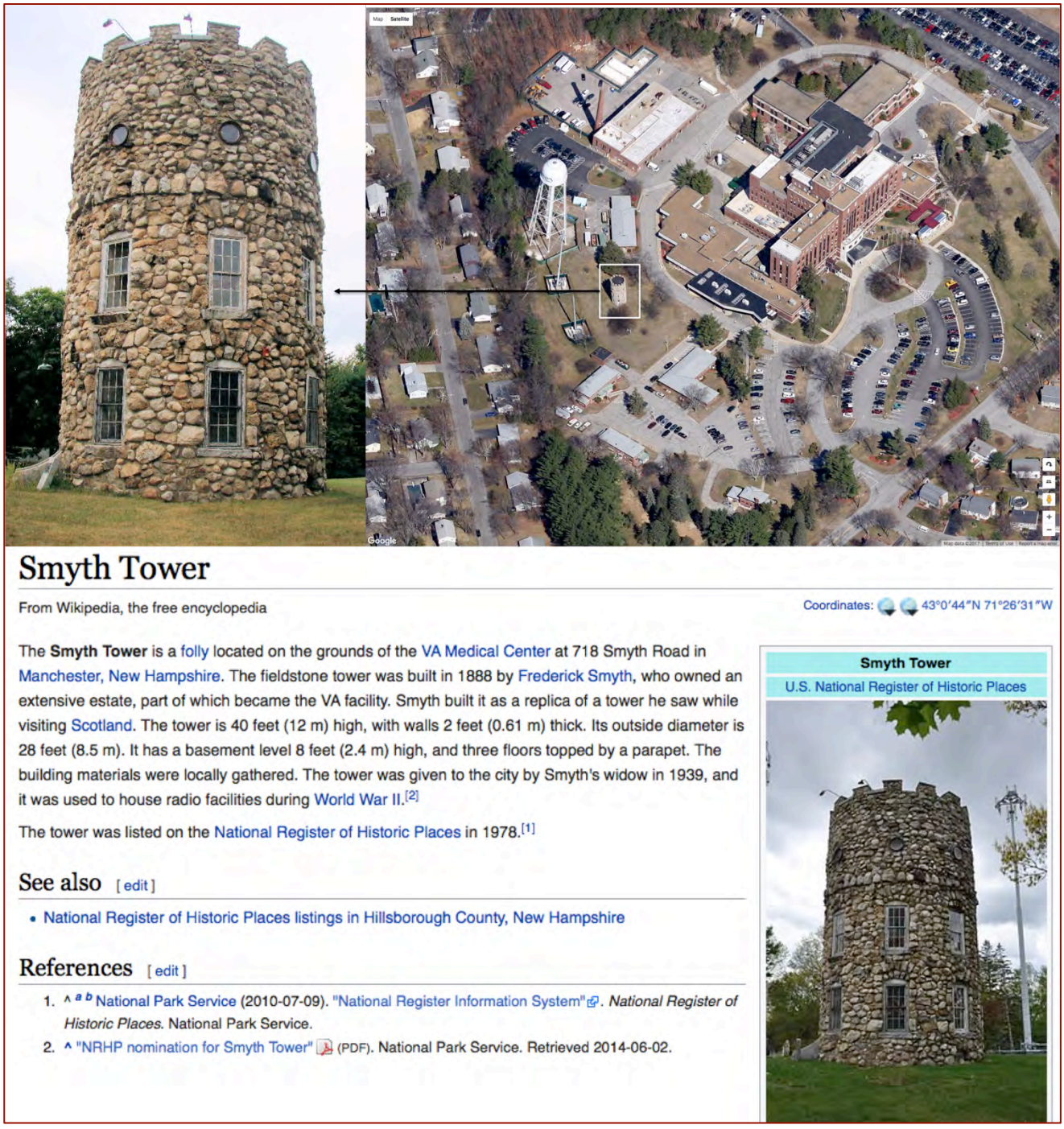

Smyth Tower

From Wikipedia, the free encyclopedia

Coordinates: 43°0′44″N 71°26′31″W

The **Smyth Tower** is a folly located on the grounds of the VA Medical Center at 718 Smyth Road in Manchester, New Hampshire. The fieldstone tower was built in 1888 by Frederick Smyth, who owned an extensive estate, part of which became the VA facility. Smyth built it as a replica of a tower he saw while visiting Scotland. The tower is 40 feet (12 m) high, with walls 2 feet (0.61 m) thick. Its outside diameter is 28 feet (8.5 m). It has a basement level 8 feet (2.4 m) high, and three floors topped by a parapet. The building materials were locally gathered. The tower was given to the city by Smyth's widow in 1939, and it was used to house radio facilities during World War II.[2]

The tower was listed on the National Register of Historic Places in 1978.[1]

Smyth Tower
U.S. National Register of Historic Places

See also [edit]

- National Register of Historic Places listings in Hillsborough County, New Hampshire

References [edit]

1. ^ a b National Park Service (2010-07-09). "National Register Information System". *National Register of Historic Places*. National Park Service.
2. ^ "NRHP nomination for Smyth Tower" (PDF). National Park Service. Retrieved 2014-06-02.

Figure 1: The Smyth Tower at 718 Smyth Road in Manchester, New Hampshire. The top right photo shows its location on the ground of the VA Medical Center.

Sample ID	Weight (grams)	Largest Piece Dimensions (mm)	Appearance	Integrity
Masonry Mortar from Smyth Tower	63.0	70.6 mm × 49.1 mm × 14.5 mm	Tan; dense, hard dry, (Figures 2 and 3)	One intact piece

Table 1: Weight, dimensions of largest fragment, color, hardness/softness, and integrity of mortar sample.

Figure 2: Shown are the two sides of the same mortar sample, as received. Notice some parallel chisel marks on one side (in the right photo) left from its retrieval from the joint.

Figure 3 shows: (a) four photomicrographs of a saw-cut section through the piece at the top (field width of each photo is 15 mm), as well as (b) lapped section of that saw-cut section at the bottom. In both photos, separate lighter gray-colored mortar fragments are detected (many are marked by white dashed lines in Figure 3) scattered throughout the overwhelming tan-colored paste of the main mortar.

During the course of this laboratory examination, these lighter-gray colored fragments were determined to be an entirely different mortar than the host mortar, used as a *recycled mortar*, probably constituted the coarser fractions of the sand. These recycled mortar fragments range in sizes from 10 mm to as small as a millimeter (finer sizes are due to the fragmented nature of this recycled mortar when incorporated). These fragments represent one of the earliest uses of recycled construction materials in a masonry tower in the US that dates back to 1888.

Figures 4 and 5 show blue dye-mixed epoxy-impregnated thin section of the mortar sectioned through the original piece. The purpose of using blue dye-mixed epoxy is to highlight the open spaces, cracks, and voids in the mortar by filling those open spaces with dyed epoxy (and also to improve the overall integrity of the sample for thin section preparation). The thin section prepared is of a large area, i.e. 50 mm × 75 mm in dimensions, which has covered a representative area of the mortar for optical microscopical examinations. These thin section photomicrographs again show many recycled mortar fragments scattered throughout the main mortar body that are characteristically lighter in color than the main mortar body (many are separated by yellow dashed lines).

Thin section photomicrographs showed that the fine, angular sand used in the recycled mortar is compositionally similar to the sand used in the main mortar, indicating a possible local quarry for both types of mortars. Opposite to sand, however, pastes in two mortar types show noticeable difference in appearances (color, porosity, etc.) due to inherent differences in their compositions, as described later.

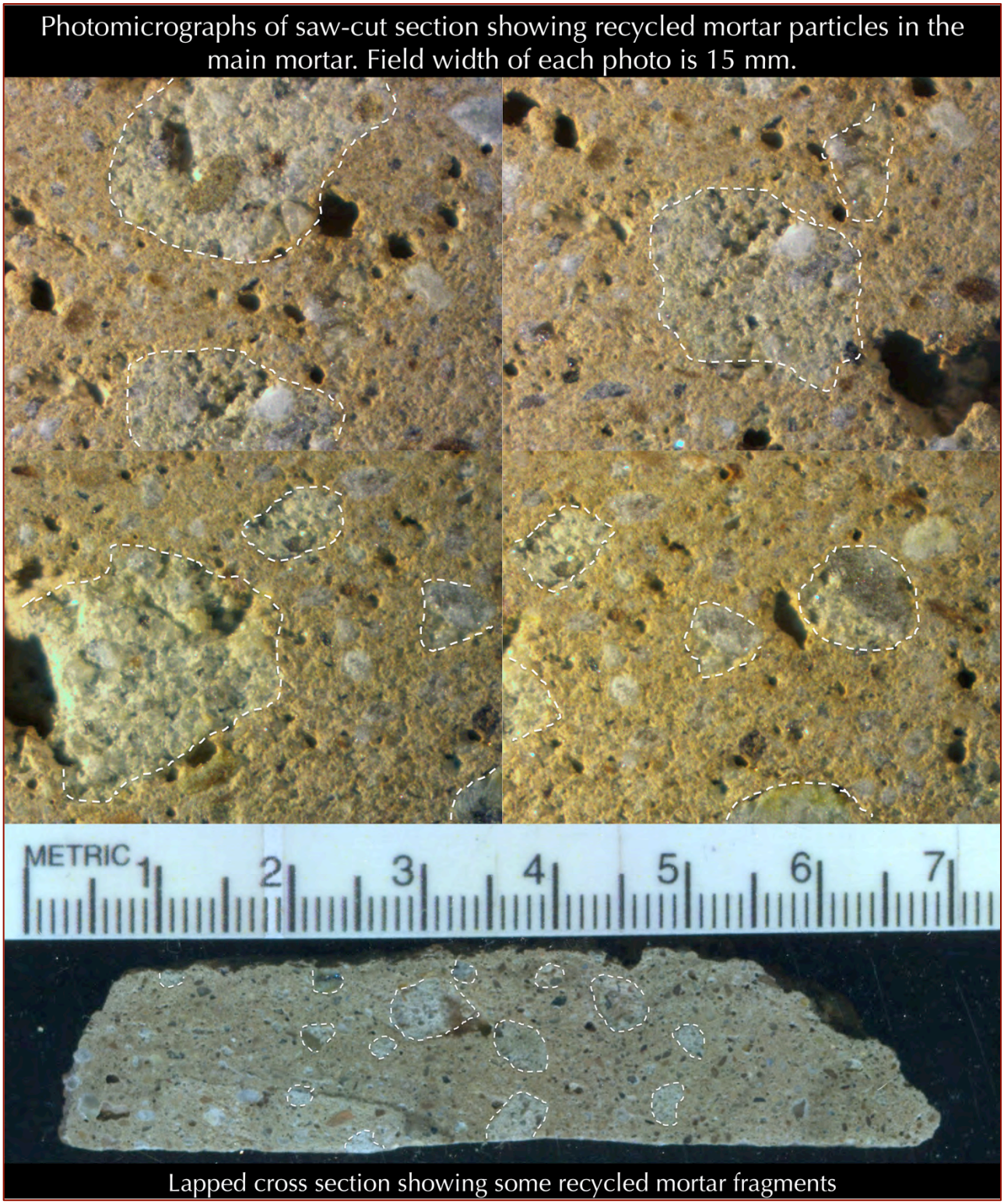

Figure 3: Photomicrographs of saw-cut section (top) and lapped cross section (bottom) of the mortar showing many lighter gray colored recycled mortar fragments (many marked with dashed white lines) within the main mortar. Therefore, a pre-existing mortar was crushed and recycled, probably as coarse sand into the present mortar.

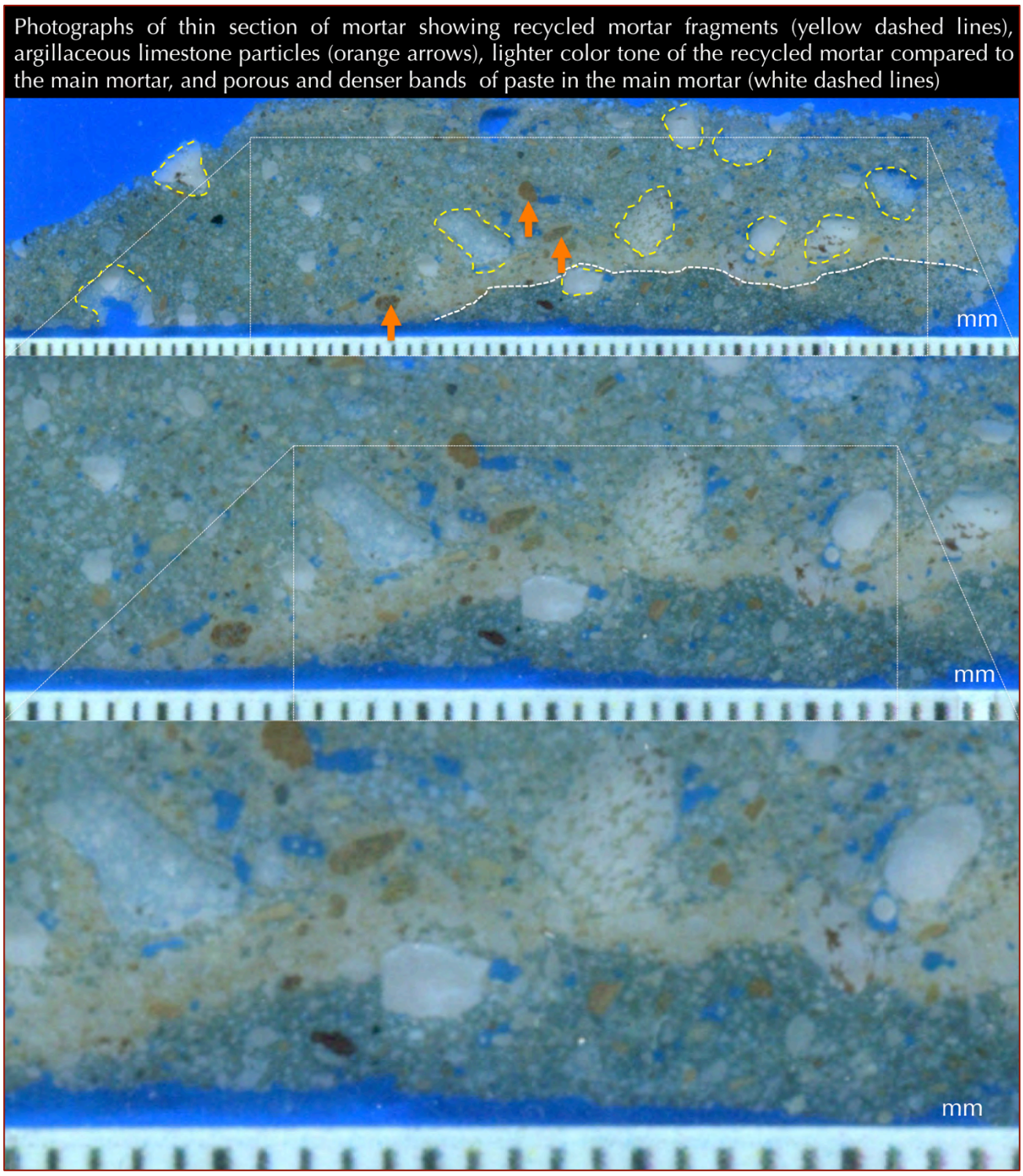

Figure 4: Blue dye-mixed epoxy-impregnated thin section of mortar sectioned through the middle of the original fragment showing size, shape, angularity, and distribution of sand aggregate and binder. Yellow dashed lines show recycled mortar fragments. White dashed line in the top photo shows different porosities of the main mortar from different degrees of absorption of blue dye. Boxed area in top and middle photos are enlarged in the respective following photos. The beige band of paste above the white dashed line in the top photo represents a denser zone of paste in the main mortar (hence less absorption of dye compared to the paste above and below where paste being porous absorbed more dye and appeared blue). Orange arrows point to some argillaceous limestone remnants. The thin section was scanned over a flatbed scanner on a white background.

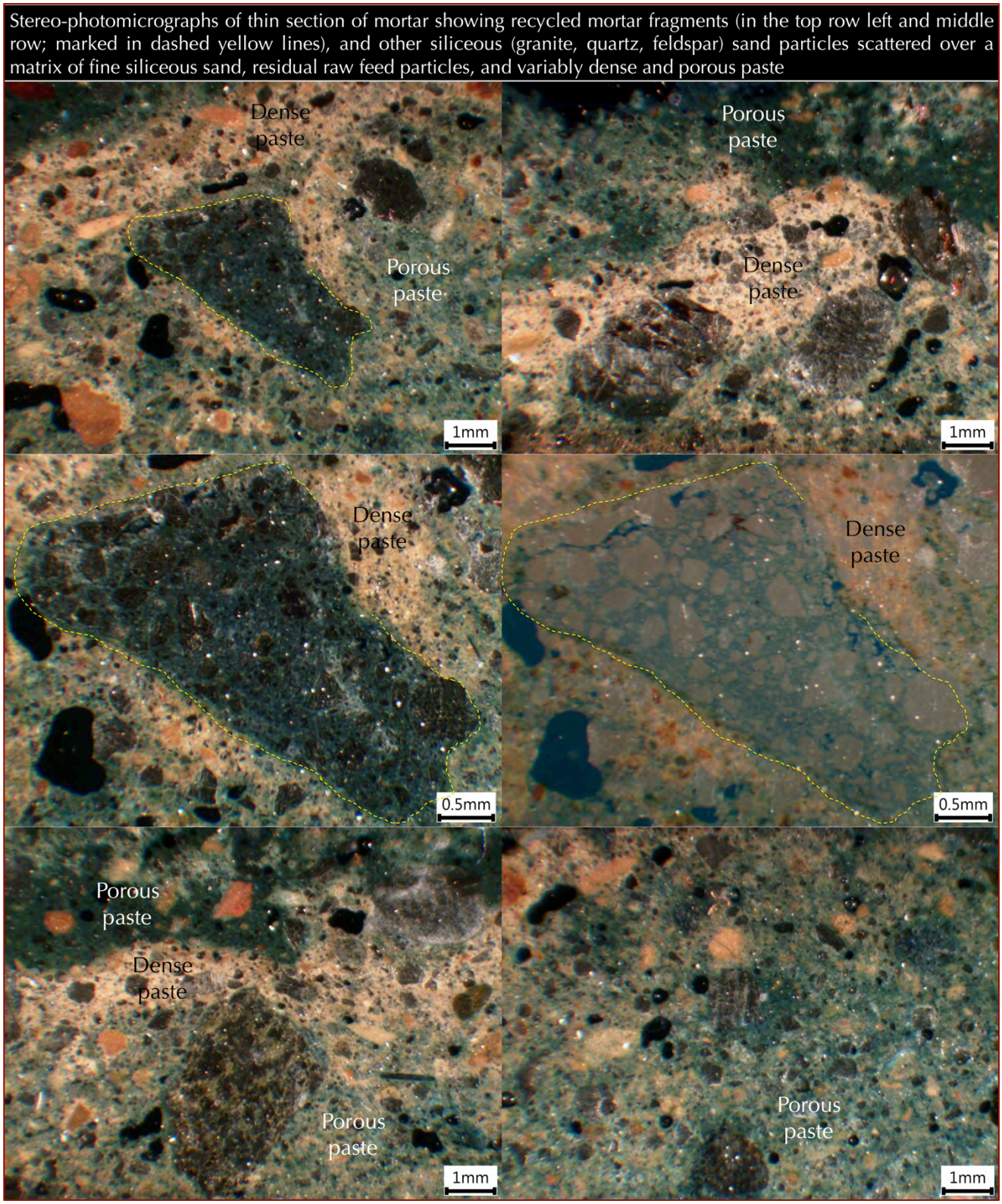

Figure 5: Photomicrographs of thin section of mortar shown in Figure 4. All photos except the middle right one were taken against a black background with a Stereozoom microscope; the middle right photo was taken against a white background. Notice some recycled mortar particles (marked with yellow dashed lines) that are scattered with other siliceous sand and residual dark brown raw feed particles over variably dense and porous paste.

METHODOLOGIES

Appendix A1 provides detailed methodologies for laboratory testing of masonry mortar that are followed by the laboratories of CMC.

The mortar sample was tested by following the methods of ASTM C 1324 "Standard Test Method for Examination and Analysis of Hardened Masonry Mortar," which includes detailed petrographic examinations, followed by chemical analyses, along with various analytical methods to test masonry mortars as described in various literatures, e.g., Erlin and Hime 1987, Doebley and Spitzer 1996, Chiari et al. 1996, Middendorf et al. 2005 a and b, Elsen 2006, Bartos et al. 2000, Valek et al. 2012, Jana 2005, 2006, and Goins 2001 and 2004.

PETROGRAPHIC EXAMINATIONS

SAW-CUT, LAPPED, TRANSPARENT (THIN), AND FRESH FRACTURED SURFACES

Continuing Figures 3, 4, and 5, the following Figure 6 shows fresh fractured surface of mortar, which was scanned on a flatbed scanner. The fractured surface shows the overall tan color tone of mortar, with isolated occurrences of light, off-white relatively coarser particles of recycled mortar, some of which are marked in dashed yellow lines. Overall mortar is very dense, hard, and lacks any coarse voids.

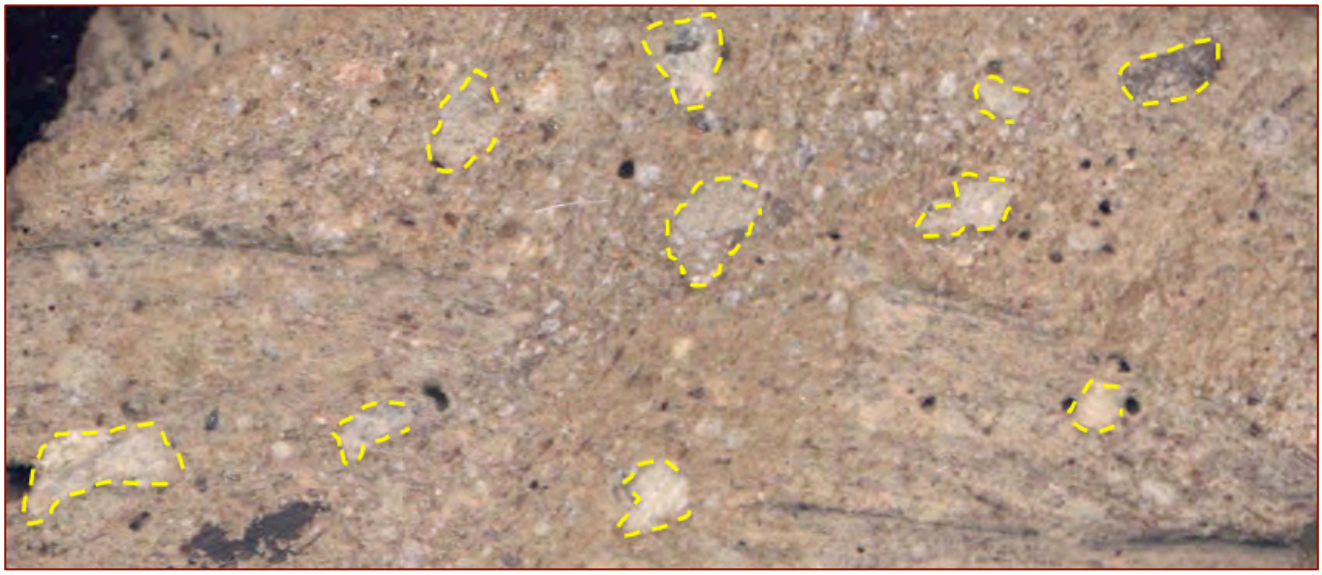

Figure 6: Fresh fractured surface of mortar showing distribution of recycled mortar fragments (marked in yellow dashed lines) in the main mortar body. This figure further shows distribution of recycled mortar fragments after seeing those fragments in the saw-cut and lapped sections in Figure 3 and in thin section in Figures 4 and 5.

POROSITY, SAND SIZE, & GRADING FROM IMAGE ANALYSES OF THIN SECTION PHOTOMICROGRAPHS

Figure 7 shows large-area photomicrographs of thin section of mortar taken with a transmitted-light Stereozoom microscope with polarizing light facilities (see Appendix A1). Four different areas of mortar were scanned and stitched in a mosaic to show overall variations in size, shape, angularity, gradation, and composition of sand used in the mortar, as well as size, shape, amount and distribution of void spaces, microcracks, and other open areas that are highlighted by the colored (blue) dye-mixed epoxy used to impregnate the sample for thin section preparation.

Photomicrographs of blue dye-mixed epoxy-impregnated thin section of mortar are used for image analyses in Adobe Photoshop to highlight the sand particles and voids separately, by turning the object of interest in black against everything else in white, and, then calculate proportions of sand and void volumes by Image J. Figures 7 through 9 show:

a) Photomicrographs of blue dye-mixed epoxy-impregnated thin section of mortar in Figure 7 from a mosaic of 4 photos taken over 4 different areas in thin section by using Olympus transmitted-light Stereozoom microscope;
b) Corresponding black-and-white binary images in Figure 8 of thin section photomicrographs in Figure 7 to highlight the open spaces in black against everything else in white to calculate an estimated pore volume of 3.8 percent.
c) Corresponding black-and-white binary images in Figure 9 of thin section photomicrographs in Figure 7 to highlight the sand particles in black against everything else in white, thus evaluate the size, shape, angularity, sphericity, gradation, and distribution of sand particles, and calculate sand volume as 36.7 percent;
d) The black and white binary images highlighting the sand or pore spaces are derived from Adobe Photoshop, and, volumetric proportions of sand and pore spaces are calculated from Image J, an open-source image analysis software developed by the National Institute of Health (www.imagej.nih.gov).
e) As seen from these photomicrographs the mortar shows a high amount of interstitial voids between sand particles and aggregate-paste separations, and close to 40 percent by volume of sand.

Sample ID	Pores, Voids, Cracks, Separations				Sand (Including Recycled Mortar)		
	Estimated (%) Volumes	Proportion of Irregular Voids	Shrinkage Microcracks	Total Volume is Contributed From:	Nominal Maximum Size (mm)	Shape, Angularity, Grading, Distribution	Estimate Volumes in Images (%)
Masonry Mortar	3.81	Many Interstitial voids between sand	Few Elongated to none	Interstitial Voids and separations along aggregate-paste interfaces	4.0	Equidimensional, Subangular to Well-rounded, Well-graded, Well-distributed	36.7

Table 2: Estimated porosity, types of pore spaces, nominal maximum size (determined from photomicrographs) of sand aggregates, and angularity and grading of sand (including recycled mortar) in the masonry mortar determined from image analysis by Image J.

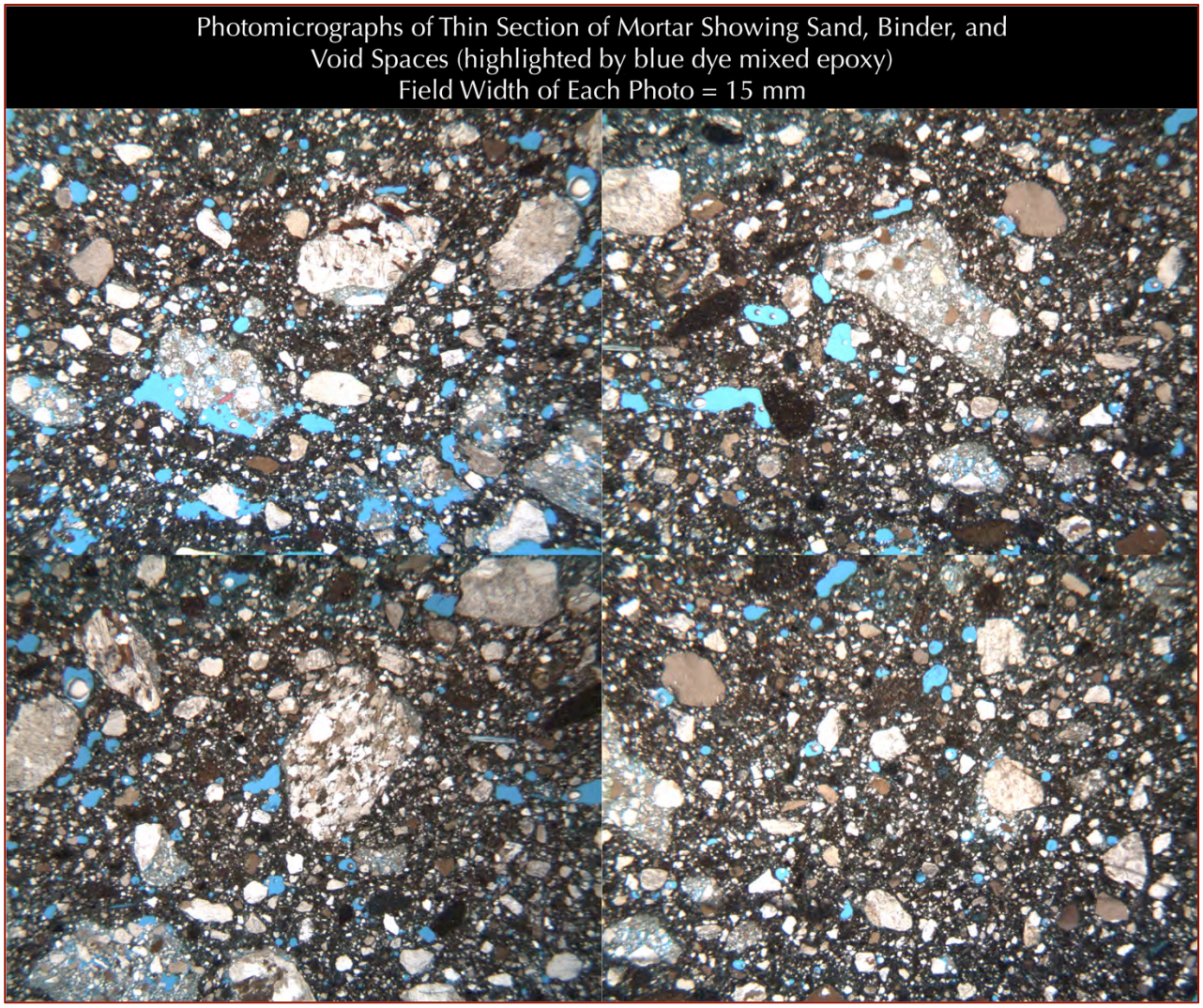

Figure 7: Mosaic of 4 photomicrographs of blue dye-mixed epoxy-impregnated thin section of mortar. Also shown in Figures 8 and 9 are the calculated volumetric proportions of interstitial void spaces and sand, respectively, from Image J (see Table 2). Field width of each photo is 15 mm.

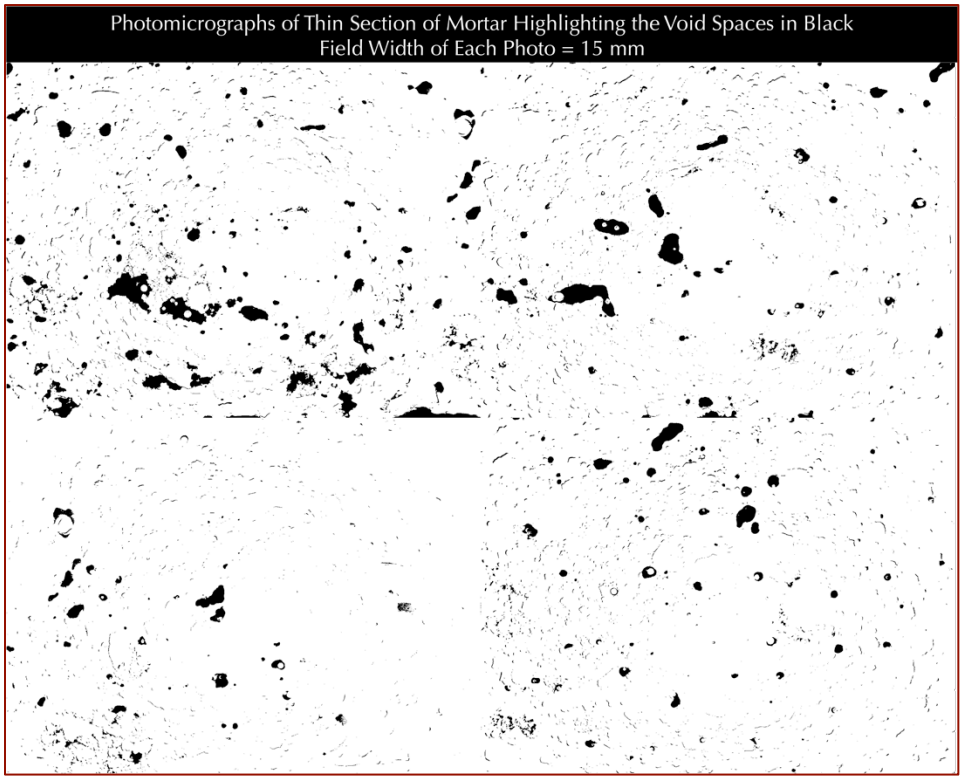

Figure 8: Corresponding black and white images of thin section photos in Figure 7 that highlight interstitial air voids in the mortar in black. Image analyses of entire mosaic of four photos determined 3.81 percent voids.

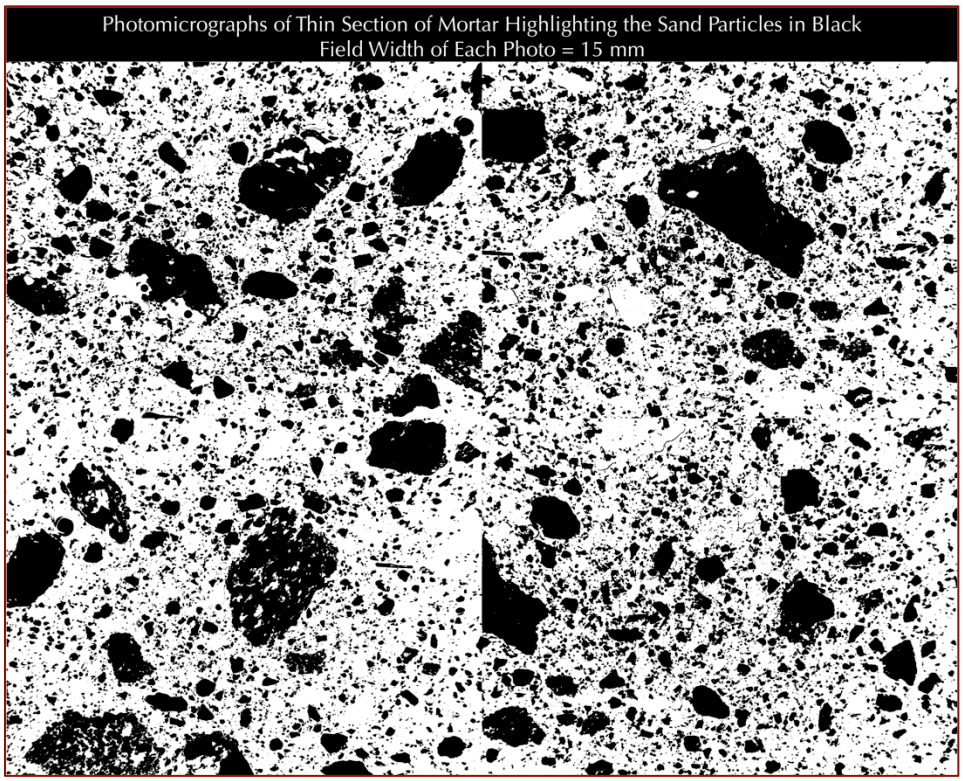

Figure 9: Corresponding black and white images of thin section photos in Figure 7 that highlight sands in the mortar in black. Image analyses of entire mosaic of four photos determined 36.7 percent sand volume.

Results of volumes of sand, and pore spaces obtained from such practices are only considered as rough estimates, since adequate numbers of such photomicrographs across the entire examined surface area of a mortar sample are needed for better accuracy of these parameters. Care is needed to select pore spaces and void areas that are inadequately filled with blue dyed epoxy, or of aggregate-paste gaps during the process of highlighting not only just the easily detectable pore spaces and voids, but also any not so distinct voids. Selection of all voids, open spaces, microcracks, etc. are done in Adobe Photoshop in the final processed blue-dyed photomicrographs, which are then transferred to Image J to calculate the volumes of pore spaces not only from entrained and entrapped air-voids but also from cracks, microcracks, and aggregate-paste separations. Shrinkage microcracks are carefully identified and separated from any sand-paste separations since they both may appear similar in the black and white binary images. With some practice, such an approach of processing a photomicrograph in Photoshop and analysis of its binary image in Image J become quick and important for rough estimation of porosities and sand volumes in the mortars, as well as size, shape, grading, and distribution of sand, a quick detection of if a mortar is over-sanded or under-sanded, and if a mortar is porous, excessively air-entrained, or dense. Stitching multiple photomicrographs (captured in an overlapping pattern) over an entire thin section of a mortar can provide meaningful information on all these aspects from such approach on image analysis.

OPTICAL MICROSCOPY OF SAND – A RECYCLED MORTAR (PROBABLY USED AS A COARSE SAND) AND A FINE CRUSHED SILICEOUS SAND COMPOSITIONLLY SIMILAR IN THE RECYCLED AND MAIN MORTARS

Figures 3, 4, 5, 6, 7, and 10 through 12 show the types, sizes, shapes, angularities, distribution, and grading of sand particles in the recycled and the main mortar, where field width of each photo is 15 mm.

As seen in all these photos, two different populations of sand are present: (a) a 'coarse sand' population where majority of the particles are 1 to 3 mm in nominal size (some as much as 10 mm), and, (b) a 'fine sand' population of nominal 1 mm or less. The 'coarse sand' population represents the recycled mortar, which consists of: (i) quartzite, (ii) biotite granitic gneiss, and (iii) isolated porous clumps or agglomerates of fine angular siliceous sand in a binder, where all three components are judged to be of 'recycled mortar,' having very different mortar composition than the main mortar. Some coarse quartzite and biotite granite particles are found to have adhered remnants of finer angular quartz and binder i.e. the finer fraction of the recycled mortar.

The finer fraction of sand inside the recycled mortar contains major amounts of quartz, which is similar to the fine quartz sand found outside in the main mortar, along with minor feldspar (microcline, orthoclase), again similar to the particles present in the main mortar sand. Sand in the main mortar are all fine, less than a millimeter to 2 mm in size and compositionally similar to the finer sand present within the recycled mortar. Therefore, the fine angular quartz, feldspar sand found in recycled and main mortars are compositionally similar and probably locally obtained and crushed. Recycled mortar fragments are subangular to subrounded to well-rounded,

indicating some effects of erosion, fragmentation either prior to or during its incorporation into the main mortar, whereas the fine, angular sand within the recycled mortar and in the outside main mortar are angular, indicating a possible manufactured origin of sand (as opposed to more rounded natural sand).

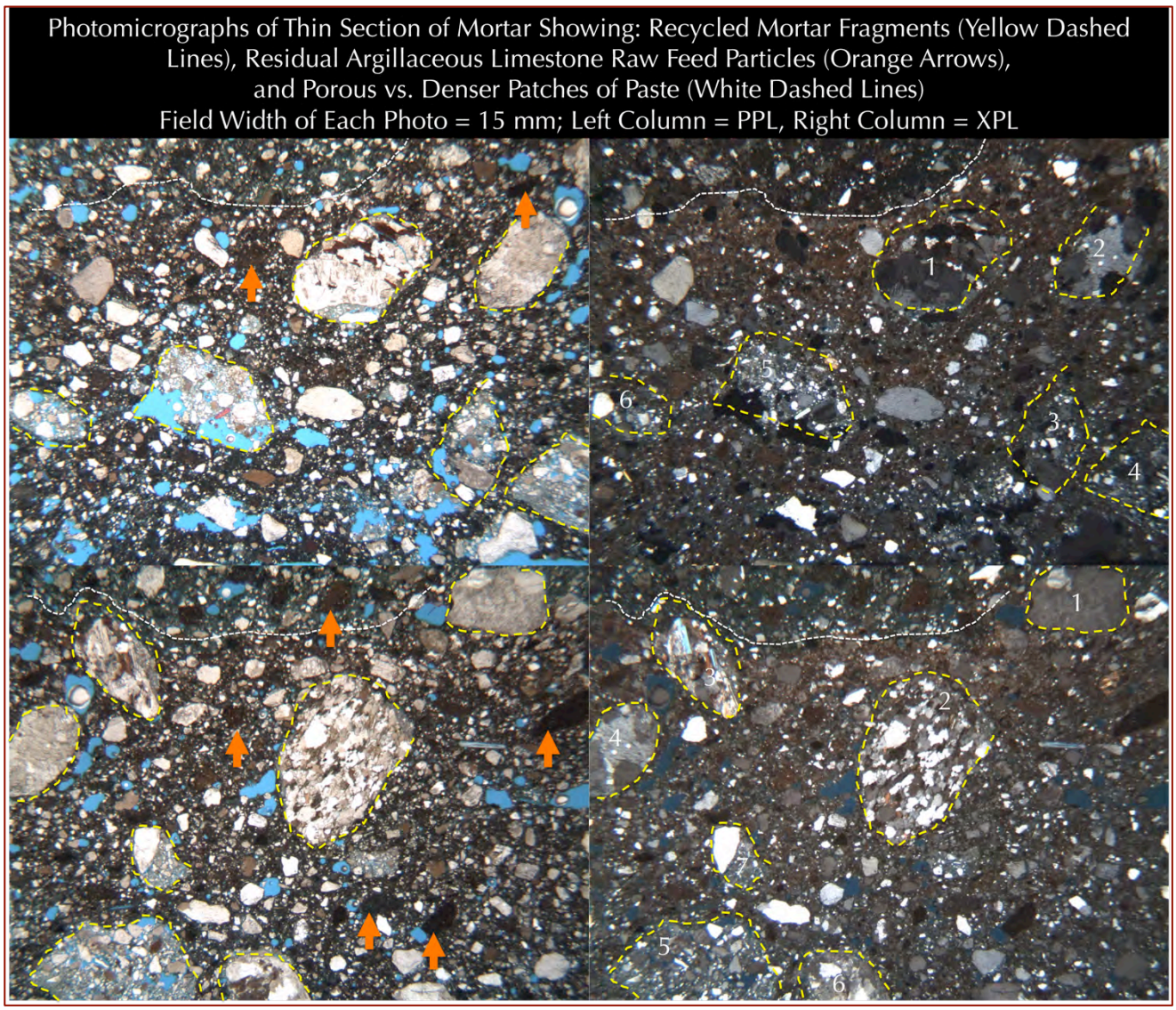

Figure 10: A mosaic of two (2) photomicrographs of blue dye-mixed epoxy-impregnated thin section of mortar showing size, shape, angularity, gradation, and distribution of various coarse to fine sand particles, where some recycled mortar fragments (probably used as coarse sand particles) are highlighted by the yellow dashed lines and are described in the following Table. White dashed lines separate pastes of variable porosities in the main mortar. Orange arrows point to some brown residual or raw feed particles of natural cement added in the main mortar.

Some coarse sand particles numbered in the top and bottom row photographs are as follows:

Row	Coarse Sand Particles	Particle Types
Top	1 to 6	1 = Biotite granite with adhered mortar; 2 = Quartzite; 3 to 6 = Recycled mortar
Bottom	1 to 6	1 and 4 = Quartzite; 2 = Biotite granite; 3 = Biotite granite with adhered mortar; 5 and 6 = Recycled mortar

Table 3: Various coarse sand particles found in the recycled and main mortar.

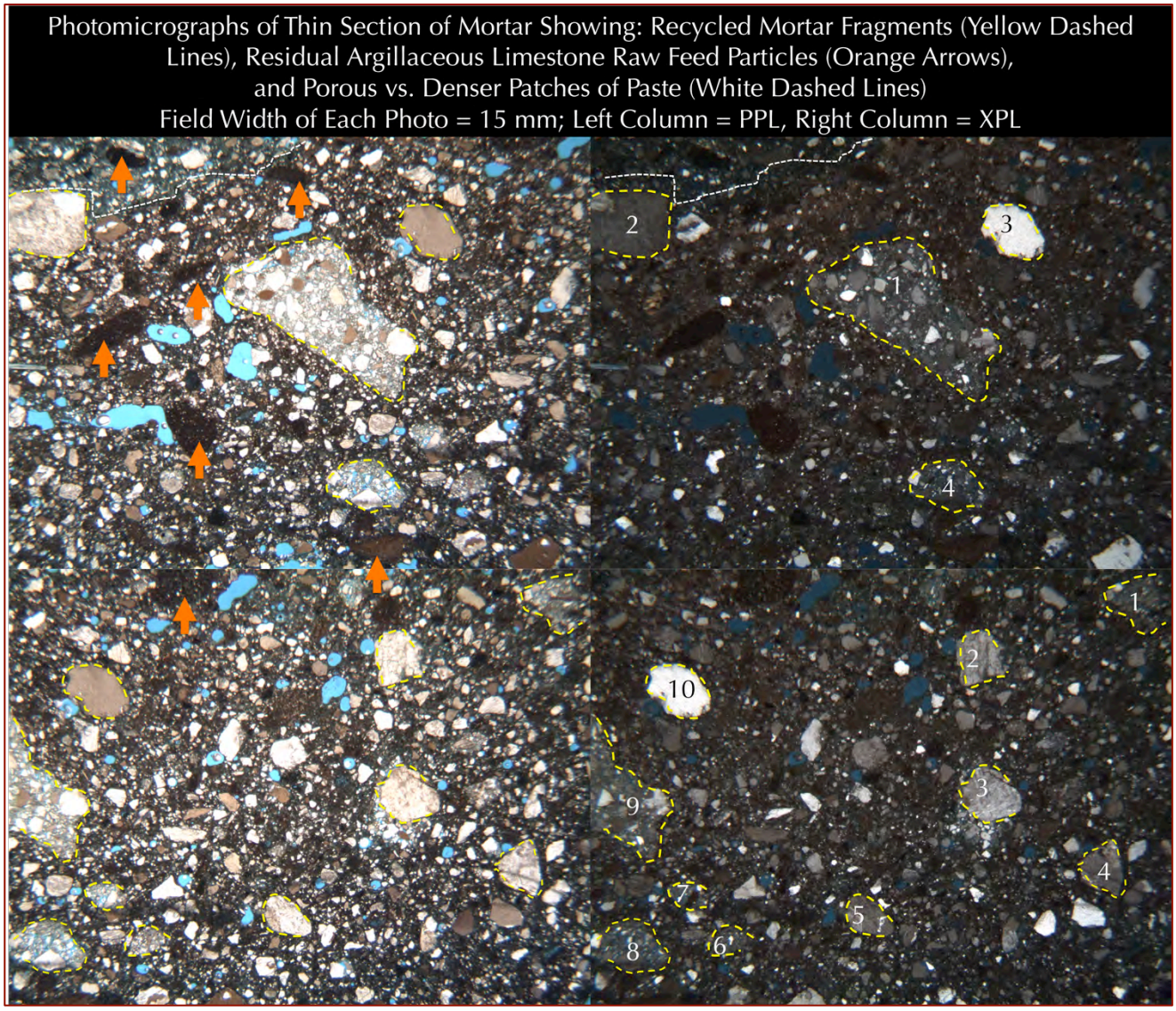

Figure 11: A mosaic of two (2) photomicrographs of blue dye-mixed epoxy-impregnated thin section of mortar showing size, shape, angularity, gradation, and distribution of various coarse to fine sand particles, where some recycled mortar fragments probably used as coarse sand particles are highlighted by the yellow dashed lines and are described in the following Table. White dashed lines separate pastes of variable porosities in the main mortar. Orange arrows point to some dark brown residual or raw feed particles of natural cement added in the main mortar.

Some coarse sand particles numbered in the top and bottom row photographs are as follows:

Row	Coarse Sand Particles	Particle Types
Top	1 to 4	1 and 4 = Recycled mortar; 2 = Quartzite; 3 = Quartz;
Bottom	1 to 10	1, 2, 3, 4, 5, and 10 = Quartz and quartzite; 6, 7, 8, and 9 = Recycled mortar

Table 4: Various sand particles found in the recycled and main mortar.

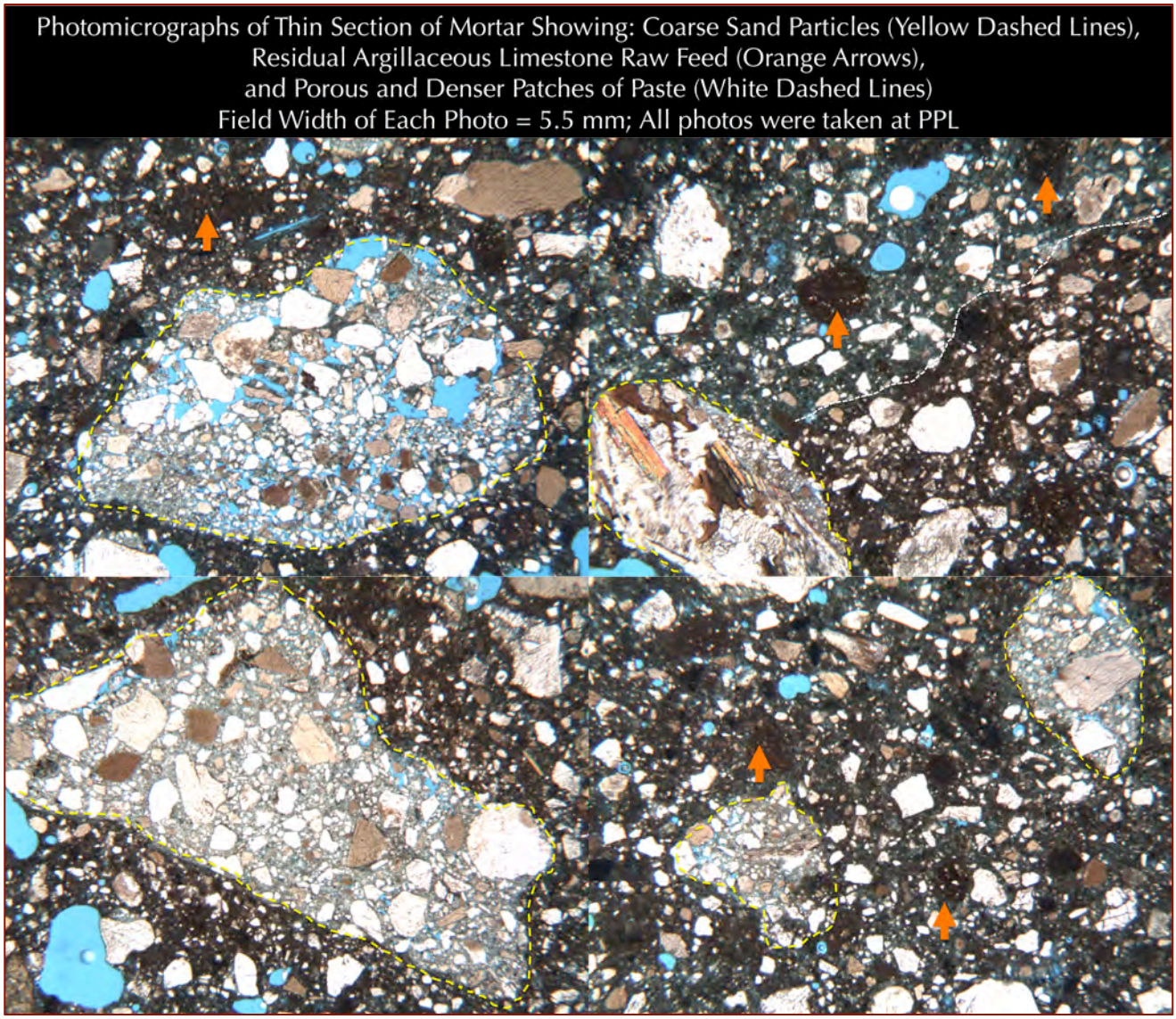

Figure 12: A mosaic of four (4) photomicrographs (all taken in PPL mode) of blue dye-mixed epoxy-impregnated thin section of mortar showing some recycled mortar fragments probably used as coarse sand particles (porous, consisting of coarse biotite granite sand and finer angular quartz sand scattered in a binder) are highlighted by the yellow dashed lines. White dashed lines separate pastes of variable porosities in the main mortar. Orange arrows point to some dark brown residual or raw feed particles of natural cement added in the main mortar.

Figures 12 and 13 concentrate on some of the recycled mortar fragments that contain two different types of particles based on their sizes – (a) biotite granite particles present as coarse sand (within the recycled mortar only), and (b) angular quartz-quartzite particles present as intermediate to fine sand. The bottom left photo in Figures 12 and 13 show the fine to intermediate quartz-quartzite particles in the mortar where biotite granite is absent, whereas the top right photo in Figure 12 and top row plus bottom right photo in Figure 13 show the coarse biotite granite with adhered fine to intermediate sized quartz-quartzite particles in the recycled mortar.

The fine sand particles are well-graded, well-distributed, and have been sound during their service in the mortar. There is no evidence of any potentially deleterious alkali-aggregate reaction of sand found in the mortar.

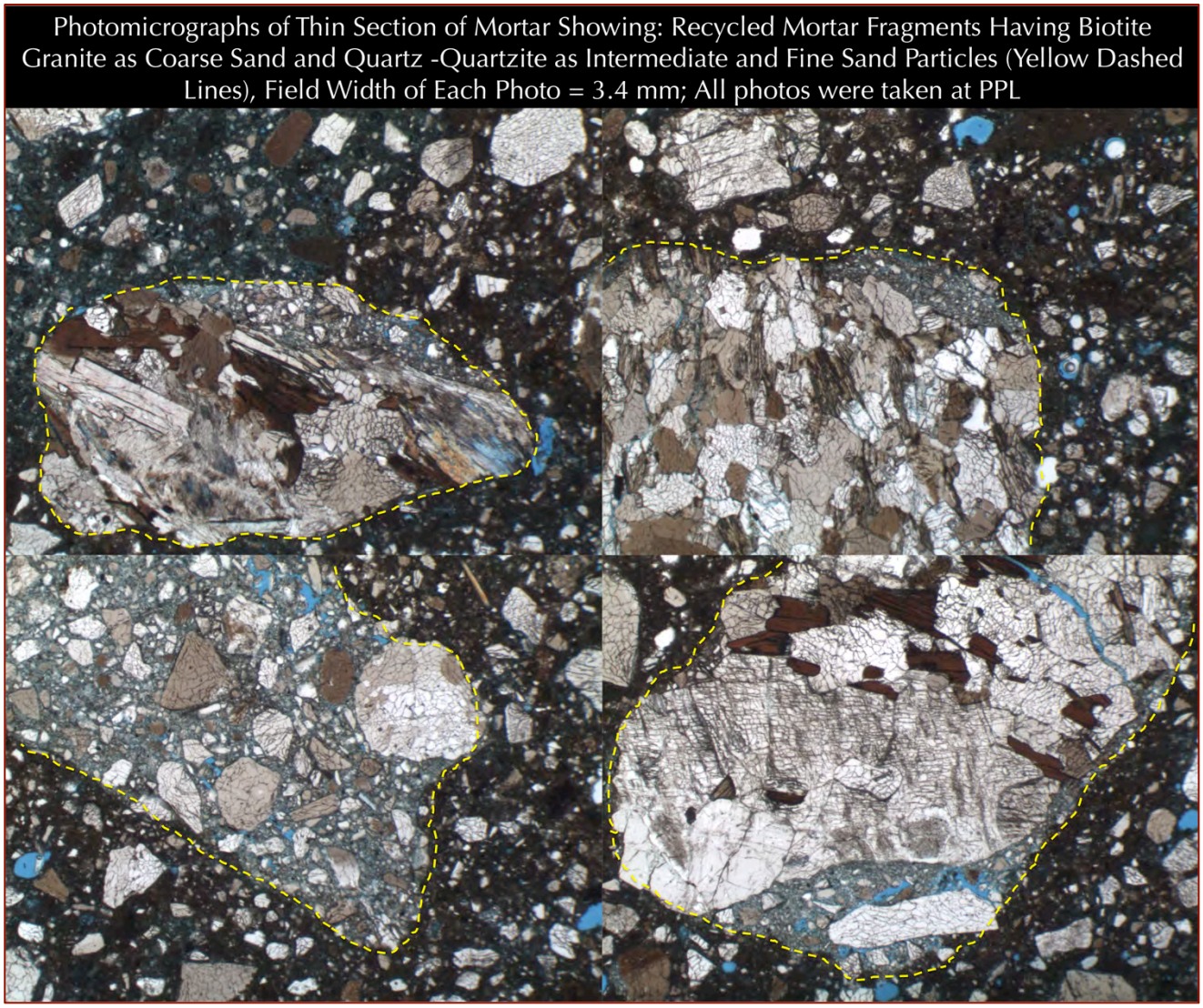

Figure 13: A mosaic of four (4) photomicrographs (all taken in PPL mode) of blue dye-mixed epoxy-impregnated thin section of mortar showing some recycled mortar fragments probably used as coarse sand particles (porous, consisting of coarse biotite granite sand and finer angular quartz sand scattered in a binder) are highlighted by the yellow dashed lines. White dashed lines separate pastes of variable porosities in the main mortar. Orange arrows point to some dark brown residual or raw feed particles of natural cement added in the main mortar.

Tables 3 and 4 list various recycled mortar fragments as detected. Figure 12 (as well as the middle row photo in Figure 5) shows a close-up of one recycled mortar fragment where many fine angular quartz sand particles are seen loosely held together by a rather porous paste. Paste within the recycled mortar is noticeably more porous than the overwhelming paste of the main mortar. Majorities of sand both within the recycled mortar, as well as the outside overwhelming population of fine sand in the main mortar consist of major amounts of quartz, and minor amounts of quartzite and feldspar. Biotite granite gneiss particles are only present within the recycled mortar but not outside in the main mortar. All sand particles are sound; there is no evidence of alkali-aggregate or any other potentially deleterious reactions of sand in the mortar.

Optical Microscopy of Sand Extracted From Acid Digestion of Pulverized Mortar

Figure 14 shows color variations in 'pulverized' sand particles after digesting a pulverized (passing No. 50 sieve) portion of mortar in hydrochloric acid (for determination of acid-insoluble residue content), and collecting the insoluble residue (siliceous sand) from the filter paper for examinations in a digital microscope. As seen, sand particles are dominantly colorless, clear to light gray with occasional dark gray or black specs. Particle sizes of sand in this figure do not represent the original sand sizes since the photo was taken after pulverization of mortar.

Sand particles seen here are contributed from the fine sand used in the main mortar as well as the sand used in the recycled mortar – both sources essentially showed use of compositionally similar clear crushed quartz sand. Recycled mortar, as mentioned, however, also contained coarser particles of biotite granite, which are not present in the main mortar.

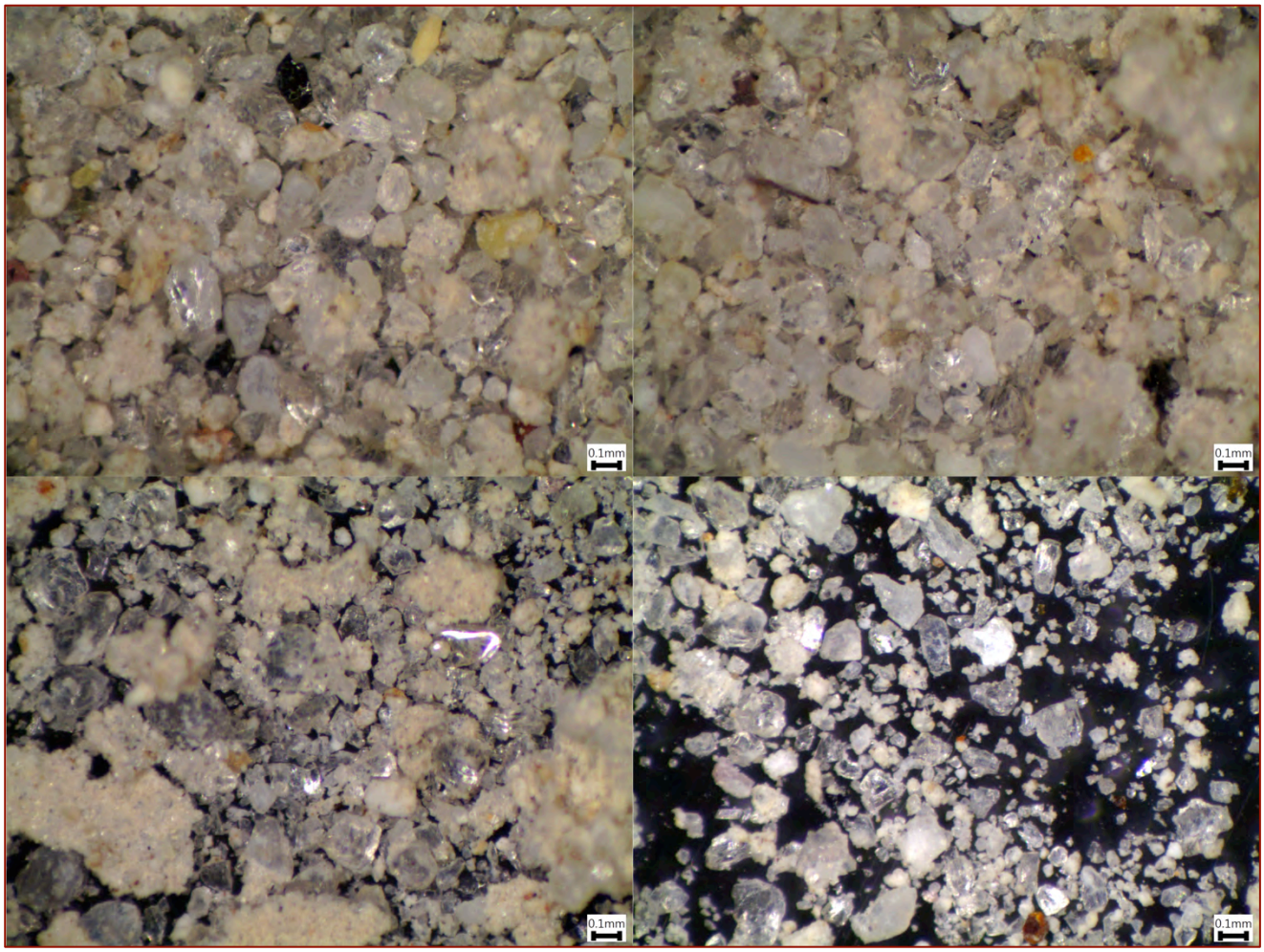

Figure 14: Sand particles left on filter paper after hydrochloric acid-digestion of a pulverized mortar fraction (passing US Sieve 50).

MORTAR PASTE – BINDER TYPE, COMPOSITION, AND MICROSTRUCTURE

Binders in the Main Mortar

Figures 15 through 24 show detailed microstructures of main mortar as well as recycled mortar (in all photomicrographs the latter are highlighted by dashed yellow lines). Binder component in the recycled mortar fragments will be addressed in the next section, after following the immediate discussion of the main mortar.

Binder Components - The majority of the binder in the main mortar shows the typical mineralogy and microstructure produced from the use of (i) a natural cement and (ii) lime as the two essential binders.

Natural Cement - Natural cement binder is characterized by (i) the characteristic light to medium to dark stained brown appearance of the overwhelming paste, and (ii) many fine medium to dark brown residue of calcined raw feed particles of natural cement, many are marked with orange arrows in Figures 16 and 19 through 24, which are remnants of argillaceous limestone and dolomite, the common raw feed used in production of natural cement (e.g., Rosendale cement).

Lime - Lime is recognized as few isolated lumps of unmixed slaked lime with characteristic shrinkage microcracks within the lime lumps, e.g., shown in orange dashed lines in the middle rows in Figures 20 and 23. Lime being extremely fine-grained cryptocrystalline to microcrystalline in nature is intimately mixed with the hydration products of natural cement and difficult to distinguish without lumps as shown in those two figures.

Matrix Components - The overall overwhelming binder in the main mortar is, therefore, a mixture of: (i) hydration and carbonation products of natural cement and (ii) carbonation product of lime, along with (iii) residual calcined raw feed argillaceous limestone/dolomite particles of natural cement, and (iv) some lime lumps.

Hydraulic Component of Binder - The only recognizable crystalline (hydraulic) component of these four binder components is the residual calcined raw feed of natural cement, which shows very typical and characteristic mineralogy and microstructure of calcined raw feed particles of other natural cements (e.g., see Figures 19, 21, 23, and 24), e.g., consisting of: (i) calcium silicate (belite), (ii) aluminate and ferrite, (iii) fine silt-sized silica as quartz, along with (iv) active silica component that had reacted with lime from limestone and alumina and iron from clay to form the calcium silicate and aluminate hydraulic phases, (v) an isotropic amorphous phase formed during calcination of raw feed of natural cement, and, (vi) the hydration and carbonation products of hydraulic phases, e.g., calcium silicate and aluminate, and the amorphous phase.

Variable Density of Matrix - The overwhelming matrix shows variable porosity from denser patches that have absorbed less blue dye-mixed epoxy to relatively porous patches that absorbed more blue dye-mixed epoxy during

impregnation of thin section and hence appeared blue in brightfield. The denser patches of paste are separated from relatively porous paste areas by white dashed lines in Figures 4, 10, 11, 12, 15, and 19.

Binder in the Recycled Mortar

As opposed to the overwhelming natural cement-lime binders in the main mortar, recycled mortar showed very different compositions that differed from the host in the following ways shown in these thin section photos, e.g., (i) binder in recycled mortar is noticeably more porous and hence absorbed more blue dye than the binder in the main mortar, (ii) natural cement is not detected in the recycled mortar, indicating a different hydraulic binder was used in the recycled mortar; (ii) lime is the most common binder detected in the recycled mortar as opposed to natural cement and occurred as fine-grained, cryptocrystalline carbonated lime matrix; and (iv) a few residual calcium silicate particles are detected in the lime-based binder of recycled mortar indicating perhaps a hydraulic lime was used in the recycled mortar, e.g., a natural hydraulic lime.

Figures 15, 16, 19, and 20 show isolated occurrences of these recycled mortars that are separated from the host by yellow dashed lines where differences in microstructures of binders in two mortars are distinct.

Figure 15 shows successively enlarged view of one recycled mortar, from top to bottom rows to show: (i) use of similar angular quartz sand in the recycled mortar as in the main body; however sand particles are loosely held together in recycled mortar by (ii) a fine-grained, cryptocrystalline, porous paste that shows (iii) typical microstructure of a carbonated calcium silicate-type paste e.g., similar to carbonated calcium silicate hydrate patches of Portland cement paste, particularly seen in the crossed polarized light photos (e.g., right columns in Figure 15 are crossed polarized light images of photos shown in the left column).

Figures 17 and 18 concentrated within one recycled mortar particle where the particle is shown in the top row in Figure 17 to show its markedly different microstructure and overall porous nature compared to the outside main mortar, whereas the middle and bottom rows in Figure 17 and all rows in Figure 18 concentrated entirely within recycled mortar to show (i) use of similar angular quartz sand as outside main mortar, where the particles are loosely held together by (ii) a porous paste that shows (iii) typical microstructure of a carbonated lime-based paste i.e. carbonated calcium silicate hydrate in crossed polarized light. The middle rows in Figures 17 and 18 point to two residual calcium silicate phases (marked with yellow arrows) that are the hydraulic phases used along with slaked lime to form the binder in the recycled mortar. These phases indicate possible use of a hydraulic lime binder in the recycled mortar. The overwhelming microstructures of binder in recycled mortar in crossed polarized light modes in right columns in Figures 17 and 18 show a startling similarity to those of many natural hydraulic lime mortars in having calcium silicate-aluminate-ferrite hydrates and their carbonation products.

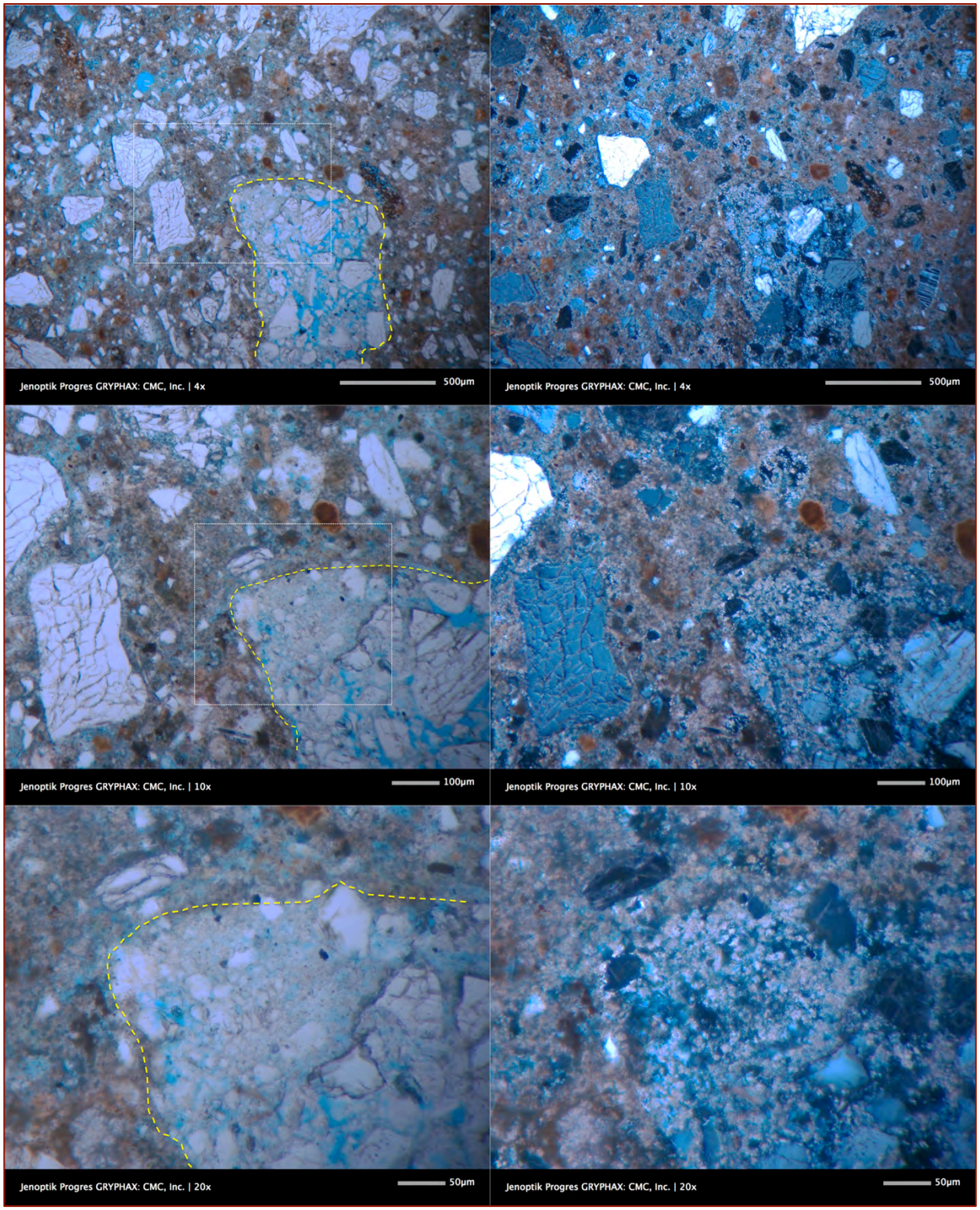

Figure 15: Photomicrographs of thin section of mortar showing: (i) a recycled mortar fragment (marked with dashed yellow lines), (ii) overall light to medium brown appearance of paste in the main mortar that shows typical characteristics of natural cement and lime binder, (iii) many dark brown residual calcium raw feed particles of natural cement, and (iv) noticeably denser nature of the overwhelming natural cement-lime binder in the main mortar as opposed to porous, fine-grained binder in the recycled mortar. Left photos were taken in PPL and right photos in corresponding XPL modes in a petrographic microscope.

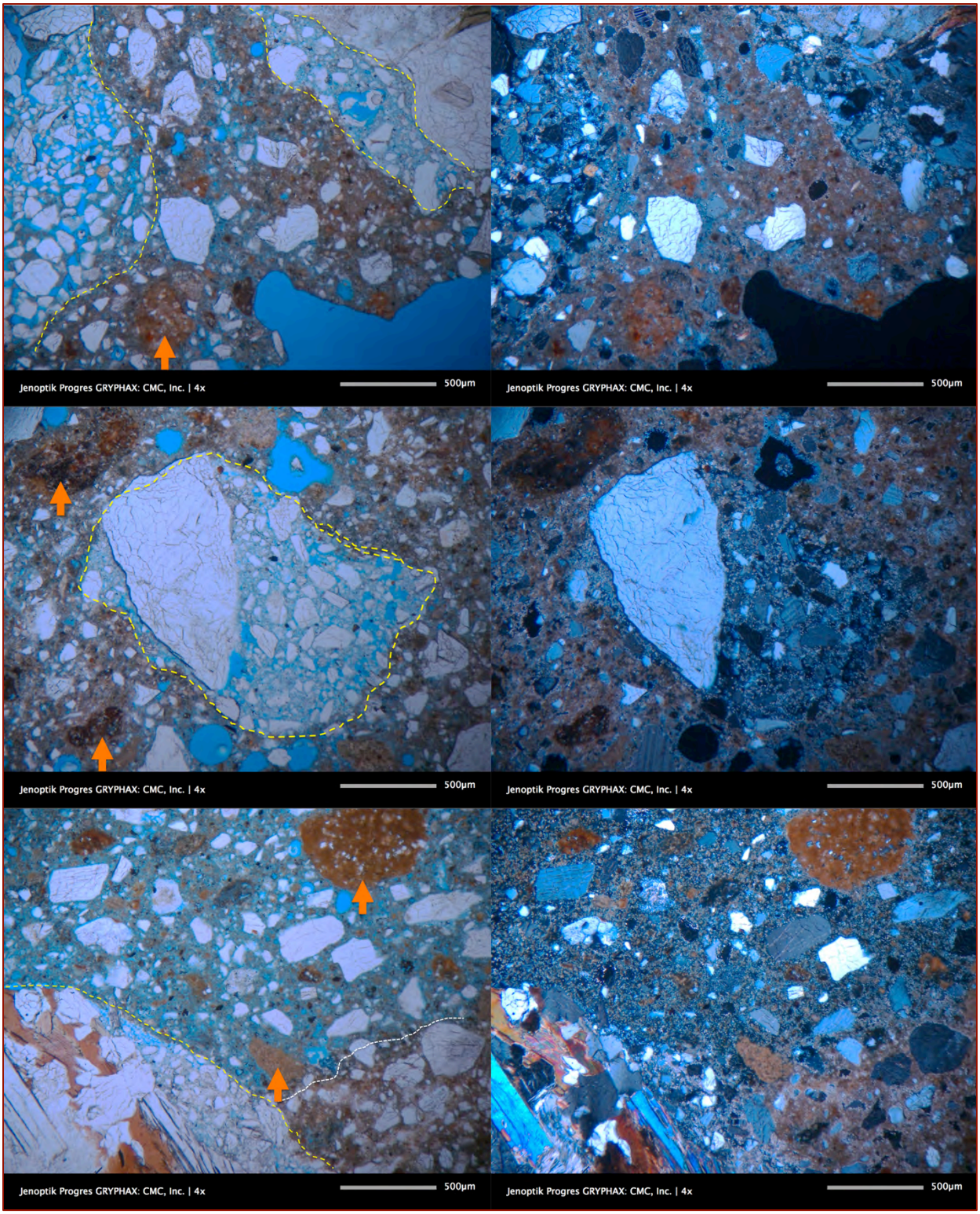

Figure 16: Photomicrographs of thin section of mortar showing: (i) recycled mortar fragments (marked with dashed yellow lines), (ii) overall light to medium brown appearance of paste in the main mortar that shows typical characteristics of natural cement and lime binder, (iii) many dark brown residual calcium raw feed particles of natural cement (marked with orange arrows), and (iv) noticeably denser nature of the overwhelming natural cement-lime binder in the main mortar as opposed to porous, fine-grained binder in the recycled mortar. Left photos were taken in PPL and right photos in corresponding XPL modes in a petrographic microscope.

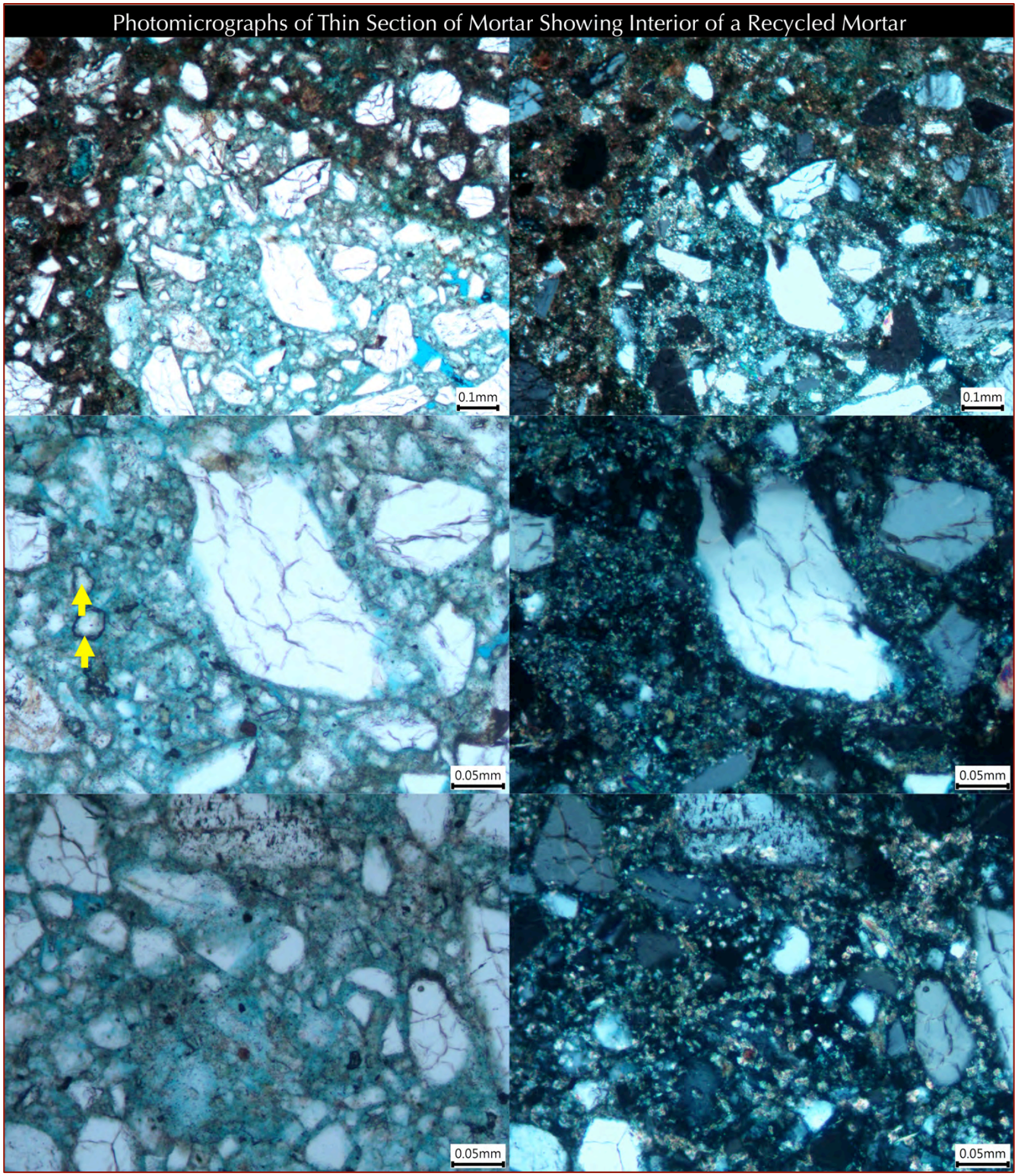

Figure 17: Photomicrographs of thin section of mortar concentrating on a recycled mortar fragment. The particle is shown in the top row against its outside main mortar, whereas the middle and bottom rows as well as all rows in Figure 18 have concentrated within this particle to show its own binder and sand. A few calcium silicate-type hydraulic phases are detected in the binder of this recycled mortar particle (marked with yellow arrows).

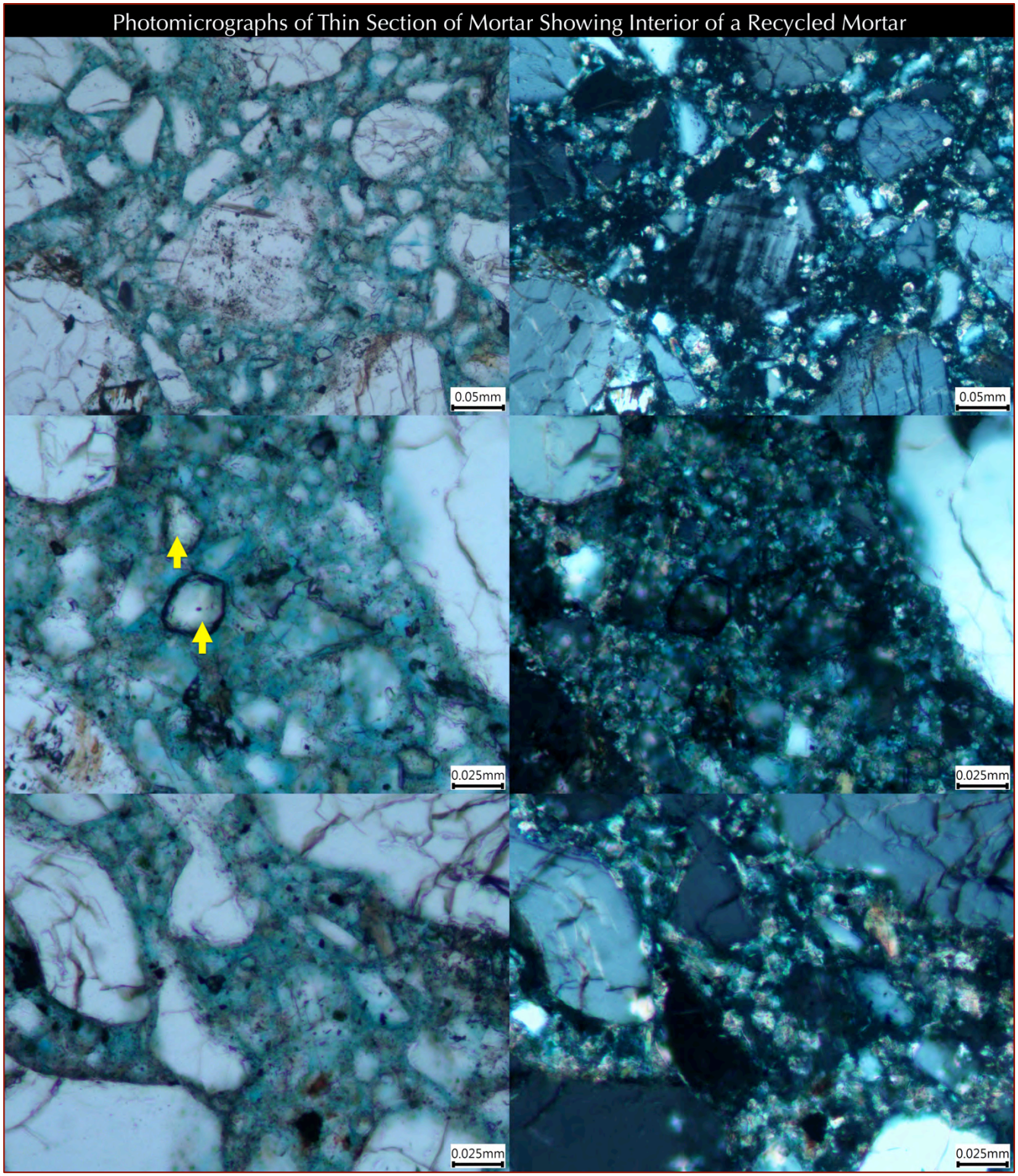

Figure 18: Continuation of previous photos of a recycled mortar particle showing quartz sand and interstitial binder, where the binder shows a few residual hydraulic phases (yellow arrows) and overwhelming paste similar in appearance to a natural hydraulic lime paste, especially in the crossed polar photos in the right column where lime-rich patches show bright interference colors.

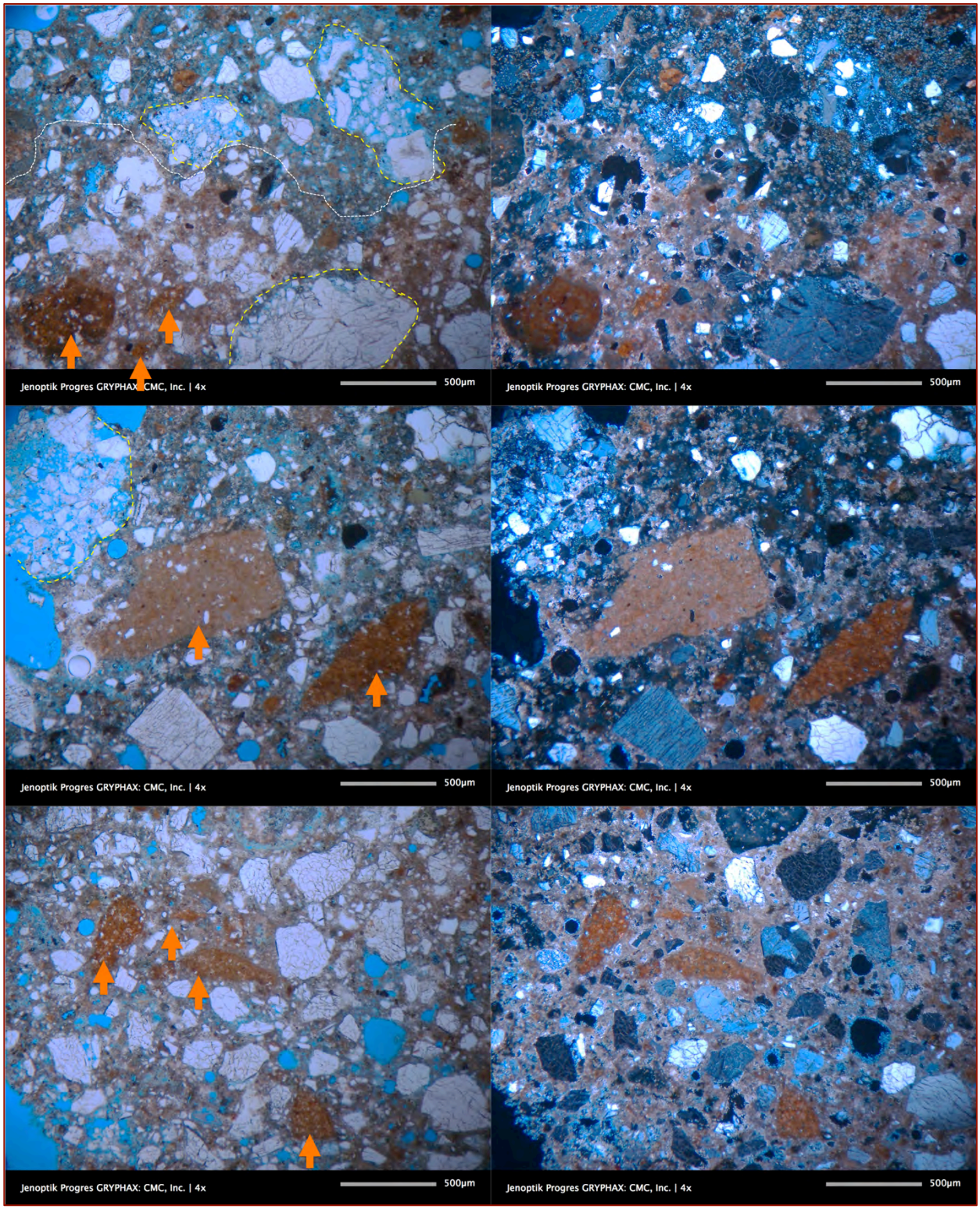

Figure 19: Photomicrographs of thin section of mortar showing: (i) recycled mortar fragments (marked with dashed yellow lines), (ii) overall light to medium brown appearance of paste in the main mortar that shows typical characteristics of natural cement and lime binder, (iii) many dark brown residual calcium raw feed particles of natural cement (marked with orange arrows), and (iv) noticeably denser nature of the overwhelming natural cement-lime binder in the main mortar as opposed to porous, fine-grained binder in the recycled mortar. Left photos were taken in PPL and right photos in corresponding XPL modes in a petrographic microscope.

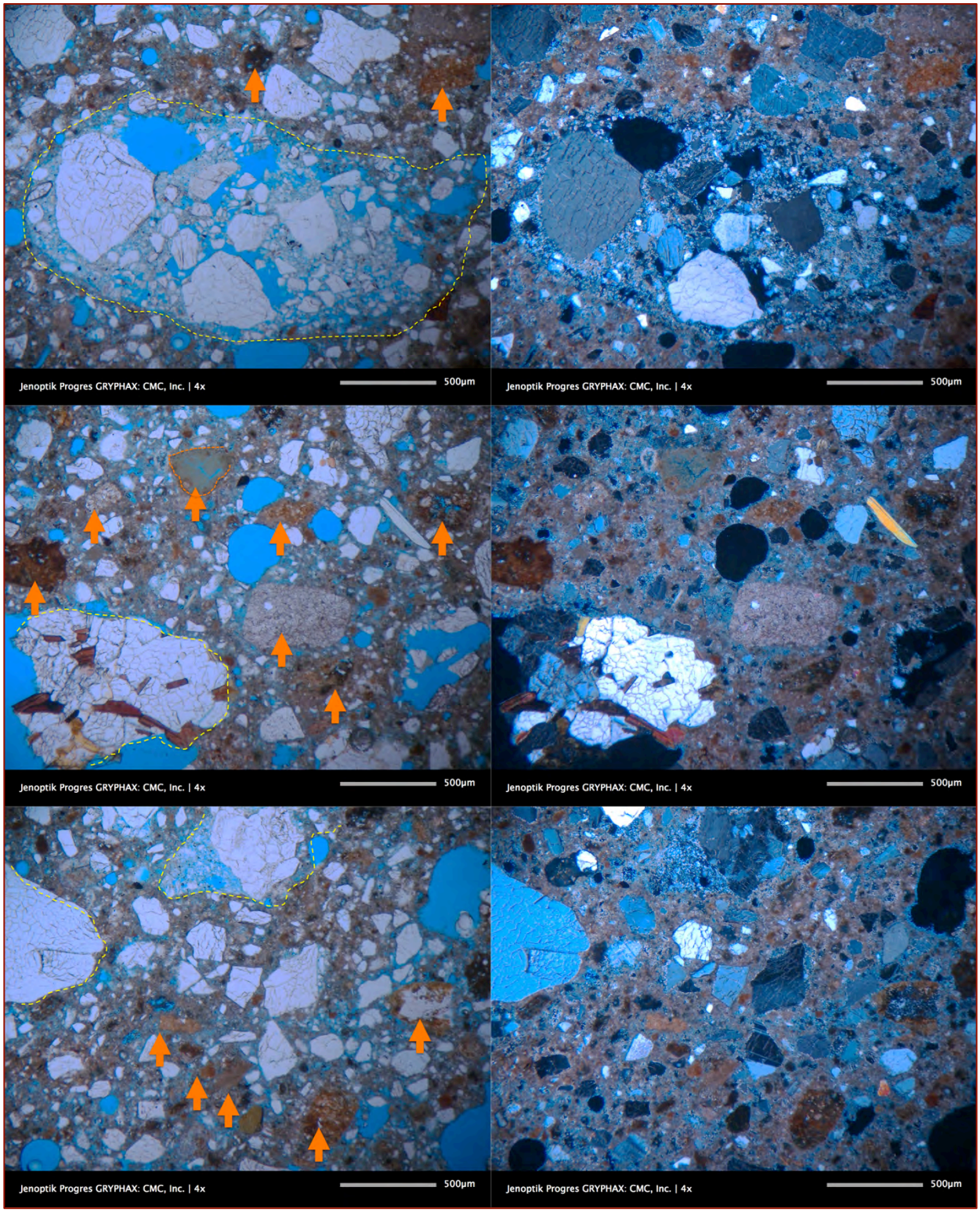

Figure 20: Photomicrographs of thin section of mortar showing: (i) recycled mortar fragments (marked with dashed yellow lines), (ii) overall light to medium brown appearance of paste in the main mortar that shows typical characteristics of natural cement and lime binder, (iii) many dark brown residual calcium raw feed particles of natural cement (marked with orange arrows), and (iv) noticeably denser nature of the overwhelming natural cement-lime binder in the main mortar as opposed to porous, fine-grained binder in the recycled mortar. Left photos were taken in PPL and right photos in corresponding XPL modes in a petrographic microscope.

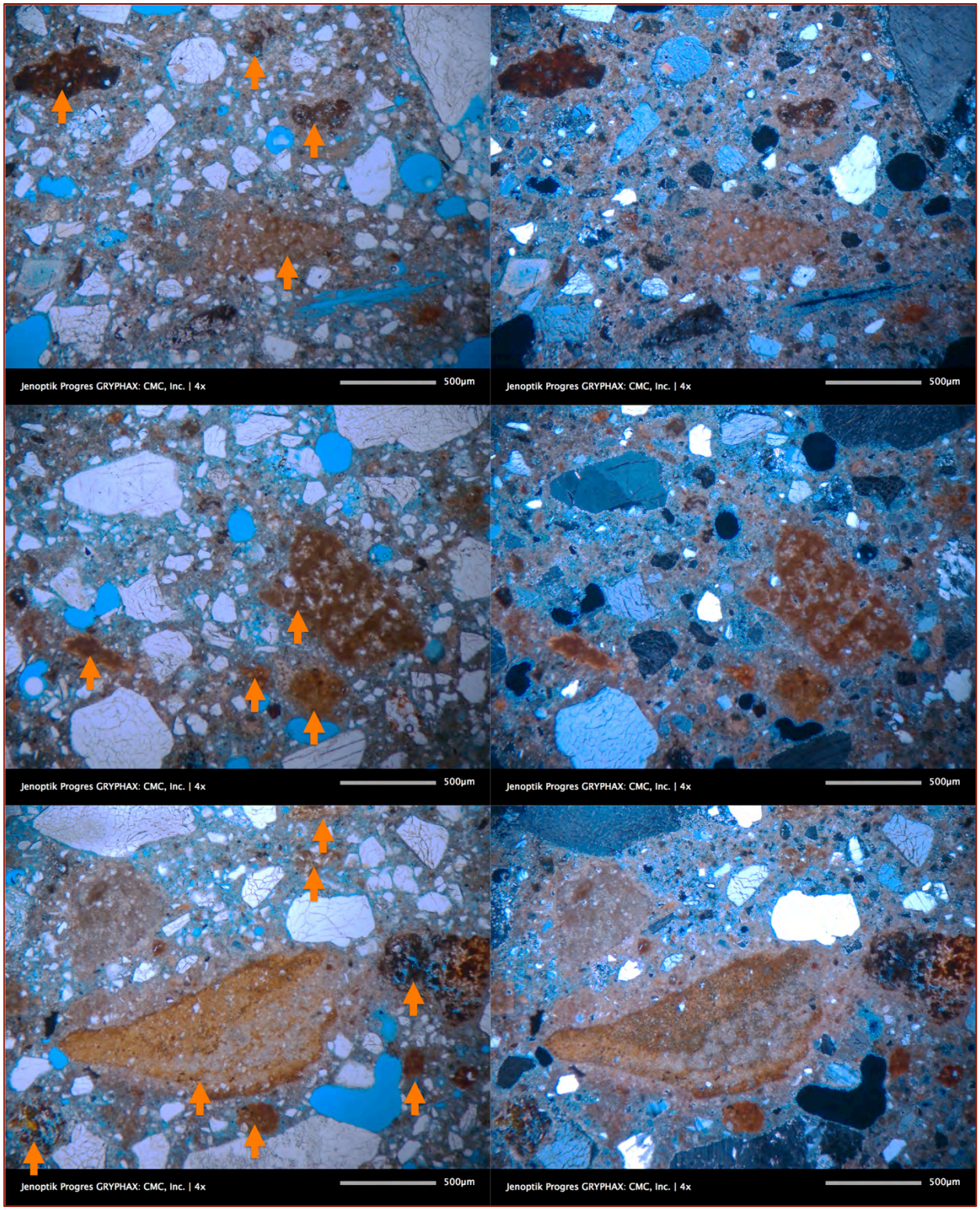

Figure 21: Photomicrographs of thin section of mortar showing: (i) overall light to medium brown appearance of paste in the main mortar that shows the typical characteristics of natural cement and lime binder, and (ii) many dark brown residual calcium raw feed particles of natural cement (marked with orange arrows). Left photos were taken in PPL and right photos in corresponding XPL modes in a petrographic microscope.

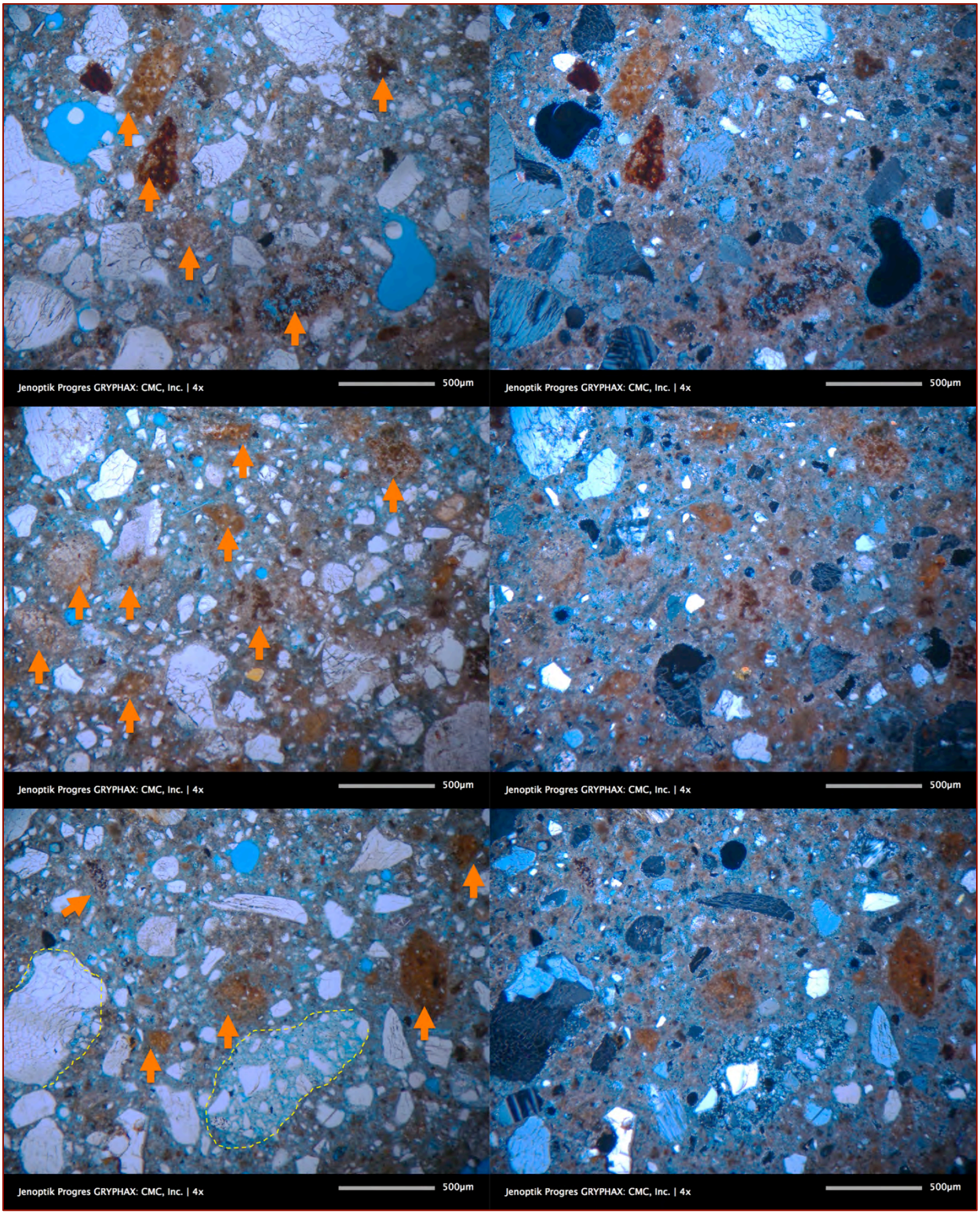

Figure 22: Photomicrographs of thin section of mortar showing many calcined limestone and argillaceous dolostone raw feed particles (many are marked with orange arrows) that are indications of use of natural cement as a binder in the main mortar. Some coarse sand particles are marked in dashed yellow lines. Left and right column photos were taken in PPL and XPL modes, respectively.

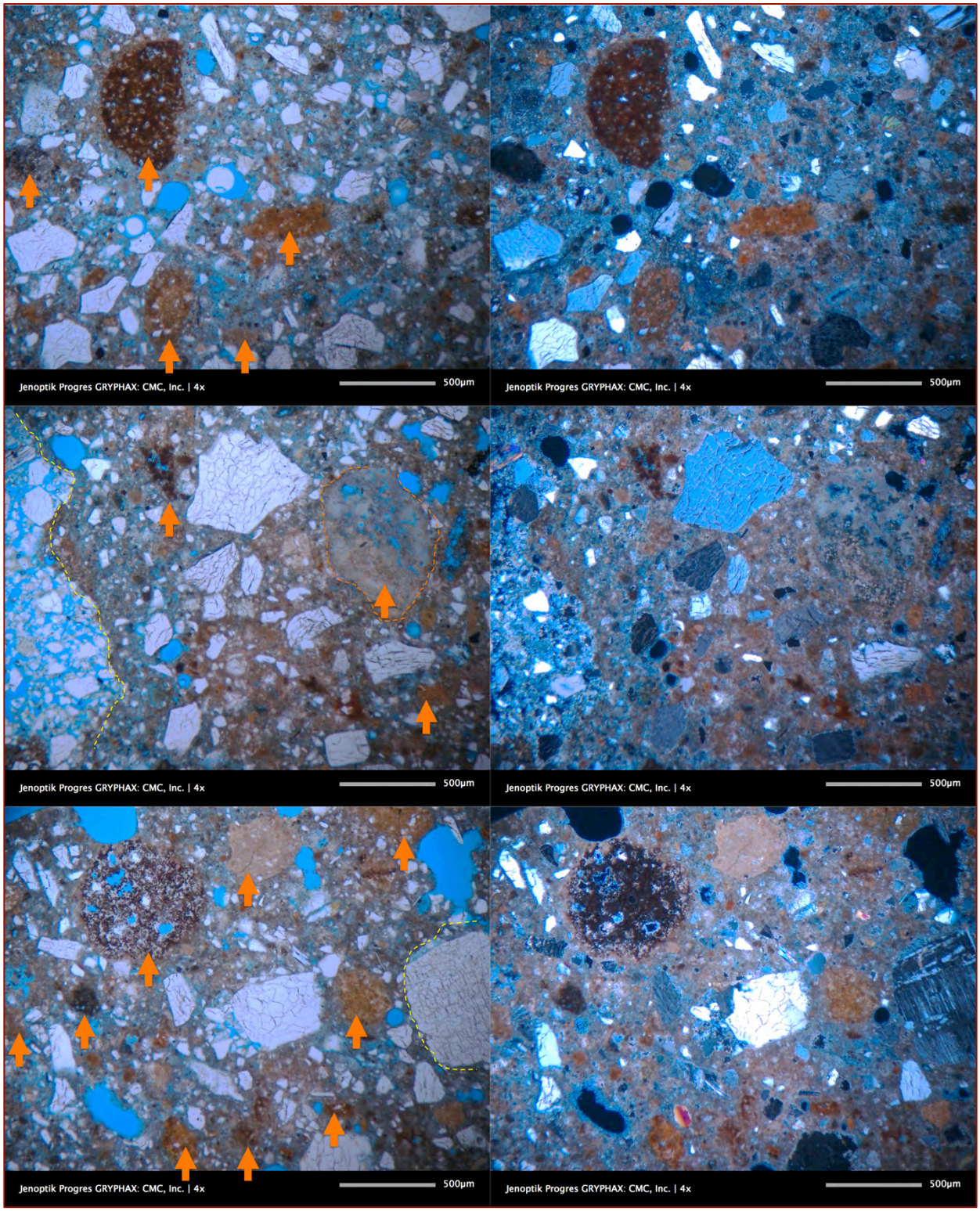

Figure 23: Photomicrographs of thin section of mortar showing many calcined limestone and argillaceous dolostone raw feed particles (many are marked with orange arrows) that are indications of use of natural cement as a binder in the main mortar. A calcined lime lump is shown by dashed orange line in the middle row. Left and right column photos were taken in PPL and XPL modes, respectively.

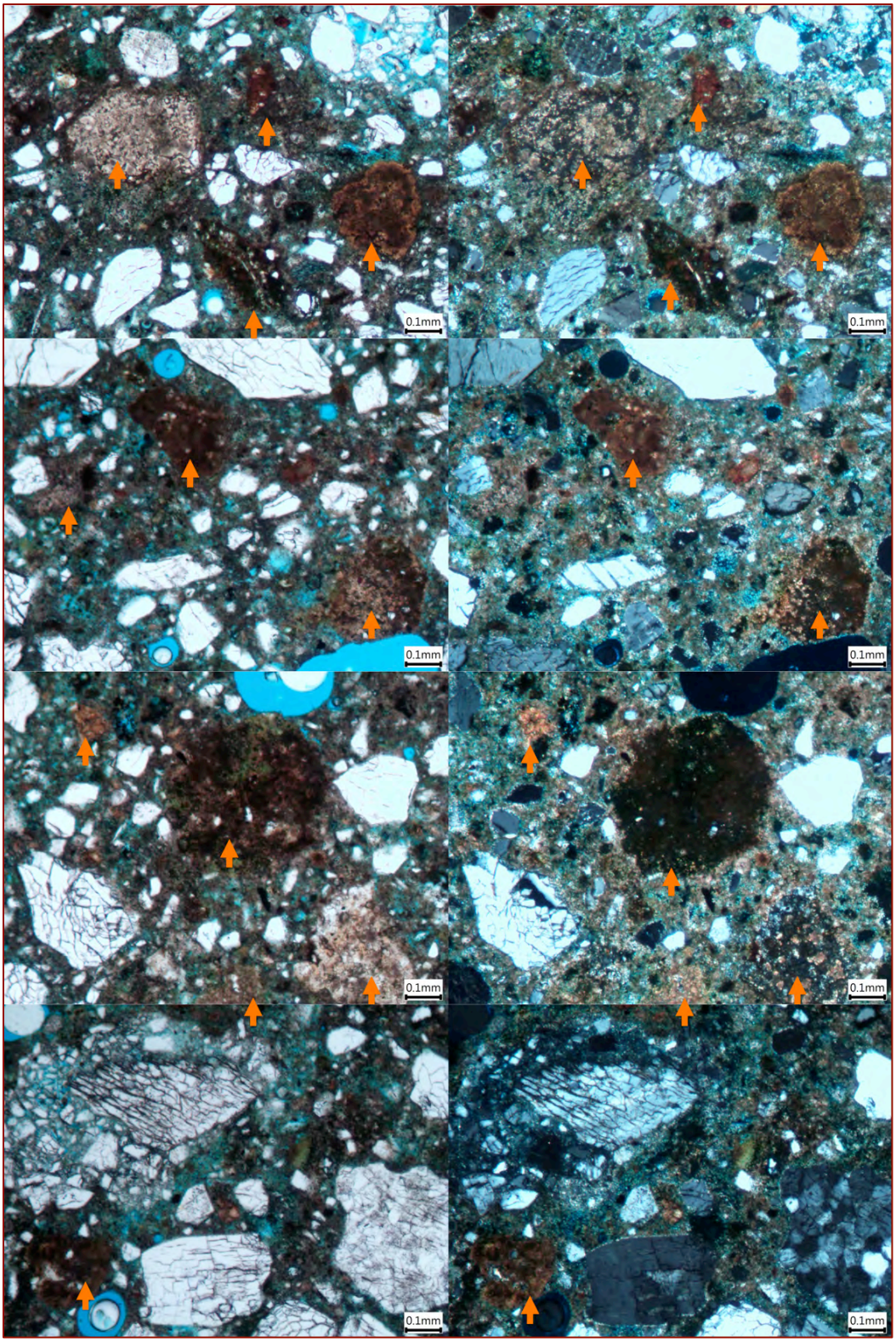

Figure 24: Photomicrographs of thin section of mortar showing: (i) overall light to medium brown appearance of paste that shows typical characteristics of natural cement and lime binder in the main mortar, and (ii) many dark brown residual calcium raw feed particles of natural cement (marked with orange arrows). Left photos were taken in PPL and right photos in corresponding XPL modes in a petrographic microscope.

SEM-EDS ANALYSES OF RECYCLED MORTAR AND MAIN (NATURAL CEMENT-LIME) MORTAR

Recycled Mortar

Figures 25 through 39 show microstructural studies of the recycled mortar, particularly the binder component in between sand particles in backscatter electron (BSE) image, X-ray elemental image, and SEM-EDS compositional analyses of various areas in BSE image. Binder compositions from these studies are finally summarized in Figure 40 to show (a) overall compositional variations of binder, and (b) identification of three different components in the binder - (i) a calcium-rich Al-K-Fe-silicate composition inherited from lime, (ii) a calcium-poor Al-K-Fe-silicate composition from silica-rich hydraulic phases of binder, and, (iii) an intermediate calcium Al-K-Fe-silicate, which is probably the mixture of two end members of lime-rich and lime-poor components of the binder, similar in composition to a *natural (high-calcium) hydraulic lime* the raw feed of which had contained limestone as the source of lime and clay as the source of silica, alumina, potassium, and iron.

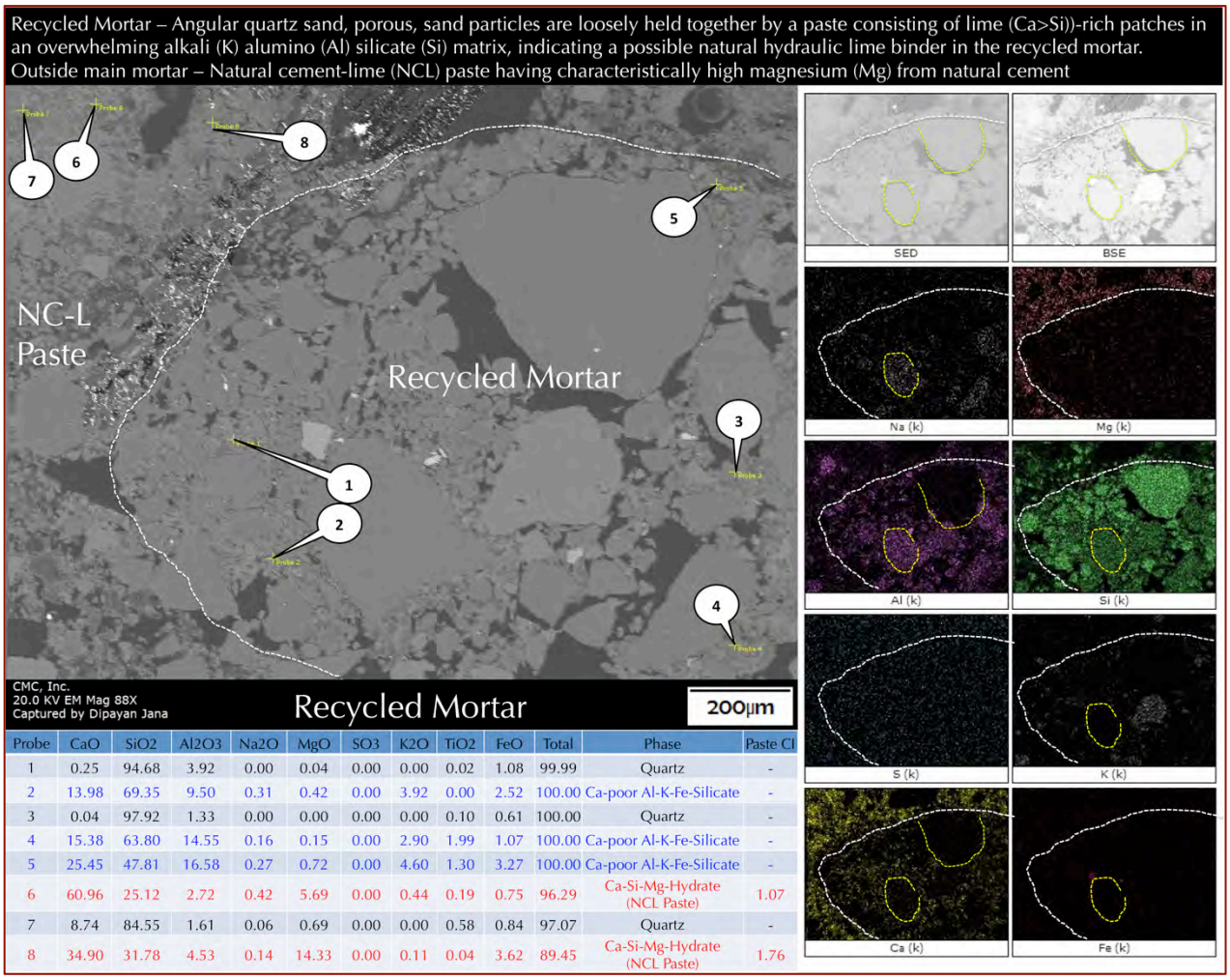

Probe	CaO	SiO2	Al2O3	Na2O	MgO	SO3	K2O	TiO2	FeO	Total	Phase	Paste Cl
1	0.25	94.68	3.92	0.00	0.04	0.00	0.00	0.02	1.08	99.99	Quartz	-
2	13.98	69.35	9.50	0.31	0.42	0.00	3.92	0.00	2.52	100.00	Ca-poor Al-K-Fe-Silicate	-
3	0.04	97.92	1.33	0.00	0.00	0.00	0.00	0.10	0.61	100.00	Quartz	-
4	15.38	63.80	14.55	0.16	0.15	0.00	2.90	1.99	1.07	100.00	Ca-poor Al-K-Fe-Silicate	-
5	25.45	47.81	16.58	0.27	0.72	0.00	4.60	1.30	3.27	100.00	Ca-poor Al-K-Fe-Silicate	-
6	60.96	25.12	2.72	0.42	5.69	0.00	0.44	0.19	0.75	96.29	Ca-Si-Mg-Hydrate (NCL Paste)	1.07
7	8.74	84.55	1.61	0.06	0.69	0.00	0.00	0.58	0.84	97.07	Quartz	-
8	34.90	31.78	4.53	0.14	14.33	0.00	0.11	0.04	3.62	89.45	Ca-Si-Mg-Hydrate (NCL Paste)	1.76

Figure 25: Backscatter electron (BSE) image (top left), X-ray elemental map (right), and EDS elemental analyses of various points on the BSE image (bottom left) showing compositional variations within a recycled mortar fragment within the white dashed line in the BSE image, and the outside the main natural cement-lime mortar.

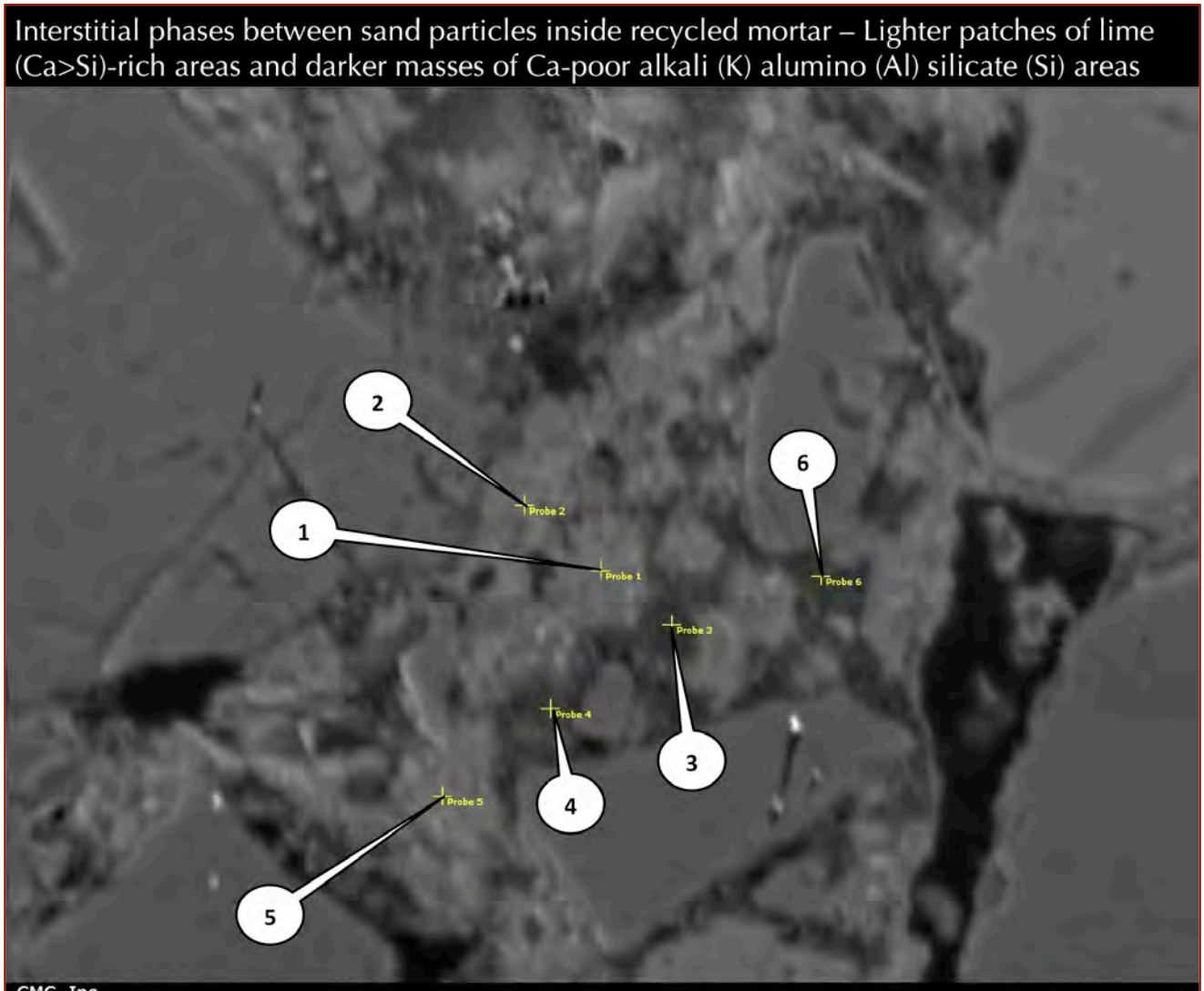

Probe	CaO	SiO2	Al2O3	Na2O	MgO	SO3	K2O	TiO2	FeO	Total	Phase	Paste CI
1	68.49	19.20	5.10	0.20	0.45	0.00	4.91	0.00	1.65	100.00	Ca-rich Al-K-Fe-Silicate	0.88
2	55.34	31.03	9.35	0.44	0.44	0.00	1.84	0.00	1.56	100.00	Ca-rich Al-K-Fe-Silicate	1.76
3	21.94	43.11	17.79	0.18	0.86	0.00	9.91	0.76	5.45	100.00	Ca-poor Al-K-Fe-Silicate	-
4	0.44	88.41	5.59	0.00	0.14	0.00	2.44	0.12	2.86	100.00	Quartz	-
5	24.89	47.04	13.19	0.07	0.86	0.00	5.65	1.10	7.19	99.99	Ca-poor Al-K-Fe-Silicate	-
6	13.04	47.59	20.10	0.13	1.12	0.00	12.60	0.52	4.88	99.98	Ca-poor Al-K-Fe-Silicate	-

Figure 26: BSE image (top) and EDS elemental analyses of various points on the BSE image (bottom) showing compositional variations within the recycled mortar shown in Figure 25.

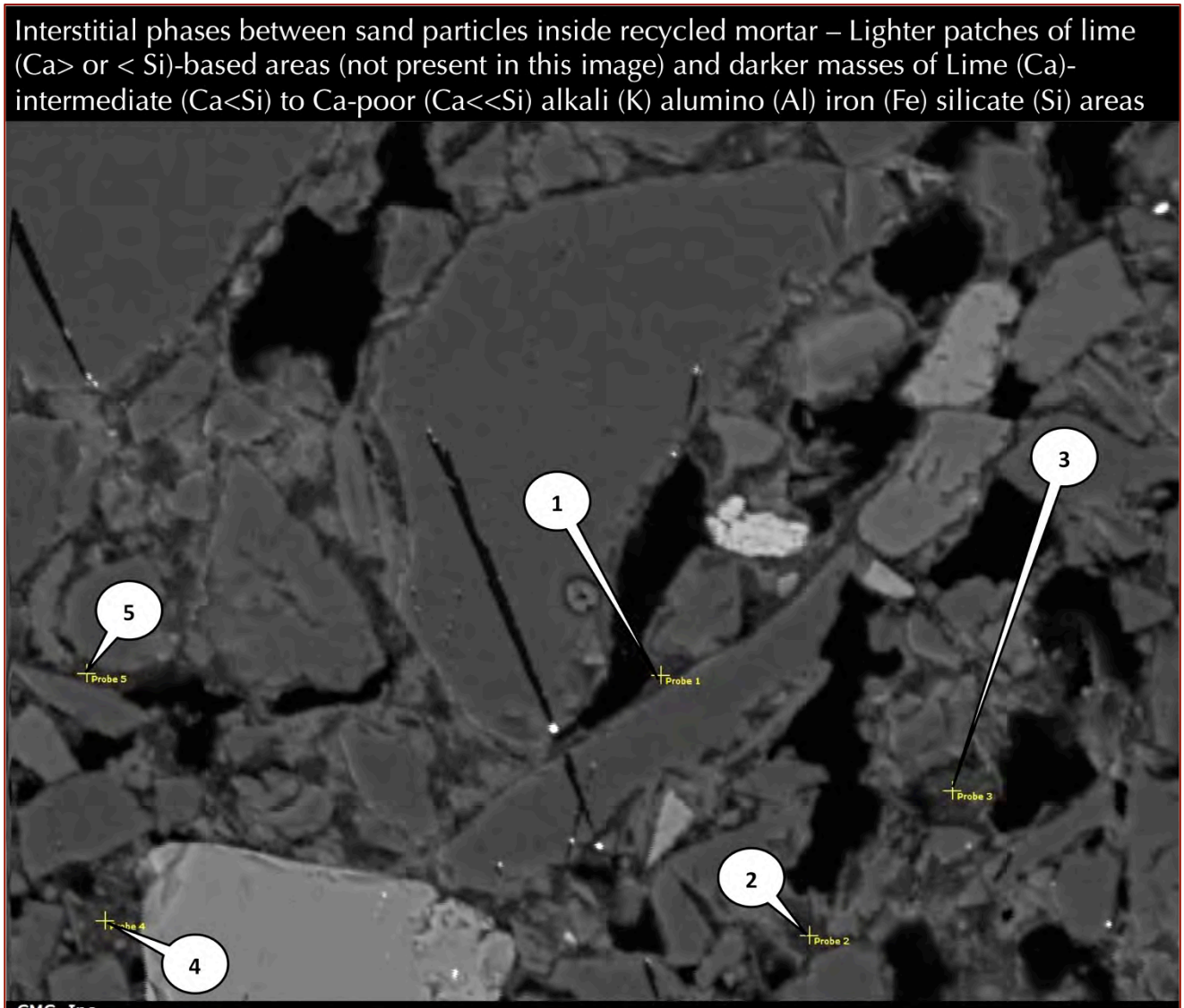

Probe	CaO	SiO2	Al2O3	Na2O	MgO	SO3	K2O	TiO2	FeO	Total	Phase	Paste CI
1	2.44	77.74	7.23	0.28	0.28	0.00	5.22	1.71	5.11	100.01	Ca-poor Al-K-Fe-Silicate	-
2	1.34	70.94	12.53	0.43	1.32	0.00	7.40	0.85	5.20	100.01	Ca-poor Al-K-Fe-Silicate	-
3	2.00	65.46	18.70	0.31	0.86	0.00	6.20	1.16	5.30	99.99	Ca-poor Al-K-Fe-Silicate	-
4	1.09	60.06	10.49	0.67	1.66	0.00	15.71	2.01	8.31	100.00	Ca-poor Al-K-Fe-Silicate	-
5	33.91	40.46	11.78	0.48	0.97	0.00	6.41	1.03	4.96	100.00	Ca-int. Al-K-Fe-Silicate	3.68

Figure 27: BSE image (top) and EDS elemental analyses of various points on the BSE image (bottom) showing compositional variations within the recycled mortar fragment shown in Figure 25.

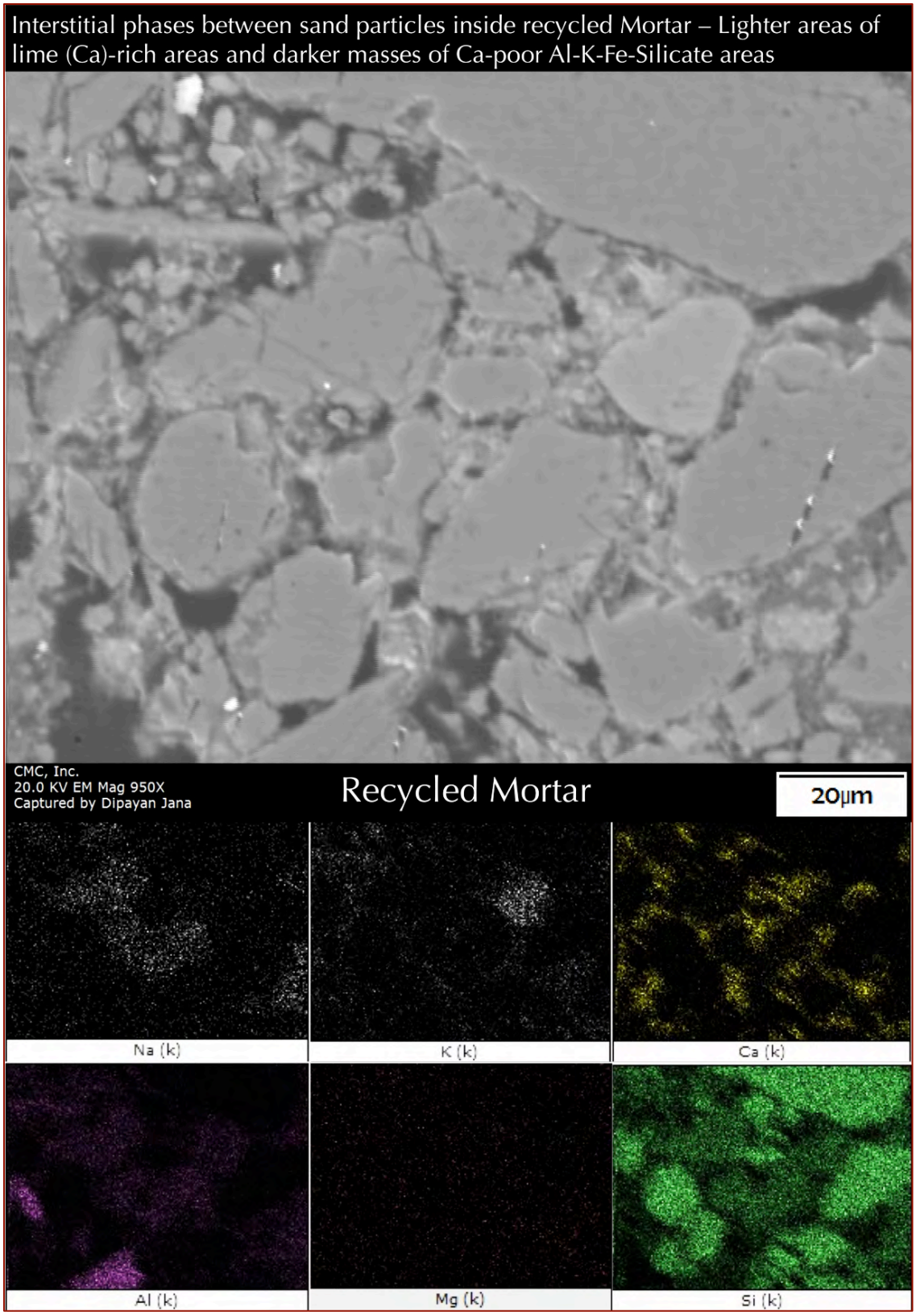

Figure 28: BSE image (top) and X-ray elemental map (bottom) showing compositional variations within the recycled mortar fragment shown in Figure 25. Notice lime-rich patchy areas, as well as some alkali- (Na, K) areas probably from feldspar in the sand fragment and/or some calcined lime-silica products of hydraulic lime.

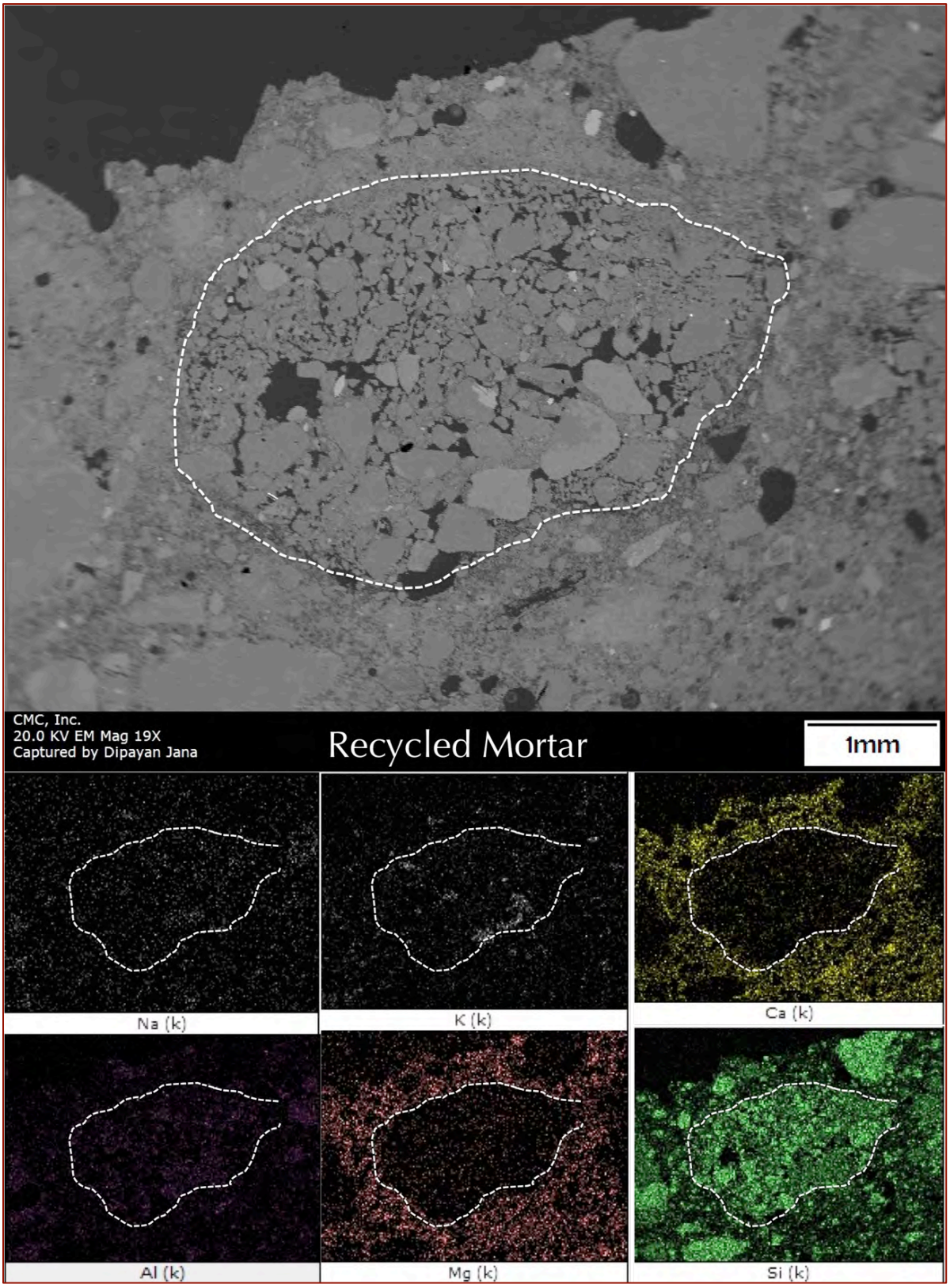

Figure 29: Backscatter electron (BSE) image (top), and X-ray elemental map (bottom) showing compositional variations within a recycled mortar fragment within the white dashed line in the BSE image, and the outside main natural cement-lime mortar.

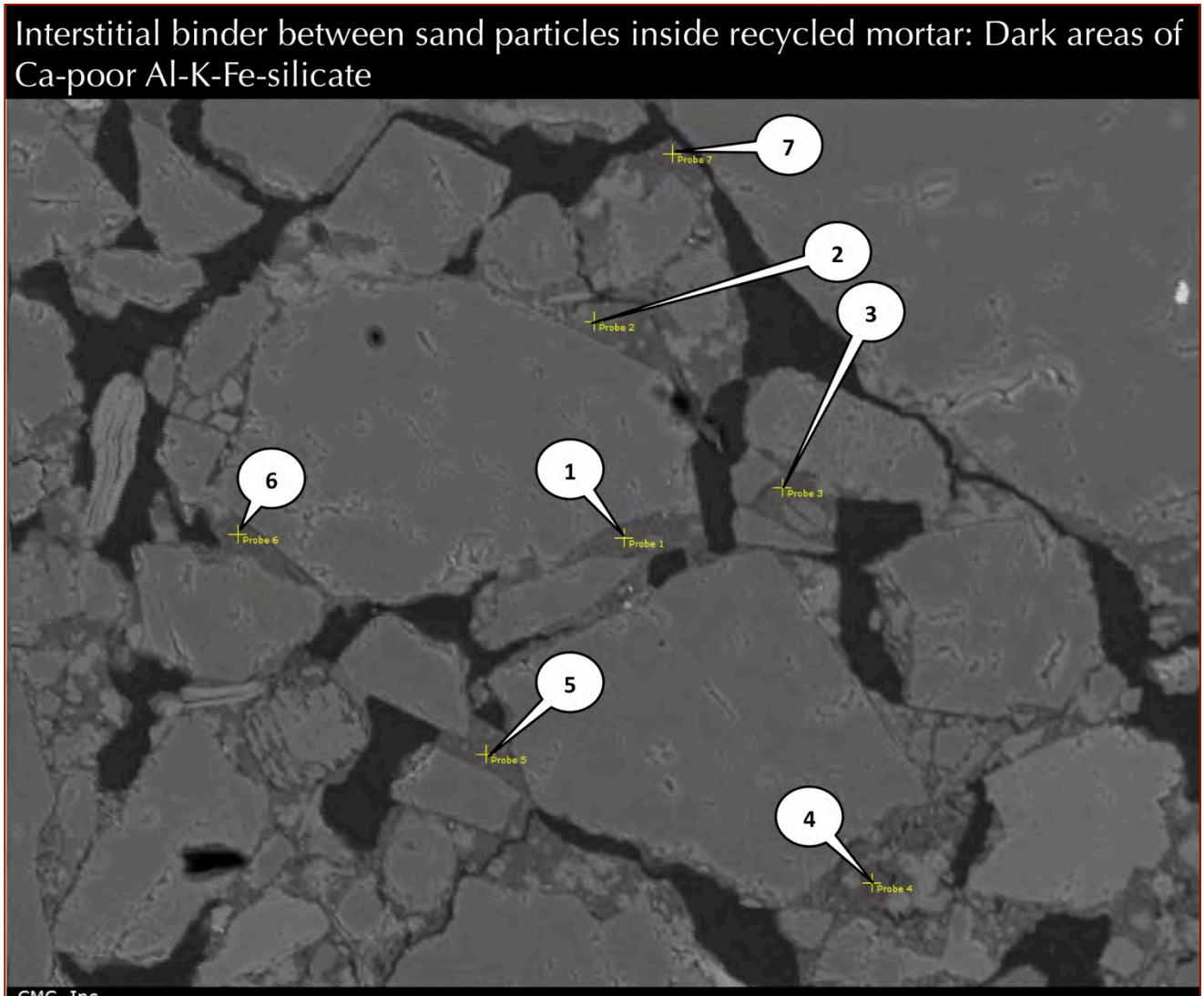

Probe	CaO	SiO2	Al2O3	Na2O	MgO	SO3	K2O	TiO2	FeO	Total	Phase	Paste Cl
1	3.45	56.04	17.37	0.50	1.52	0.00	11.17	4.08	5.86	99.99	Ca-poor Al-K-Fe-Silicate	-
2	5.41	55.54	18.08	0.30	0.79	0.00	12.08	0.97	6.84	100.01	Ca-poor Al-K-Fe-Silicate	-
3	6.30	57.05	16.88	0.53	0.86	0.00	11.70	0.57	6.11	100.00	Ca-poor Al-K-Fe-Silicate	-
4	1.55	53.03	20.40	0.16	0.69	0.00	13.17	2.09	8.91	100.00	Ca-poor Al-K-Fe-Silicate	-
5	3.30	57.28	18.30	0.64	0.75	0.00	11.70	1.19	6.84	100.00	Ca-poor Al-K-Fe-Silicate	-
6	2.61	54.11	19.43	0.35	1.13	0.00	10.43	1.72	10.20	99.98	Ca-poor Al-K-Fe-Silicate	-
7	1.69	52.49	23.81	0.30	0.91	0.00	10.19	2.25	8.36	100.00	Ca-poor Al-K-Fe-Silicate	-

Figure 30: BSE image (top) and EDS elemental analyses of various points on the BSE image (bottom) showing compositional variations within the recycled mortar fragment shown in Figure 29.

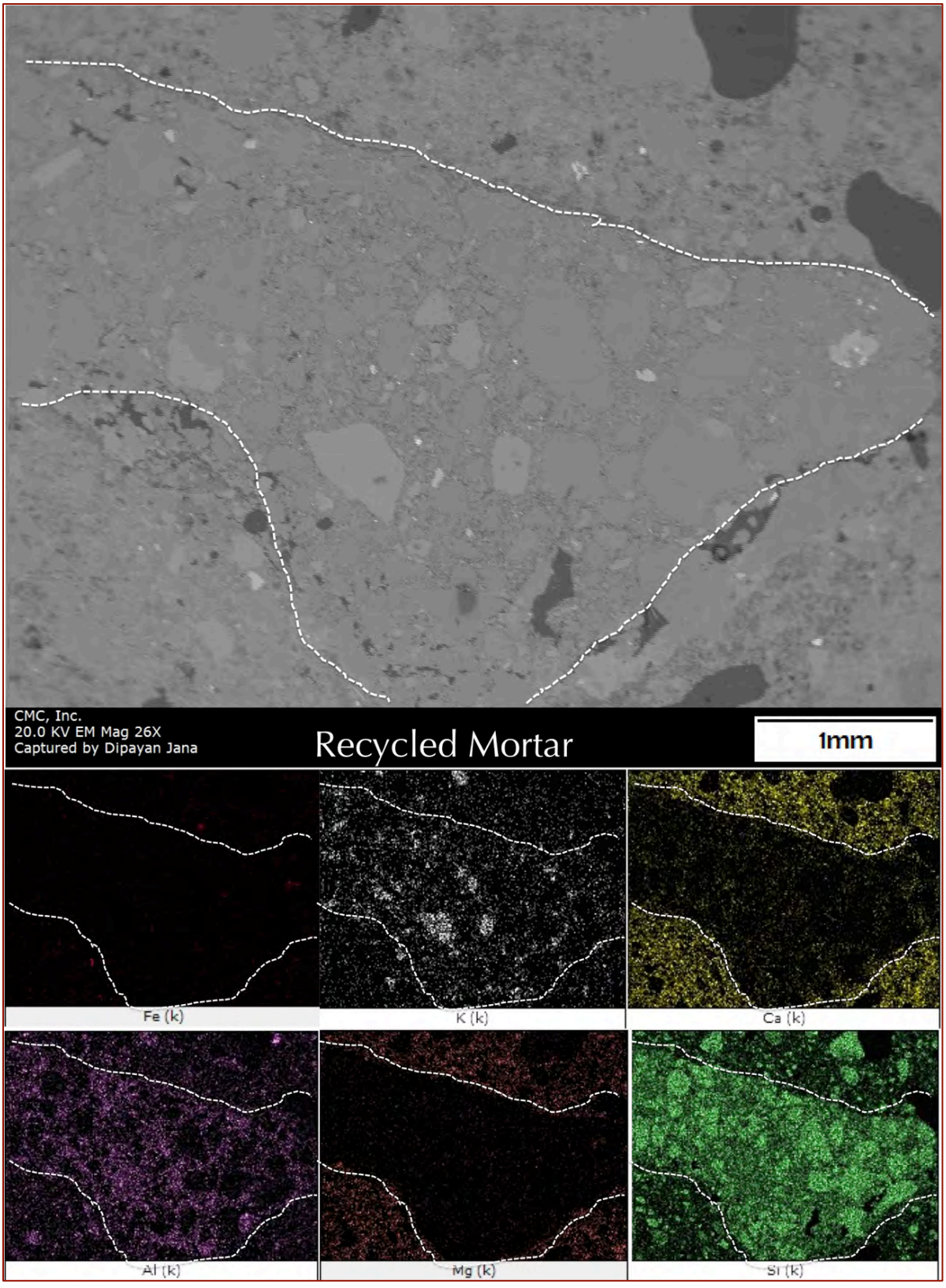

Figure 31: Backscatter electron (BSE) image (top), and X-ray elemental map (bottom) showing compositional variations within a recycled mortar fragment within the white dashed line in the BSE image, and the outside main natural cement-lime mortar.

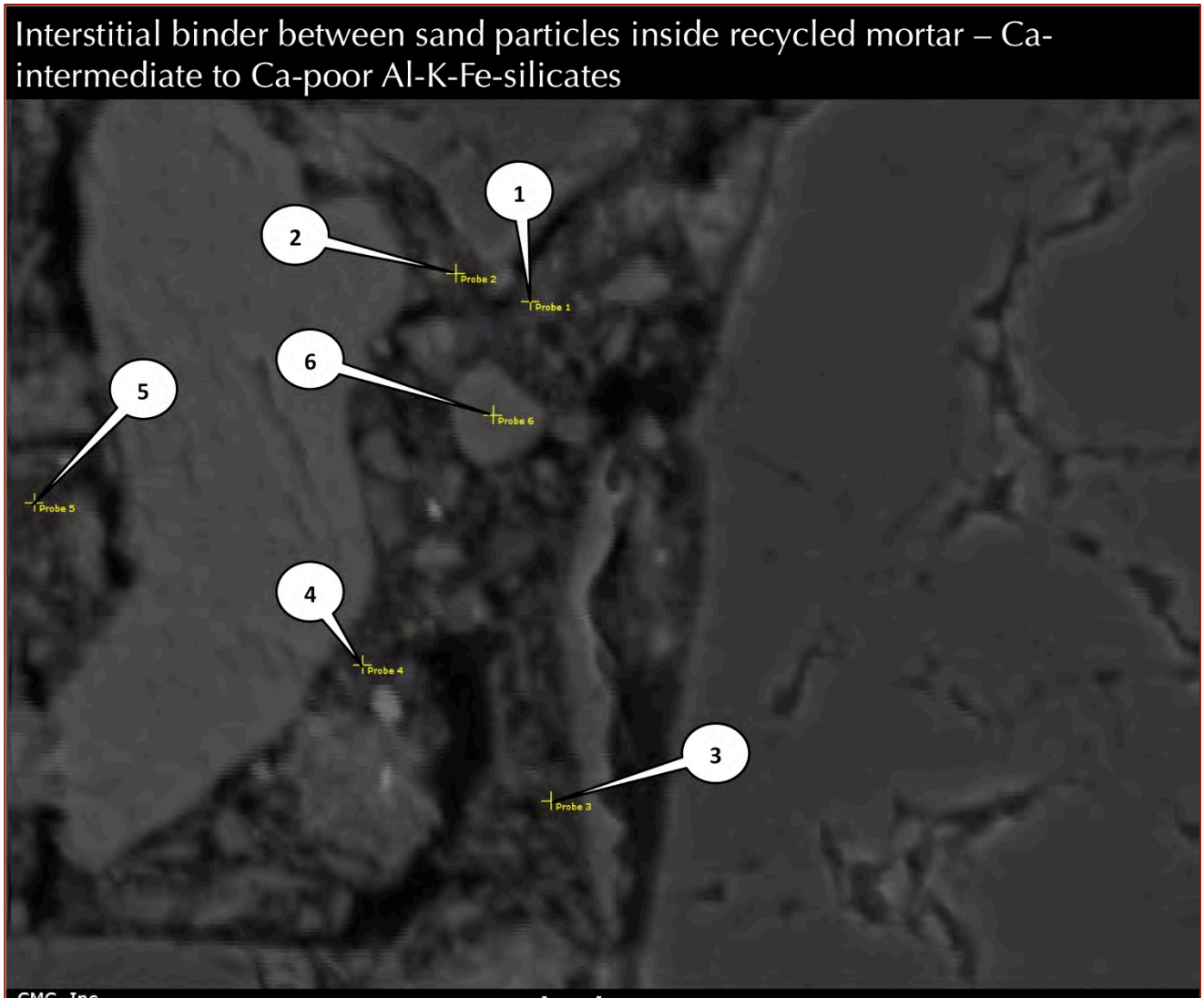

Probe	CaO	SiO2	Al2O3	Na2O	MgO	SO3	K2O	TiO2	FeO	Total	Phase	Paste Cl
1	4.23	56.04	14.87	0.16	0.38	0.00	4.01	0.50	2.35	100.00	Ca-poor Al-K-Fe-Silicate	-
2	21.74	55.54	15.15	0.00	0.77	0.00	4.41	0.67	3.87	99.99	Ca-int. Al-K-Fe-Silicate	-
3	1.68	57.05	17.25	0.00	2.45	0.00	6.95	0.20	4.88	99.99	Ca-poor Al-K-Fe-Silicate	-
4	11.99	53.03	18.63	0.09	0.29	0.00	14.35	2.25	3.28	100.00	Ca-int. Al-K-Fe-Silicate	-
5	3.08	57.28	21.22	1.02	1.92	0.00	10.06	0.01	6.51	100.00	Ca-poor Al-K-Fe-Silicate	-
6	0.86	54.11	15.60	0.05	0.06	0.00	25.97	0.54	1.18	100.01	Ca-poor Al-K-Fe-Silicate	-

Figure 32: BSE image (top) and EDS elemental analyses of various points on the BSE image (bottom) showing compositional variations within the recycled mortar fragment shown in Figure 31.

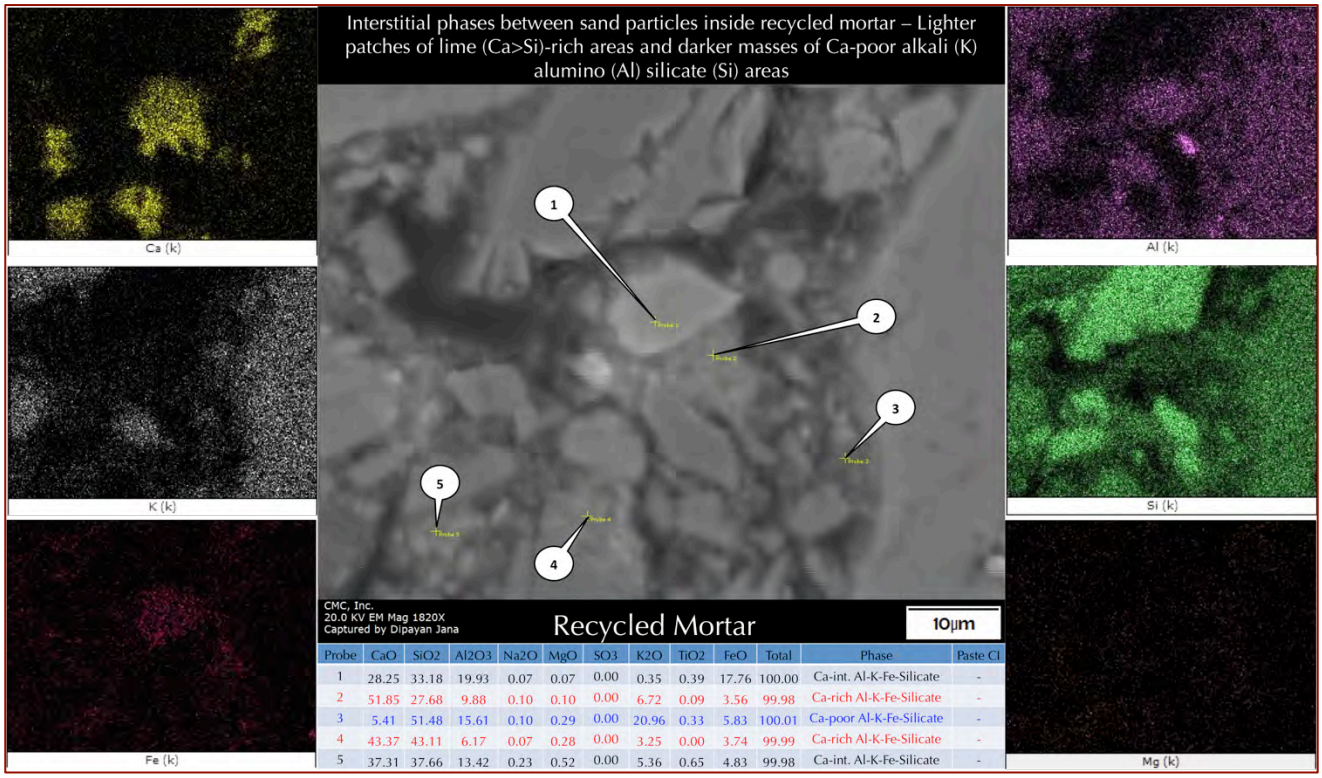

Probe	CaO	SiO2	Al2O3	Na2O	MgO	SO3	K2O	TiO2	FeO	Total	Phase	Paste Cl
1	28.25	33.18	19.93	0.07	0.07	0.00	0.35	0.39	17.76	100.00	Ca-int. Al-K-Fe-Silicate	-
2	51.85	27.68	9.88	0.10	0.10	0.00	6.72	0.09	3.56	99.98	Ca-rich Al-K-Fe-Silicate	-
3	5.41	51.48	15.61	0.10	0.29	0.00	20.96	0.33	5.83	100.01	Ca-poor Al-K-Fe-Silicate	-
4	43.37	43.11	6.17	0.07	0.28	0.00	3.25	0.00	3.74	99.99	Ca-rich Al-K-Fe-Silicate	-
5	37.31	37.66	13.42	0.23	0.52	0.00	5.36	0.65	4.83	99.98	Ca-int. Al-K-Fe-Silicate	-

Figure 33: Backscatter electron (BSE) image, X-ray elemental map, and EDS elemental analyses of various points on the BSE image showing compositional variations within a recycled mortar fragment.

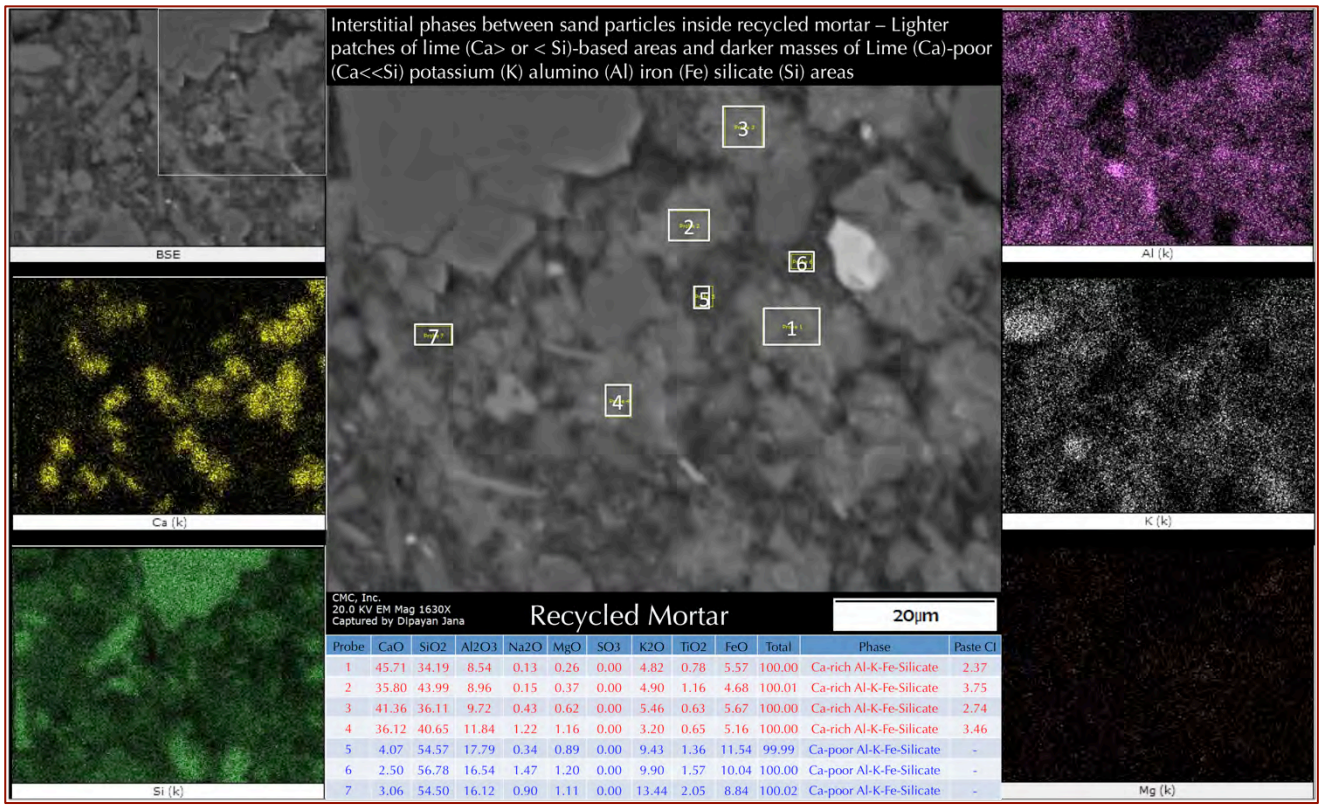

Probe	CaO	SiO2	Al2O3	Na2O	MgO	SO3	K2O	TiO2	FeO	Total	Phase	Paste Cl
1	45.71	34.19	8.54	0.13	0.26	0.00	4.82	0.78	5.57	100.00	Ca-rich Al-K-Fe-Silicate	2.37
2	35.80	43.99	8.96	0.15	0.37	0.00	4.90	1.16	4.68	100.01	Ca-rich Al-K-Fe-Silicate	3.75
3	41.36	36.11	9.72	0.43	0.62	0.00	5.46	0.63	5.67	100.00	Ca-rich Al-K-Fe-Silicate	2.74
4	36.12	40.65	11.84	1.22	1.16	0.00	3.20	0.65	5.16	100.00	Ca-rich Al-K-Fe-Silicate	3.46
5	4.07	54.57	17.79	0.34	0.89	0.00	9.43	1.36	11.54	99.99	Ca-poor Al-K-Fe-Silicate	-
6	2.50	56.78	16.54	1.47	1.20	0.00	9.90	1.57	10.04	100.00	Ca-poor Al-K-Fe-Silicate	-
7	3.06	54.50	16.12	0.90	1.11	0.00	13.44	2.05	8.84	100.02	Ca-poor Al-K-Fe-Silicate	-

Figure 34: Backscatter electron (BSE) image, X-ray elemental map, and EDS elemental analyses of various boxed areas on the BSE image showing compositional variations within a recycled mortar fragment.

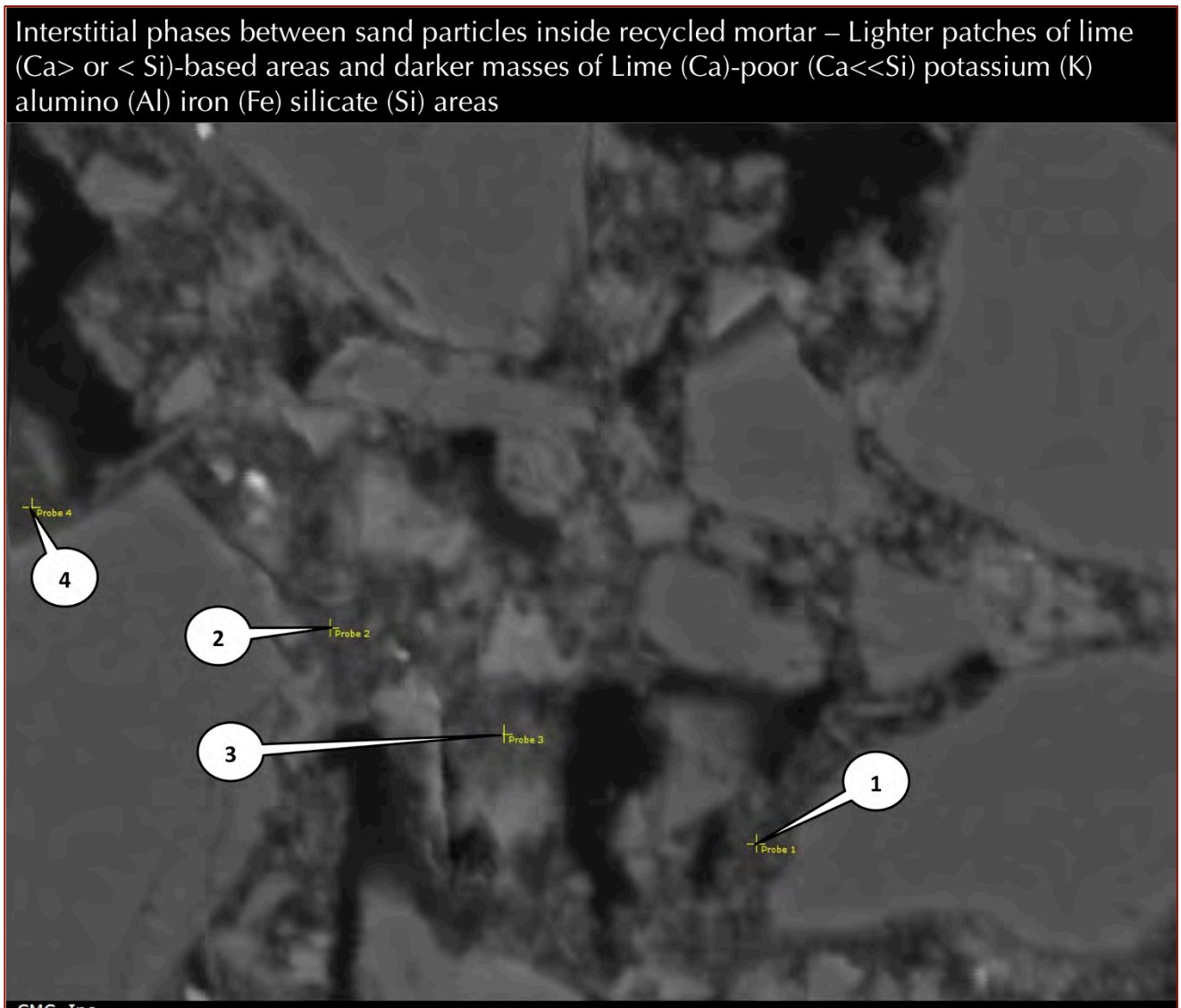

Probe	CaO	SiO2	Al2O3	Na2O	MgO	SO3	K2O	TiO2	FeO	Total	Phase	Paste Cl
1	1.62	89.19	4.78	0.00	0.35	0.00	2.47	0.44	1.15	100.00	Ca-poor Al-K-Fe-Silicate	-
2	3.42	59.86	17.54	0.49	0.50	0.00	10.70	0.58	6.89	99.98	Ca-poor Al-K-Fe-Silicate	-
3	4.54	66.05	15.97	0.11	0.71	0.00	6.66	1.43	4.53	100.00	Ca-poor Al-K-Fe-Silicate	-
4	1.36	76.15	11.38	0.18	0.60	0.01	4.16	0.64	5.52	99.99	Ca-poor Al-K-Fe-Silicate	-

Figure 35: BSE image (top) and EDS elemental analyses of various points on the BSE image (bottom) showing compositional variations within the recycled mortar fragment shown in Figure 34.

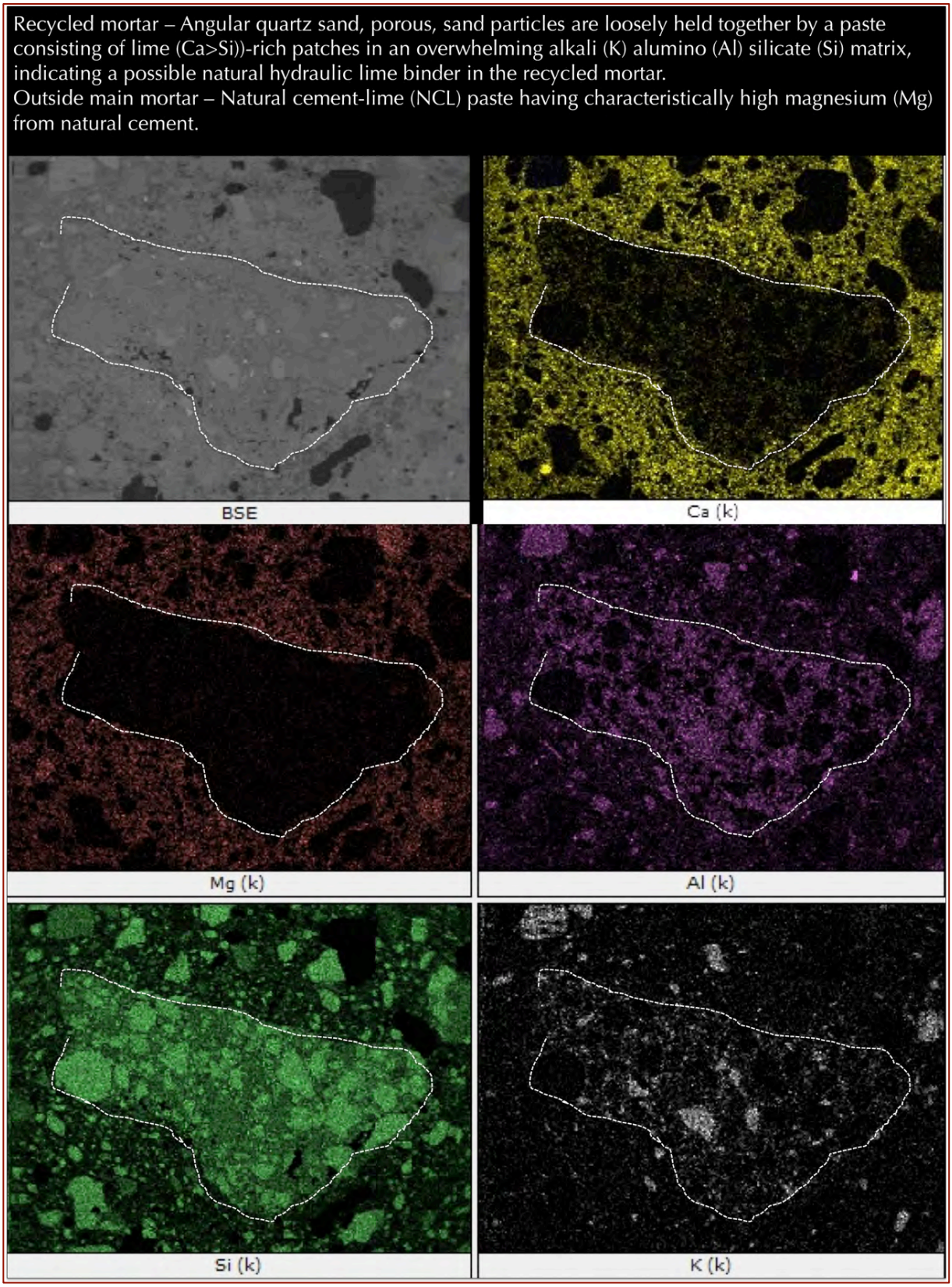

Figure 36: BSE image (top left), and X-ray elemental map (rest) showing compositional variations within a recycled mortar fragment within the white dashed line, and the outside main natural cement-lime mortar.

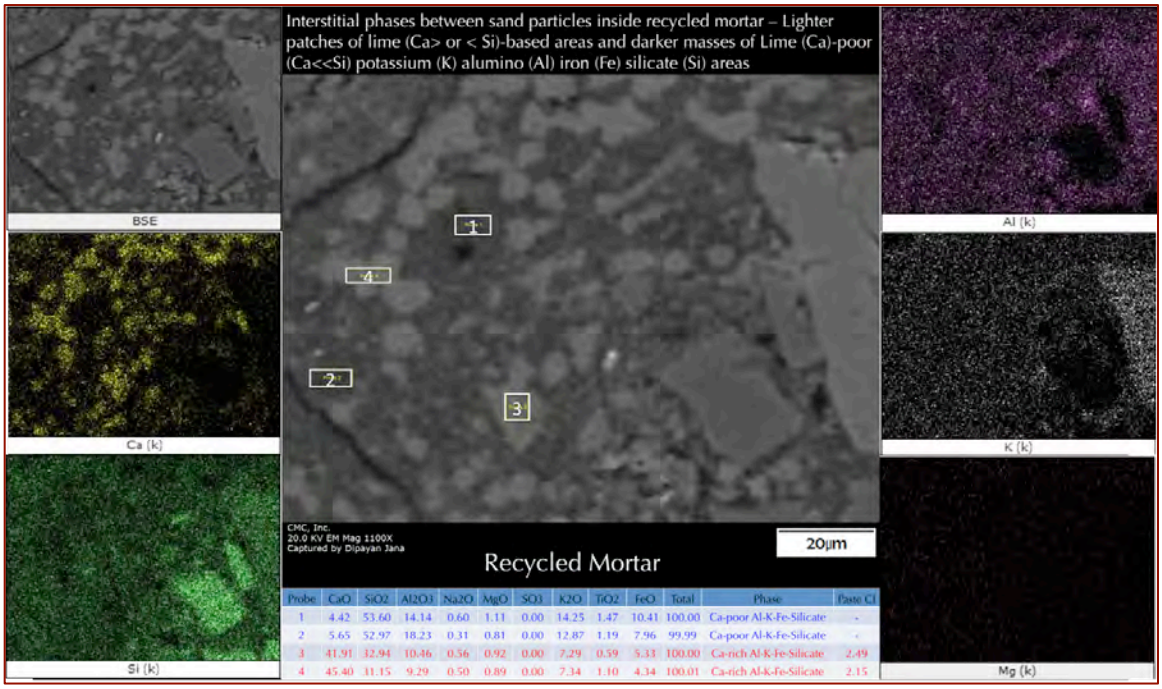

Figure 37: Backscatter electron (BSE) image, X-ray elemental map, and EDS elemental analyses of various boxed areas on the BSE image showing compositional variations within a recycled mortar fragment shown in Figure 36.

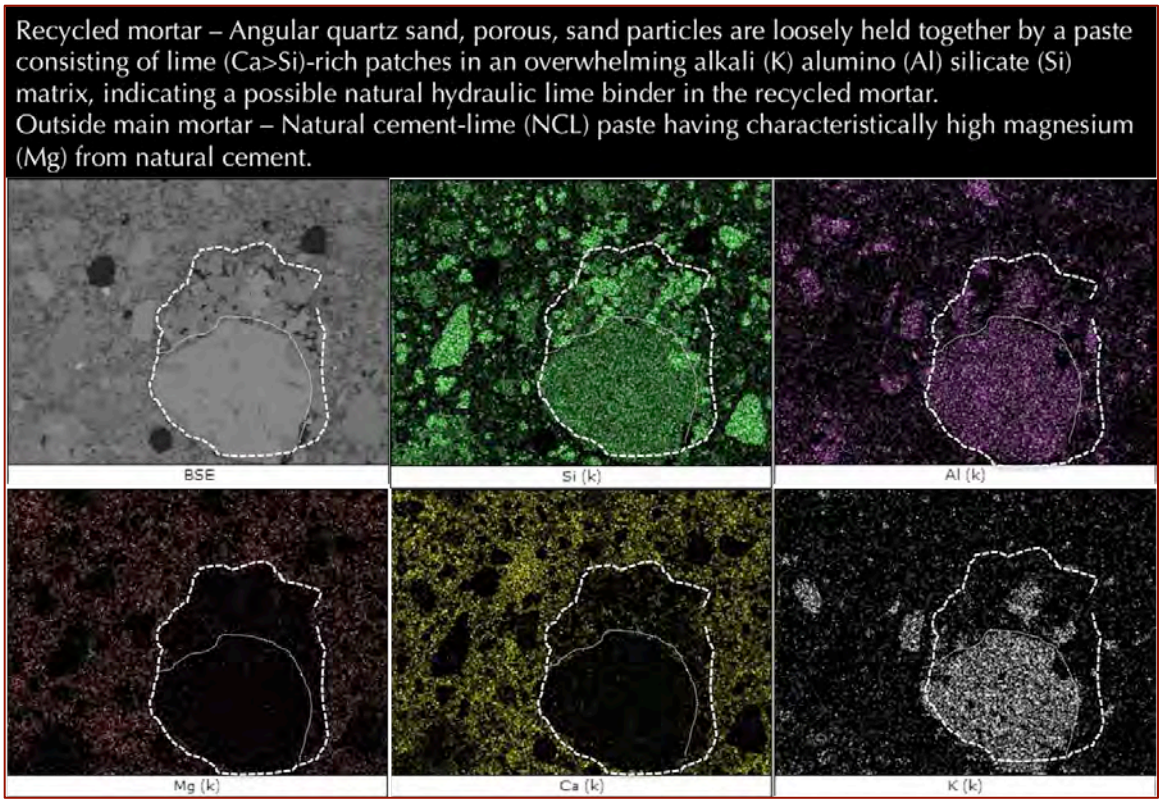

Figure 38: BSE image (top left), and X-ray elemental map (rest) showing compositional variations within a recycled mortar fragment within the white dashed line (with a large K-feldspar as shown by Al-Si-K maps), and the outside host natural cement-lime mortar.

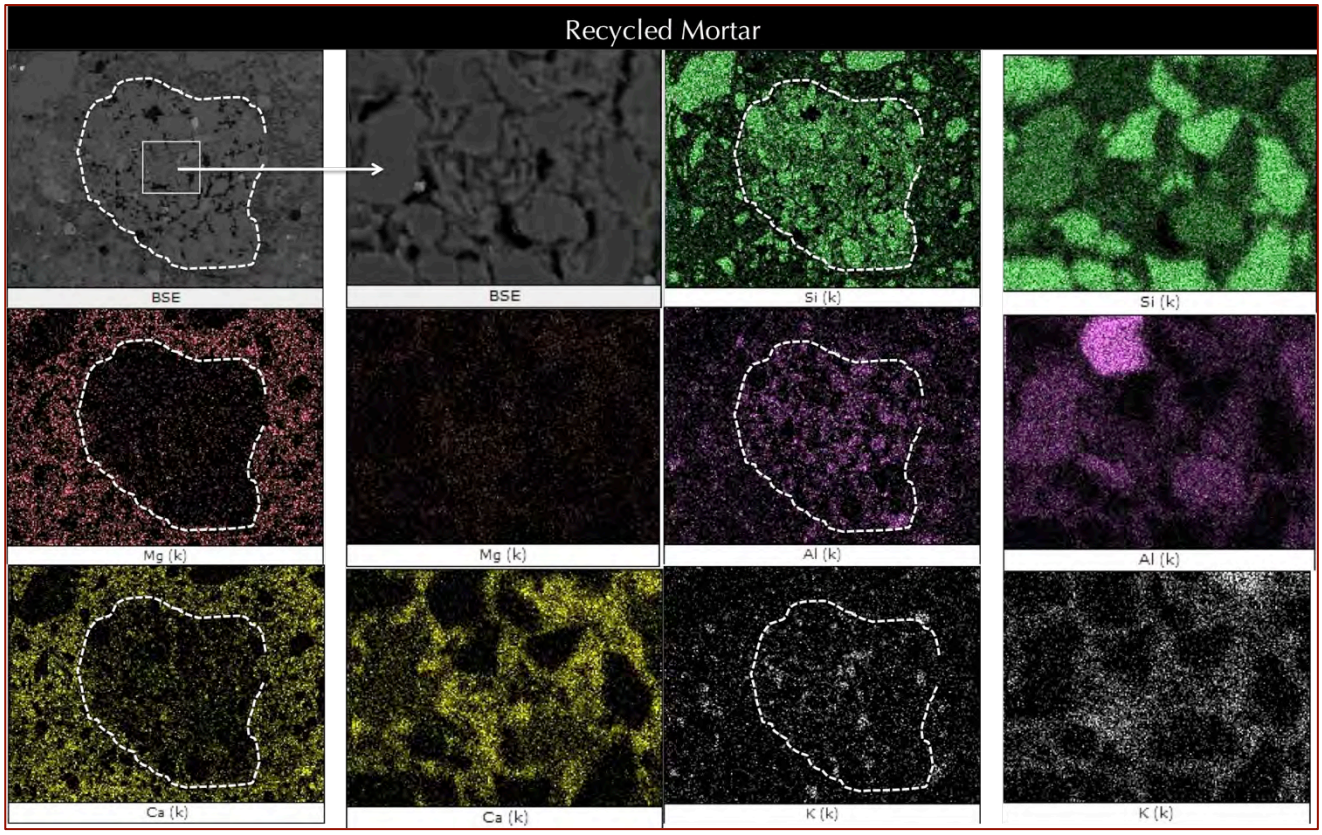

Figure 39: BSE image (top left), and X-ray elemental map (rest) showing compositional variations within a recycled mortar fragment within the white dashed line, and the outside main natural cement-lime mortar. For each elemental map, the corresponding map on right shows the interior of the recycled mortar within the boxed area marked on the BSE image of the recycled mortar. Notice in this and all previous X-ray images of interiors of recycled mortars the K-Al-Si compositions occur as the overwhelming matrix within the recycled mortar where lime occurs as isolated patches of areas having Ca-Al-K-Fe silicate hydrates (e.g., see Figures 33, 34, 37, etc. for lime patches), similar to the patches of bright lime-rich areas seen in the thin section photomicrograph of interior of a recycled mortar in Figure 18. Compared to the host natural cement-lime mortar, the central recycled mortar fragment shows clear enrichments in alkalis and alumina and silica, and, depletion in magnesia and lime.

Figure 40 summarizes compositional variations of recycled mortar fragments amongst three detectable components:

(a) A calcium-rich Al-K-Fe-silicate (red diamonds) from lime,

(b) A calcium-poor Al-K-Fe-silicate (blue squares) from a hydraulic component, and,

(c) An intermediate calcium Al-K-Fe-silicate (black triangles), which is probably the mixture of two end members of lime-rich and lime-poor components.

Oxide compositional variations clearly show a trend between the two end member (lime-rich and lime-poor) components, which is similar to the trends of compositional variations of pastes of a natural hydraulic lime mortar having lime-rich and lime-poor silica-rich components.

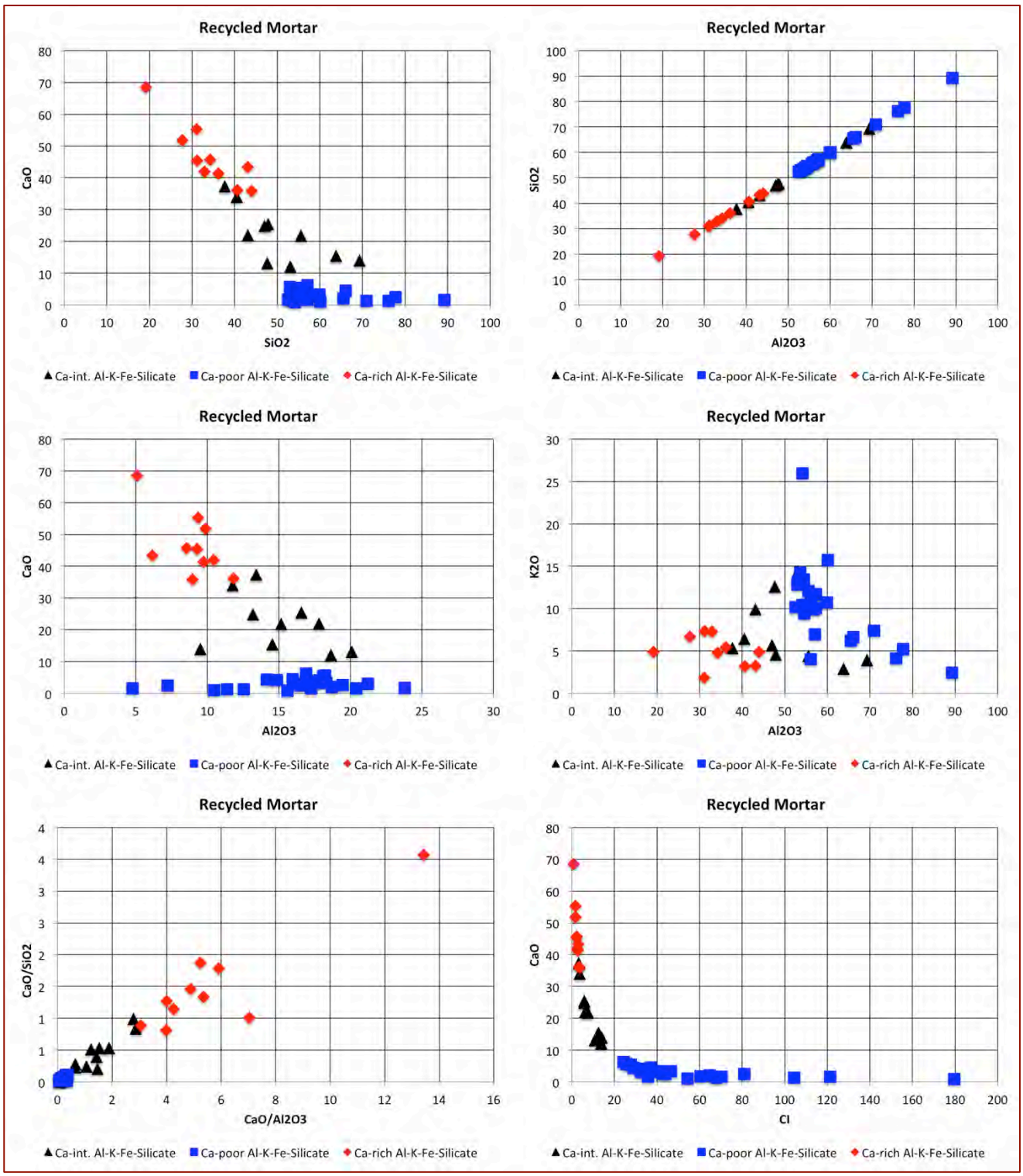

Figure 40: Compositional variations of recycled mortars amongst three detectable main components: (a) a calcium-rich Al-K-Fe-silicate (red diamonds) from lime, (b) a calcium-poor Al-K-Fe-silicate (blue squares) from a hydraulic component, and, (c) an intermediate calcium Al-K-Fe-silicate (black triangles), which is probably the mixture of two end members of lime-rich and lime-poor components. Oxide compositional variations clearly show a trend between the two end member (lime-rich and lime-poor) components.

Natural Cement – Lime Paste

Compositional variations of natural cement – lime paste: (a) Lime-rich areas (Ca-rich Mg-Al-Fe-silicate) of paste (light gray); (b) lime-poor, magnesia-rich areas (Ca-poor Mg-Al-Fe-silicate hydrate) of paste (dark gray); and (c) intermediate lime-magnesia areas – showing compositions from lime-rich to magnesia-rich silicate hydrates

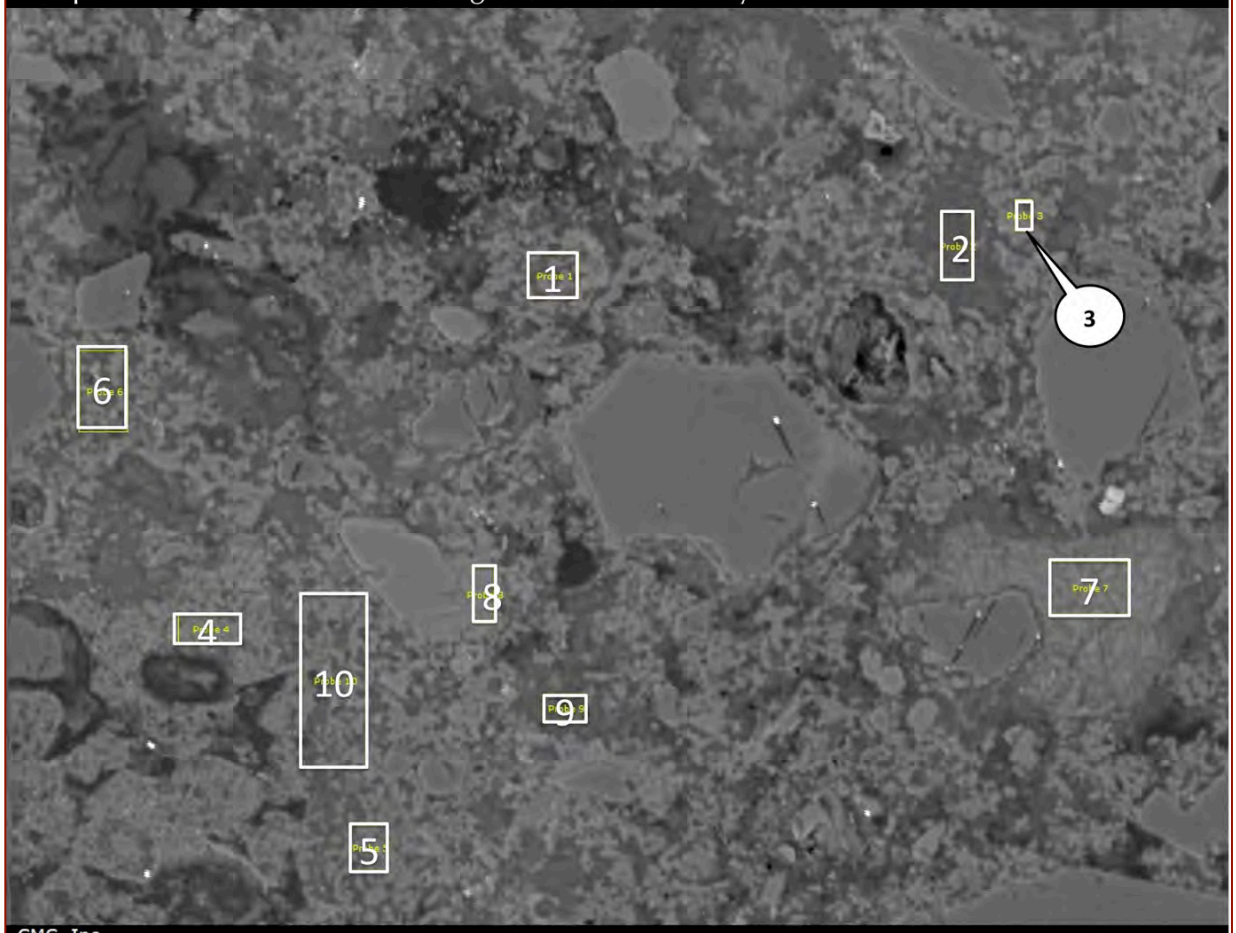

Probe	CaO	SiO2	Al2O3	Na2O	MgO	SO3	K2O	TiO2	FeO	Total	Phase	Paste Cl
1	45.54	32.49	8.37	0.05	8.40	0.00	0.71	0.59	3.85	100.00	Ca-rich Mg-Al-Fe-Silicate	1.80
2	4.18	58.02	16.03	0.00	20.77	0.00	0.16	0.03	0.80	99.99	Ca-poor Mg-Al-Fe-Silicate	5.43
3	25.05	47.80	10.94	0.21	6.58	0.00	6.77	0.15	2.50	100.00	Si>Ca>Al-Mg-Silicate	4.31
4	60.26	15.22	3.60	0.36	6.87	0.00	0.84	0.27	12.59	100.01	Ca-rich Mg-Al-Fe-Silicate	0.79
5	46.66	29.76	7.50	0.05	11.61	0.00	1.15	0.00	3.27	100.00	Ca-rich Mg-Al-Fe-Silicate	1.49
6	40.13	37.44	7.34	0.21	9.19	0.00	1.03	1.29	3.37	100.00	Ca-rich Mg-Al-Fe-Silicate	2.17
7	57.88	16.17	4.15	0.09	9.81	0.00	1.28	1.70	8.92	100.00	Ca-rich Mg-Al-Fe-Silicate	0.78
8	46.18	29.78	9.19	0.22	0.95	0.00	8.62	0.80	4.25	99.99	Ca>Si>Al>K>Fe Paste	2.03
9	9.83	57.42	14.52	0.45	12.44	0.00	0.11	0.50	4.72	99.99	Ca-poor Mg-Al-Fe-Silicate	6.61
10	38.17	31.64	10.89	0.12	11.10	0.00	0.53	0.03	7.53	100.01	Ca-rich Mg-Al-Fe-Silicate	1.97

Figure 41: BSE image (top) and EDS elemental analyses of various areas on the BSE image (bottom) showing compositional variations within the natural cement-lime paste.

Compositional variations of natural cement – lime paste: (a) Lime-rich areas (Ca-rich Mg-Al-Fe-silicate) of paste (light gray); (b) lime-poor, magnesia-rich areas (Ca-poor Mg-Al-Fe-silicate hydrate) of paste (dark gray); and (c) intermediate lime-magnesia areas – showing compositions from lime-rich to magnesia-rich silicate hydrates

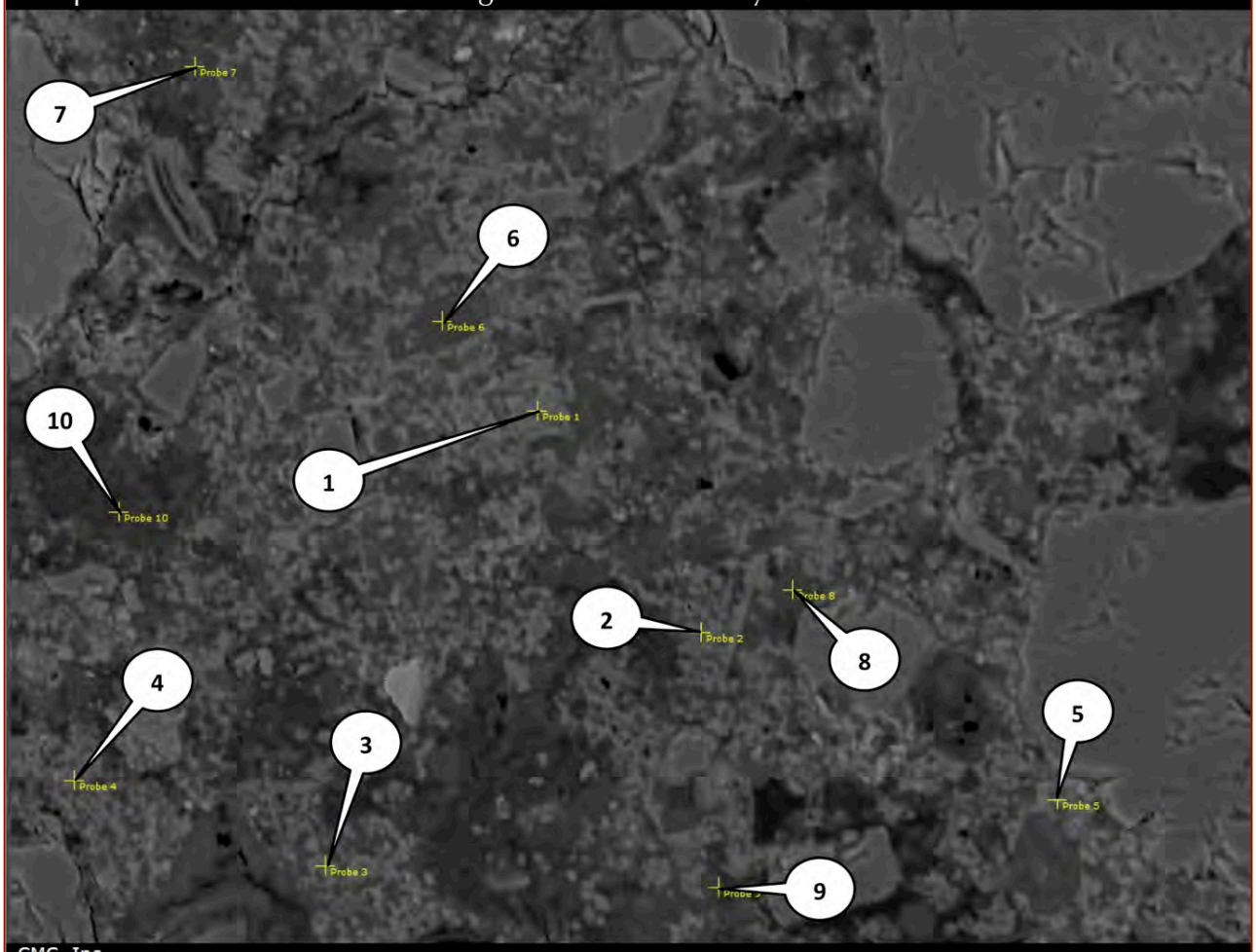

Probe	CaO	SiO2	Al2O3	Na2O	MgO	SO3	K2O	TiO2	FeO	Total	Phase	Paste Cl
1	9.41	69.69	14.94	2.41	0.47	0.00	2.29	0.19	0.60	100.00	Ca-Al-Silicate	21.06
2	78.54	12.55	1.83	0.02	3.76	0.00	0.71	0.00	2.58	99.99	Ca-rich Mg-Al-Fe-Silicate	0.46
3	81.03	10.77	1.81	0.04	3.56	0.00	0.59	0.17	2.04	100.01	Ca-rich Mg-Al-Fe-Silicate	0.39
4	69.64	16.24	2.66	0.06	7.42	0.00	0.20	0.00	3.77	99.99	Ca-rich Mg-Al-Fe-Silicate	0.64
5	48.52	21.97	9.94	0.00	11.73	0.00	0.71	0.11	7.02	100.00	Ca-rich Mg-Al-Fe-Silicate	1.19
6	14.29	36.00	16.78	0.00	24.22	0.00	0.43	0.00	8.27	99.99	Ca-poor Mg-Al-Fe-Silicate	2.59
7	3.09	66.24	12.38	0.17	14.60	0.00	1.00	0.00	2.51	99.99	Ca-poor Mg-Al-Fe-Silicate	8.54
8	5.63	71.95	16.14	1.32	2.80	0.00	0.73	0.08	1.35	100.00	Ca-Al-Silicate	23.05
9	18.35	53.44	9.69	0.20	13.54	0.00	0.27	0.00	4.51	100.00	Ca-poor Mg-Al-Fe-Silicate	4.38
10	17.92	39.92	13.90	0.00	19.63	0.00	0.66	0.29	7.68	100.00	Ca-poor Mg-Al-Fe-Silicate	2.92

Figure 42: BSE image (top) and EDS elemental analyses of various points on the BSE image (bottom) showing compositional variations within the natural cement-lime paste.

Compositional variations of natural cement – lime paste: (a) Lime-rich areas (Ca-rich Mg-Al-Fe-silicate) of paste (light gray); (b) lime-poor, magnesia-rich areas (Ca-poor Mg-Al-Fe-silicate hydrate) of paste (dark gray); and (c) intermediate lime-magnesia areas – showing compositions from lime-rich to magnesia-rich silicate hydrates

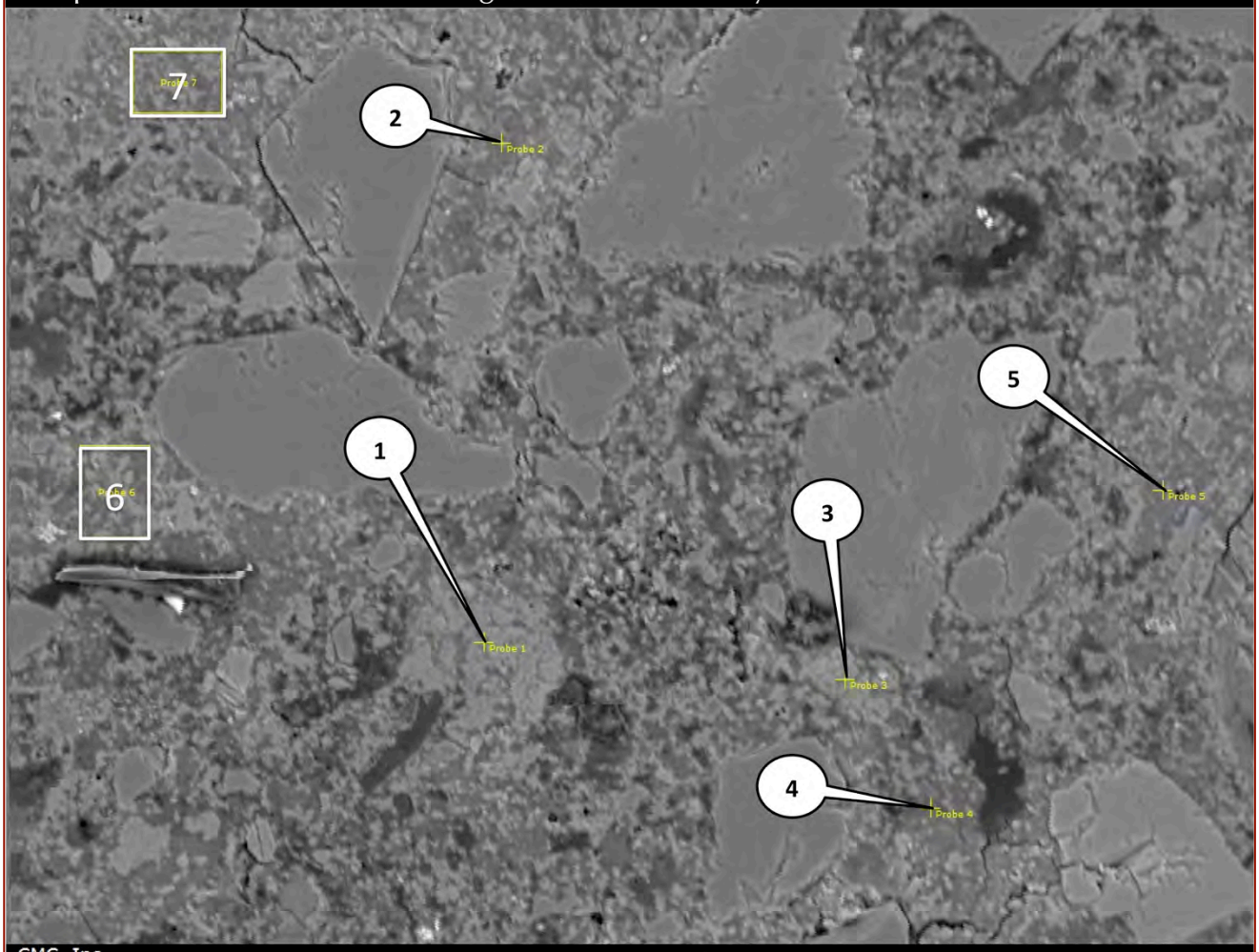

Probe	CaO	SiO2	Al2O3	Na2O	MgO	SO3	K2O	TiO2	FeO	Total	Phase	Paste CI
1	77.53	8.36	1.22	0.00	7.56	0.00	0.07	0.00	5.26	100.00	Ca-rich Mg-Al-Fe-Silicate	0.32
2	20.93	50.65	8.43	0.14	13.88	0.00	0.65	0.21	5.12	100.01	Ca-poor Mg-Al-Fe-Silicate	3.83
3	75.00	6.47	2.65	0.00	8.78	0.00	0.61	0.36	6.12	99.99	Ca-rich Mg-Al-Fe-Silicate	0.29
4	16.14	49.56	11.61	0.13	14.05	0.00	0.29	0.58	7.64	100.00	Ca-poor Mg-Al-Fe-Silicate	4.38
5	13.12	57.06	9.16	0.21	11.54	0.00	0.55	1.19	7.16	99.99	Ca-poor Mg-Al-Fe-Silicate	5.97
6	37.64	37.71	6.92	0.07	11.82	0.00	0.68	0.77	4.40	100.01	Ca-Mg-Al-Silicate	2.15
7	41.27	35.72	6.96	0.18	10.57	0.00	1.13	0.00	4.16	99.99	Ca-Mg-Al-Silicate	1.97

Figure 43: BSE image (top) and EDS elemental analyses of various points and areas on the BSE image (bottom) showing compositional variations within the natural cement-lime paste.

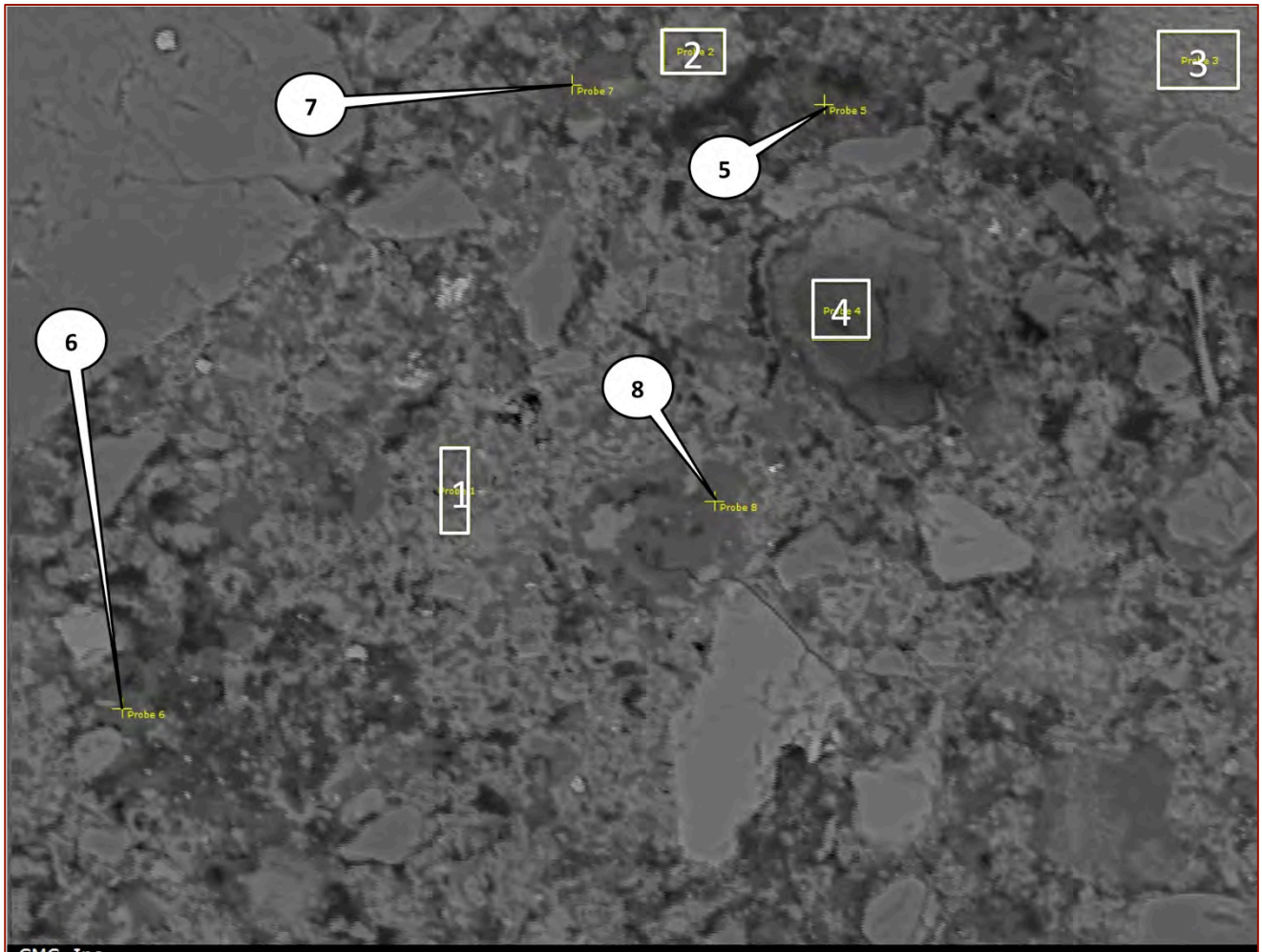

Probe	CaO	SiO2	Al2O3	Na2O	MgO	SO3	K2O	TiO2	FeO	Total	Phase	Paste CI
1	48.44	29.04	6.28	0.04	11.87	0.00	0.98	0.00	3.34	99.99	Ca-rich Mg-Al-Fe-Silicate	1.39
2	64.15	16.13	3.33	0.29	7.96	0.00	0.88	0.16	7.10	100.00	Ca-rich Mg-Al-Fe-Silicate	0.71
3	70.24	8.23	2.72	0.00	10.00	0.00	0.56	0.57	7.68	100.00	Ca-rich Mg-Al-Fe-Silicate	0.37
4	3.55	71.12	1.35	0.51	20.83	0.01	1.96	0.29	0.38	100.00	Ca-poor Mg-Al-Fe-Silicate	6.14
5	12.49	41.80	8.13	0.31	20.38	0.00	0.83	0.65	15.41	100.00	Ca-poor Mg-Al-Fe-Silicate	3.33
6	3.85	57.88	9.55	0.22	16.45	0.00	0.51	0.80	10.74	100.00	Ca-poor Mg-Al-Fe-Silicate	6.70
7	0.98	32.59	6.71	0.18	35.62	0.18	12.84	3.80	7.09	99.99	Ca-poor Mg-Al-Fe-Silicate	2.04
8	1.85	67.77	5.05	0.42	13.45	0.01	0.04	0.18	11.23	100.00	Ca-poor Mg-Al-Fe-Silicate	9.82

Figure 44: BSE image (top) and EDS elemental analyses of various points and areas on the BSE image (bottom) showing compositional variations within the natural cement-lime paste.

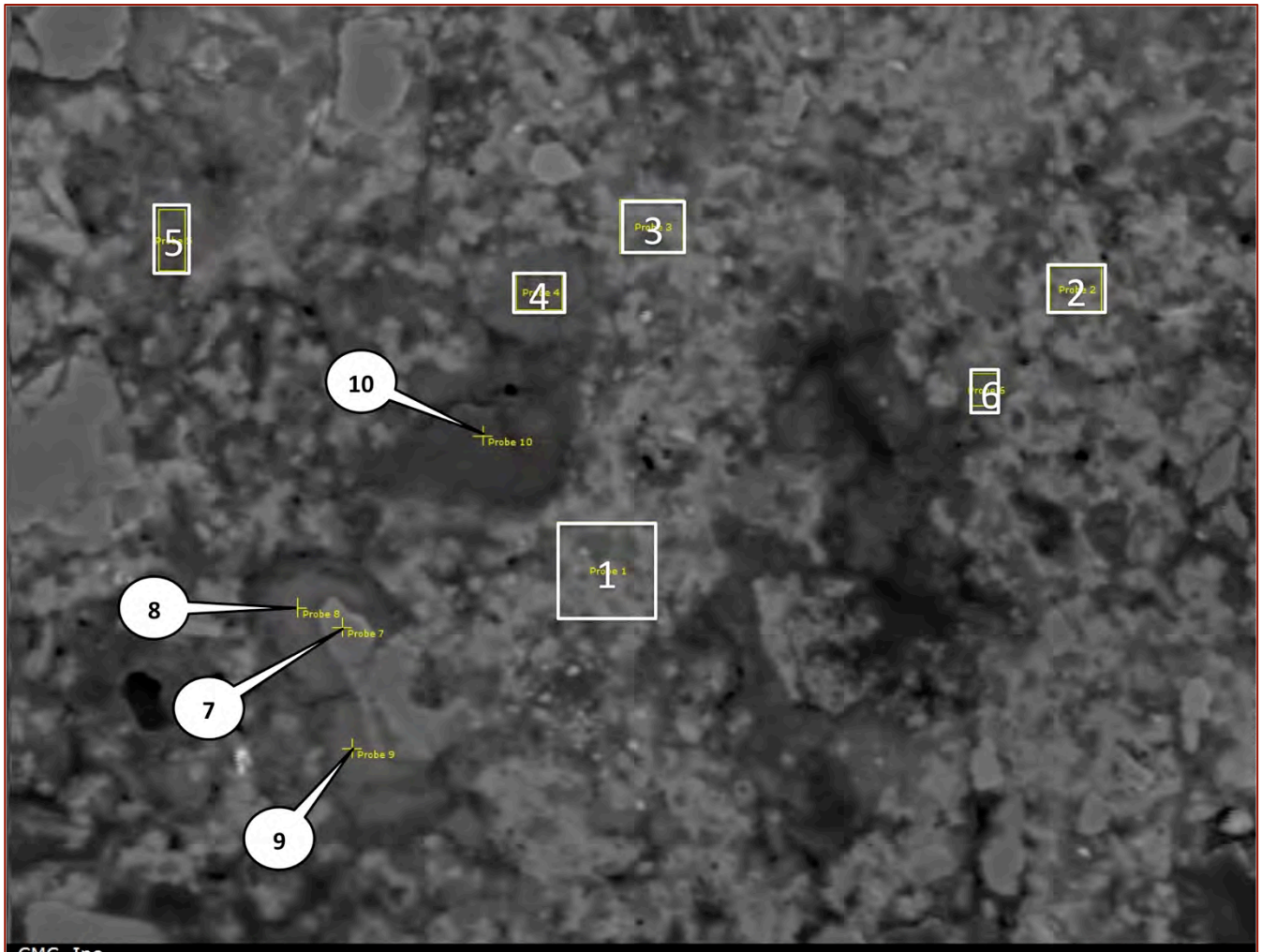

Probe	CaO	SiO2	Al2O3	Na2O	MgO	SO3	K2O	TiO2	FeO	Total	Phase	Paste Cl
1	53.56	20.96	5.19	0.00	13.39	0.00	1.02	0.15	5.73	100.00	Ca-rich Mg-Al-Fe-Silicate	0.95
2	61.75	15.50	4.99	0.00	10.64	0.00	0.94	0.77	5.40	99.99	Ca-rich Mg-Al-Fe-Silicate	0.69
3	53.10	21.69	5.41	0.00	10.61	0.00	2.07	1.34	5.78	100.00	Ca-rich Mg-Al-Fe-Silicate	1.04
4	6.83	63.74	9.58	0.35	8.44	0.00	1.80	0.00	9.25	99.99	Ca-poor Mg-Al-Fe-Silicate	10.48
5	6.43	57.75	11.96	0.20	12.58	0.00	1.08	0.53	9.46	99.99	Ca-poor Mg-Al-Fe-Silicate	7.55
6	11.28	55.40	9.42	0.10	17.67	0.00	0.39	0.17	5.57	100.00	Si>Ca>Mg>Al>Fe Paste	4.70
7	27.08	49.56	6.13	0.05	10.45	0.00	0.69	0.49	5.55	100.00	Si>Ca>Mg>Al>Fe Paste	3.58
8	2.69	68.14	10.16	0.16	15.47	0.00	1.19	0.55	1.65	100.01	Ca-poor Mg-Al-Fe-Silicate	8.34
9	2.54	68.26	8.61	0.00	17.06	0.00	1.66	0.08	1.79	100.00	Ca-poor Mg-Al-Fe-Silicate	7.64
10	0.71	62.50	13.59	0.00	12.78	0.00	0.23	0.10	10.08	99.99	Ca-poor Mg-Al-Fe-Silicate	10.59

Figure 45: BSE image (top) and EDS elemental analyses of various points and areas on the BSE image (bottom) showing compositional variations within the natural cement-lime paste.

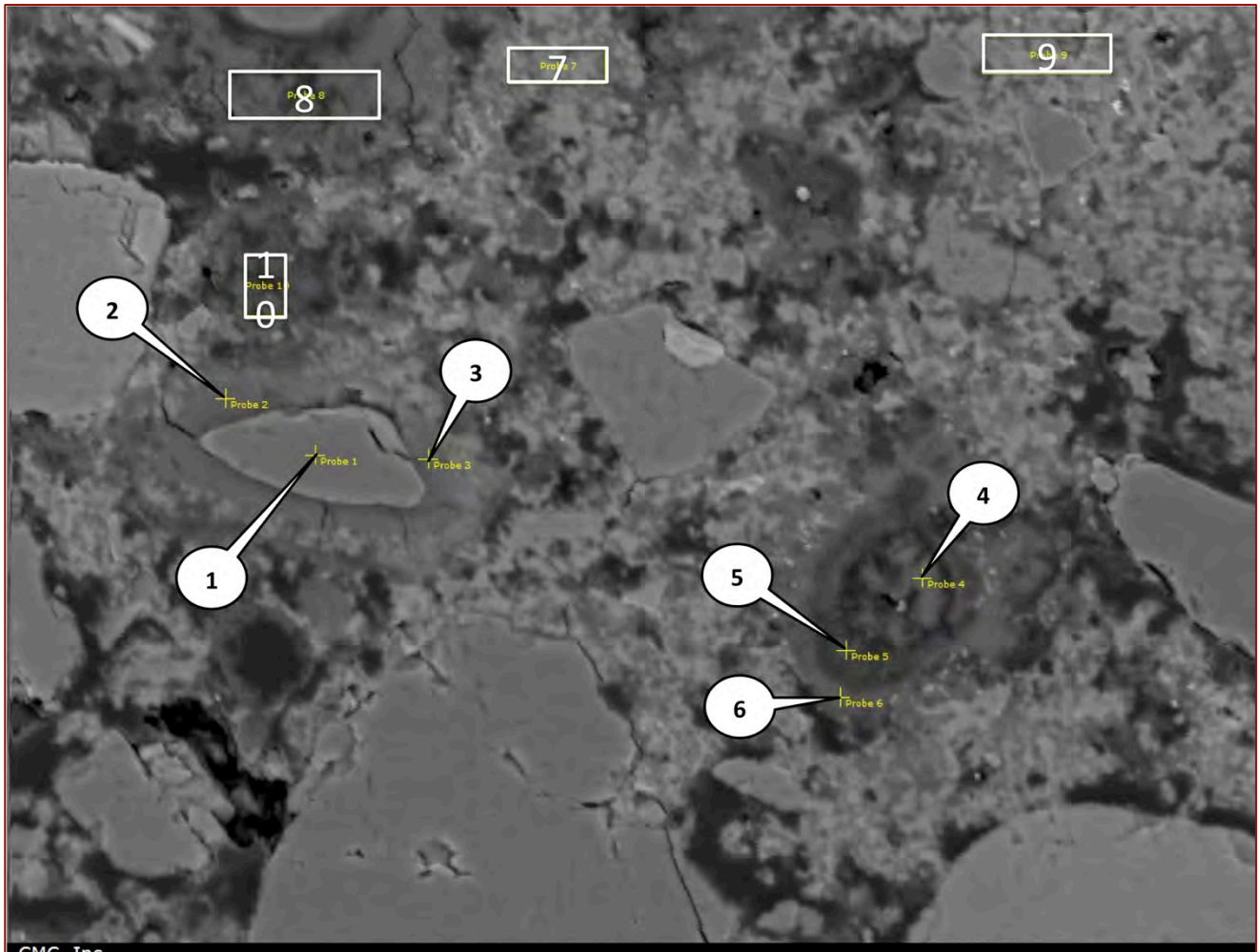

Probe	CaO	SiO2	Al2O3	Na2O	MgO	SO3	K2O	TiO2	FeO	Total	Phase	Paste CI
1	0.00	98.22	1.10	0.00	0.01	0.00	0.04	0.36	0.27	100.00	Quartz	-
2	2.13	72.85	6.36	0.05	14.27	0.00	0.34	0.20	3.80	100.00	Ca-poor Mg-Al-Fe-Silicate	9.66
3	1.80	73.54	5.36	0.35	14.05	0.00	0.89	0.20	3.80	99.99	Ca-poor Mg-Al-Fe-Silicate	9.99
4	1.50	72.35	13.61	0.19	3.64	0.00	7.15	0.33	1.23	100.00	Mg-Al-K-Silicate	-
5	1.74	75.46	10.02	0.17	8.54	0.00	1.52	0.46	2.09	100.00	Ca-poor Mg-Al-Fe-Silicate	16.34
6	1.86	65.18	10.57	0.03	16.52	0.00	1.27	0.46	4.10	99.99	Ca-poor Mg-Al-Fe-Silicate	7.88
7	60.67	19.51	4.37	0.00	9.99	0.00	0.86	0.22	4.37	99.99	Ca-rich Mg-Al-Fe-Silicate	0.84
8	2.03	64.32	7.67	0.24	17.65	0.00	1.94	1.20	4.96	100.01	Ca-poor Mg-Al-Fe-Silicate	7.18
9	73.95	14.45	3.75	0.20	2.93	0.00	0.39	0.38	3.94	99.99	Ca-rich Mg-Al-Fe-Silicate	0.61
10	1.80	57.73	12.07	0.01	15.26	0.01	0.03	2.78	10.30	99.99	Ca-poor Mg-Al-Fe-Silicate	7.86

Figure 46: BSE image (top) and EDS elemental analyses of various points and areas on the BSE image (bottom) showing compositional variations within the natural cement-lime paste.

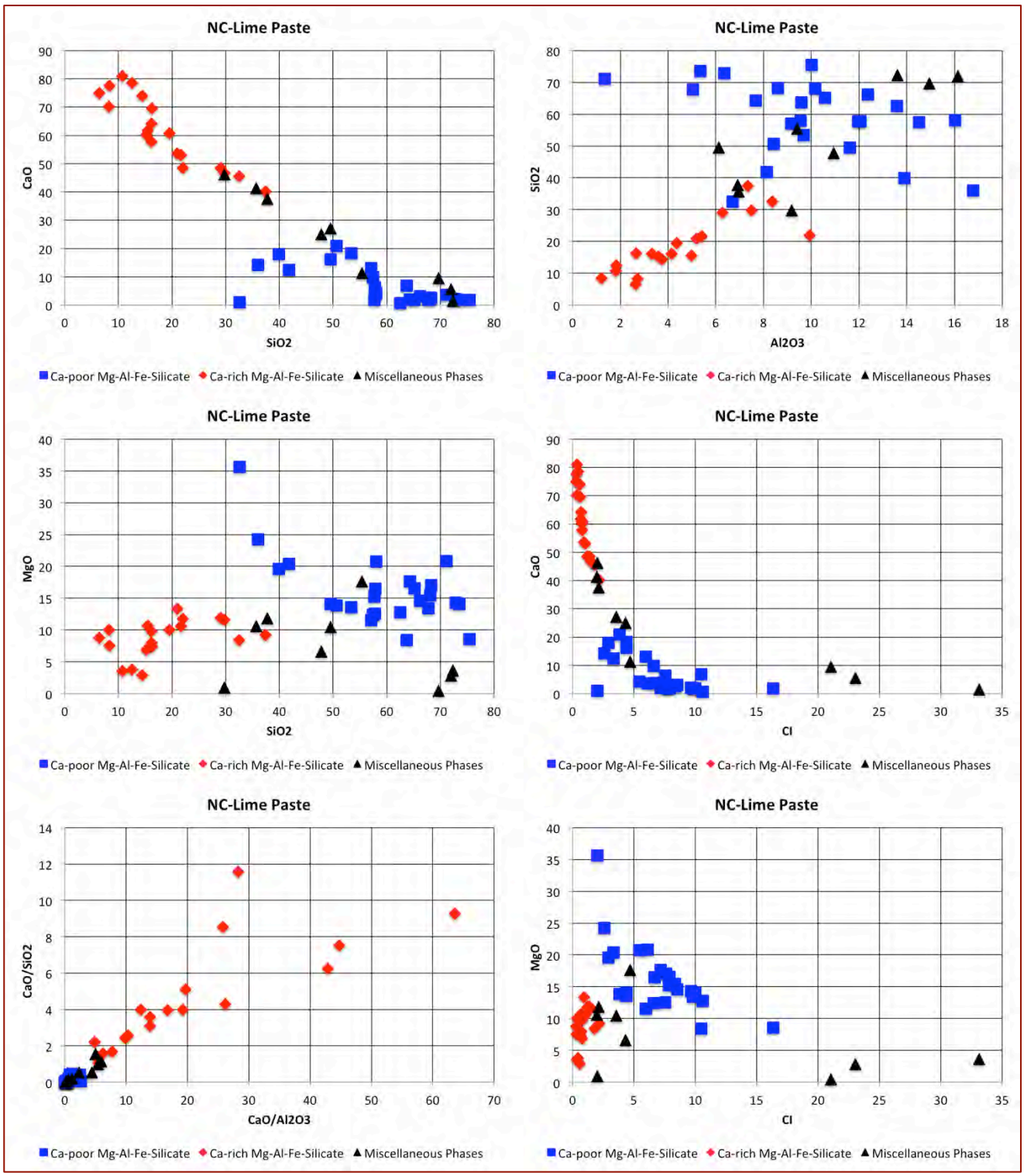

Figure 47: Compositional variations of natural cement-lime paste amongst three detectable components: (a) a calcium-rich Mg-Al-Fe-silicate (red diamonds) from lime, (b) a calcium-poor Mg-Al-Fe -silicate (blue squares) from natural cement, and, (c) a few miscellaneous minor components (black triangles), which is probably the mixture of two end members of lime-rich and lime-poor components. Oxide compositional variations clearly show a mixing-like trend between the two end member (lime-rich and lime-poor) components.

Figure 47 summarizes compositional variations of natural cement-lime paste in the main mortar amongst three detectable components: (a) a calcium-rich Mg-Al-Fe-silicate from lime and natural cement, (b) a calcium-poor to intermediate-calcium Mg-Al-Fe -silicate from natural cement, and, (c) a few miscellaneous minor components, which are probably the mixture of two end members of lime-rich (lime) and lime-poor (natural cement) components. Oxide compositional variations clearly show a trend between the two end member (lime-rich and lime-poor) components, indicating use of lime and natural cement as two separate binders.

Residual Natural Cement Particles

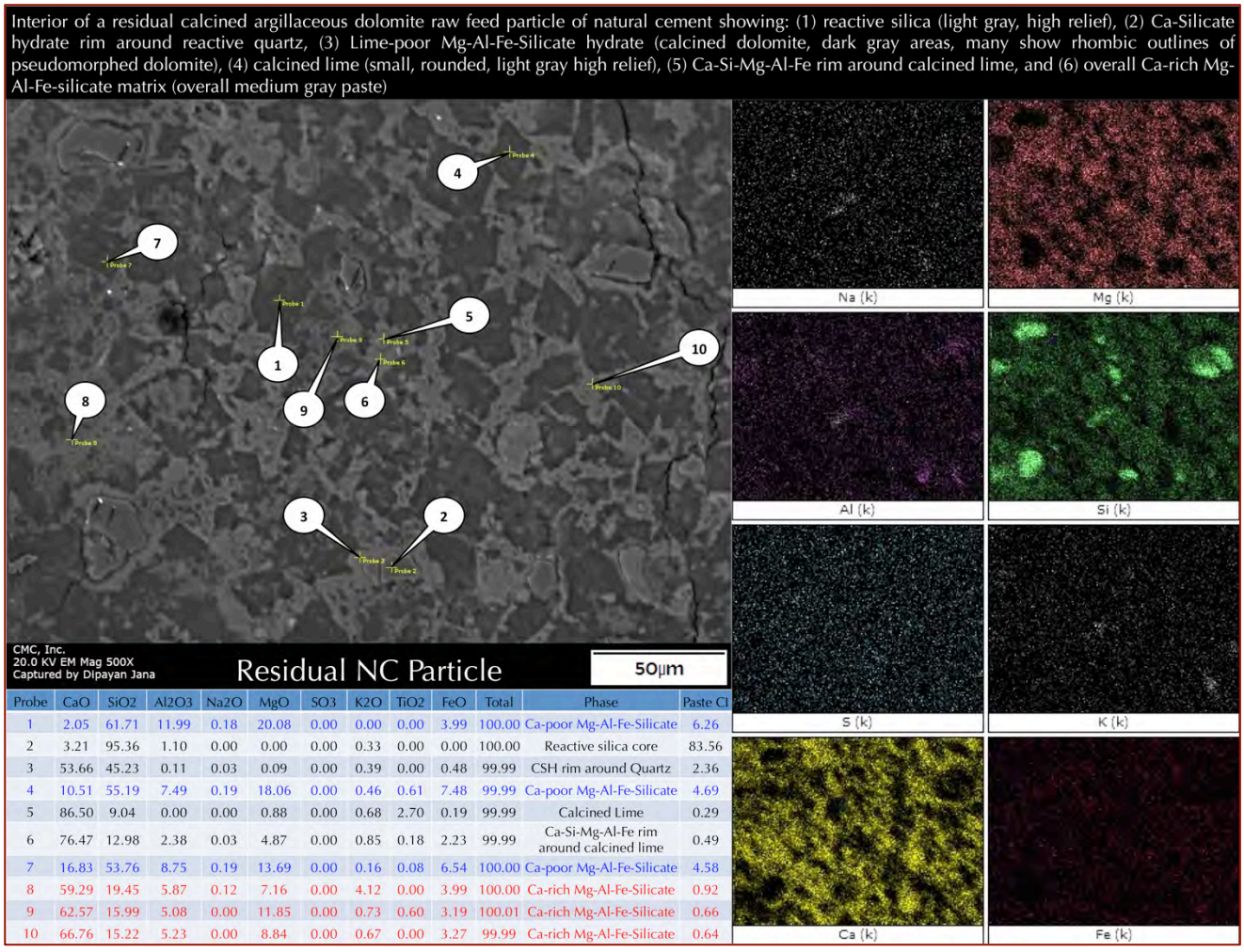

Probe	CaO	SiO2	Al2O3	Na2O	MgO	SO3	K2O	TiO2	FeO	Total	Phase	Paste Cl
1	2.05	61.71	11.99	0.18	20.08	0.00	0.00	0.00	3.99	100.00	Ca-poor Mg-Al-Fe-Silicate	6.26
2	3.21	95.36	1.10	0.00	0.00	0.00	0.33	0.00	0.00	100.00	Reactive silica core	83.56
3	53.66	45.23	0.11	0.03	0.09	0.00	0.39	0.00	0.48	99.99	CSH rim around Quartz	2.36
4	10.51	55.19	7.49	0.19	18.06	0.00	0.46	0.61	7.48	99.99	Ca-poor Mg-Al-Fe-Silicate	4.69
5	86.50	9.04	0.00	0.00	0.88	0.00	0.68	2.70	0.19	99.99	Calcined Lime	0.29
6	76.47	12.98	2.38	0.03	4.87	0.00	0.85	0.18	2.23	99.99	Ca-Si-Mg-Al-Fe rim around calcined lime	0.49
7	16.83	53.76	8.75	0.19	13.69	0.00	0.16	0.08	6.54	100.00	Ca-poor Mg-Al-Fe-Silicate	4.58
8	59.29	19.45	5.87	0.12	7.16	0.00	4.12	0.00	3.99	100.00	Ca-rich Mg-Al-Fe-Silicate	0.92
9	62.57	15.99	5.08	0.00	11.85	0.00	0.73	0.60	3.19	100.01	Ca-rich Mg-Al-Fe-Silicate	0.66
10	66.76	15.22	5.23	0.00	8.84	0.00	0.67	0.00	3.27	99.99	Ca-rich Mg-Al-Fe-Silicate	0.64

Figure 48: Backscatter electron (BSE) image (left), X-ray elemental map (right), and EDS elemental analyses of various points on the BSE image (bottom left) showing compositional variations within a residual natural cement particle from a calcined argillaceous dolomite raw feed. Notice dark rhombic-shaped areas of calcined dolomite grains in the BSE image (having Ca-poor Mg-Al-Fe-silicate composition due to solid state reaction between calcined dolomite and interstitial silica), and interstitial brighter gray areas of Ca-rich Mg-Al-Fe-silicates (and/or Ca-rich Mg-Si-Fe-aluminates).

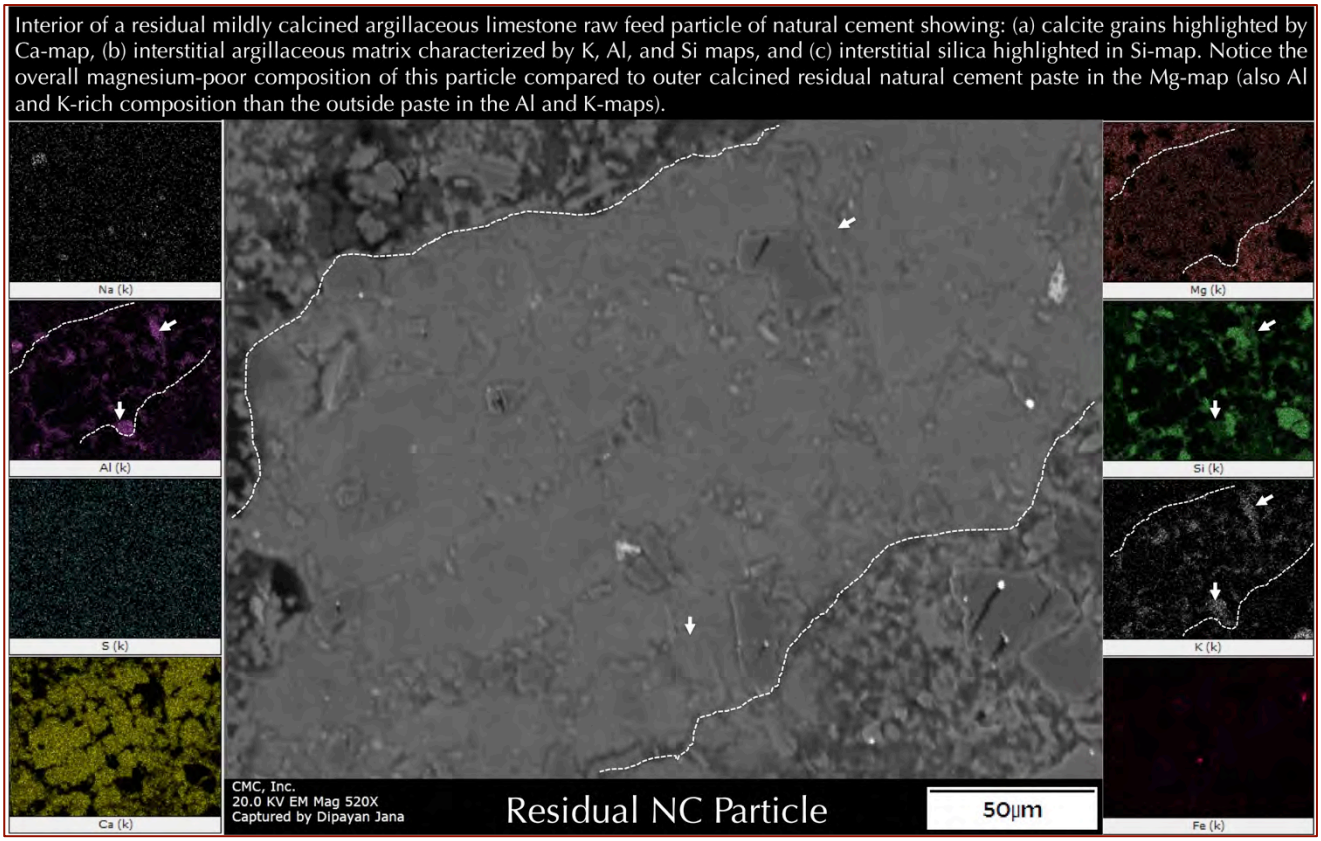

Figure 49: Backscatter electron (BSE) image, and X-ray elemental map showing compositional variations within a residual natural cement particle (marked by dashed white lines in BSE image) and its difference from the outside natural cement-lime paste. Notice the particle has relatively higher lime and lower magnesia than outside, which is indicative of a calcitic limestone particle.

Since the natural cement binder was derived from calcination of various argillaceous limestone and dolomite raw feed, it is anticipated to find many residual, variably calcined particles of raw feed, and many such particles are already identified in the thin section photomicrographs. These SEM-EDS studies in Figures 48 through 54 took a deeper look at some of these residual natural cement particles that represents variably calcined argillaceous limestone/dolomite raw feed particles of natural cement.

Figure 55 summarizes compositional variations of residual natural cement particles and found two end member components, similar to natural cement and lime paste of the main mortar, consisting of: (a) a calcium-rich Mg-Al-Fe-silicate (and/or Ca-rich Mg-Si-Fe-aluminate) from burnt lime in the raw feed, (b) a calcium-poor to intermediate-calcium Mg-Al-Fe-silicate from lime-silica reactions of interstitial silica-rich areas during calcination of raw feed.

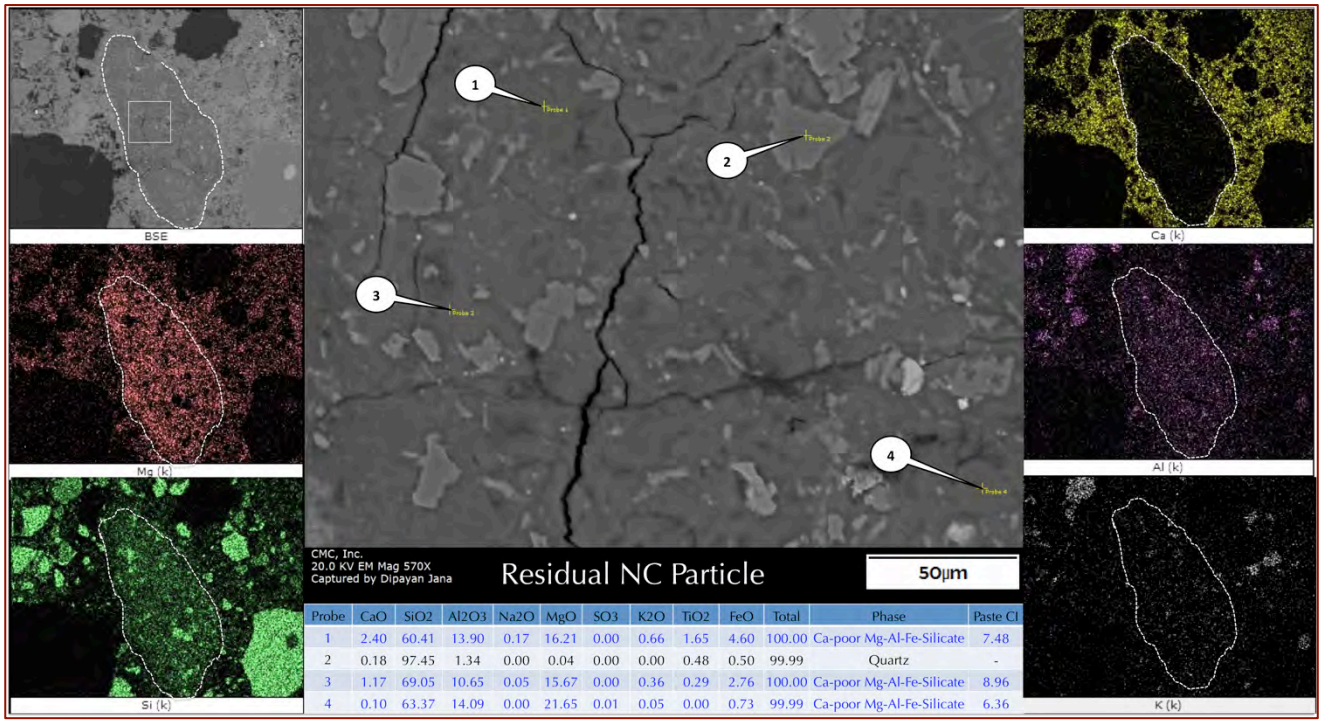

Probe	CaO	SiO2	Al2O3	Na2O	MgO	SO3	K2O	TiO2	FeO	Total	Phase	Paste Cl
1	2.40	60.41	13.90	0.17	16.21	0.00	0.66	1.65	4.60	100.00	Ca-poor Mg-Al-Fe-Silicate	7.48
2	0.18	97.45	1.34	0.00	0.04	0.00	0.00	0.48	0.50	99.99	Quartz	-
3	1.17	69.05	10.65	0.05	15.67	0.00	0.36	0.29	2.76	100.00	Ca-poor Mg-Al-Fe-Silicate	8.96
4	0.10	63.37	14.09	0.00	21.65	0.01	0.05	0.00	0.73	99.99	Ca-poor Mg-Al-Fe-Silicate	6.36

Figure 50: Backscatter electron (BSE) image, X-ray elemental map, and EDS elemental analyses of various points on the BSE image showing compositional variations within a residual natural cement particle (white dashed line).

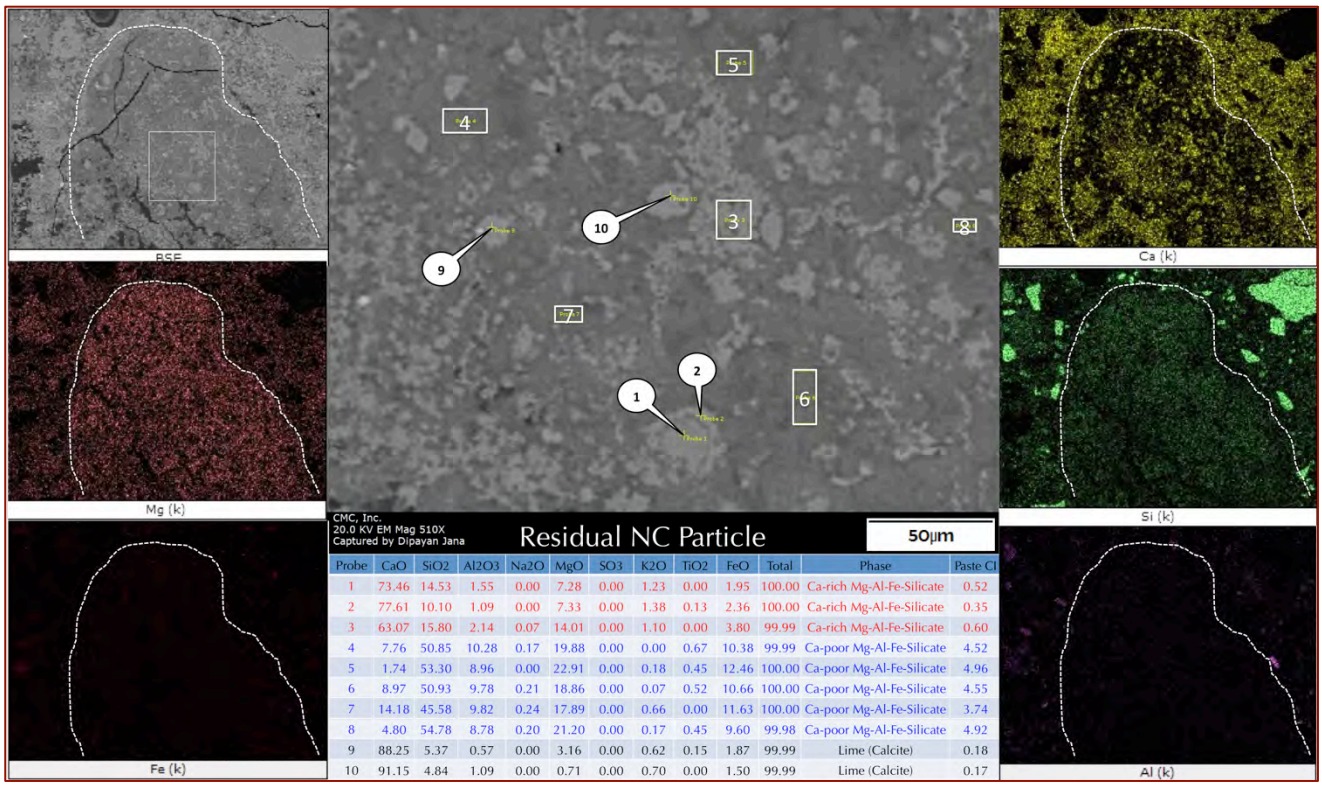

Probe	CaO	SiO2	Al2O3	Na2O	MgO	SO3	K2O	TiO2	FeO	Total	Phase	Paste Cl
1	73.46	14.53	1.55	0.00	7.28	0.00	1.23	0.00	1.95	100.00	Ca-rich Mg-Al-Fe-Silicate	0.52
2	77.61	10.10	1.09	0.00	7.33	0.00	1.38	0.13	2.36	100.00	Ca-rich Mg-Al-Fe-Silicate	0.35
3	63.07	15.80	2.14	0.07	14.01	0.00	1.10	0.00	3.80	99.99	Ca-rich Mg-Al-Fe-Silicate	0.60
4	7.76	50.85	10.28	0.17	19.88	0.00	0.00	0.67	10.38	99.99	Ca-poor Mg-Al-Fe-Silicate	4.52
5	1.74	53.30	8.96	0.00	22.91	0.00	0.18	0.45	12.46	100.00	Ca-poor Mg-Al-Fe-Silicate	4.96
6	8.97	50.93	9.78	0.21	18.86	0.00	0.07	0.52	10.66	100.00	Ca-poor Mg-Al-Fe-Silicate	4.55
7	14.18	45.58	9.82	0.24	17.89	0.00	0.66	0.00	11.63	100.00	Ca-poor Mg-Al-Fe-Silicate	3.74
8	4.80	54.78	8.78	0.20	21.20	0.00	0.17	0.45	9.60	99.98	Ca-poor Mg-Al-Fe-Silicate	4.92
9	88.25	5.37	0.57	0.00	3.16	0.00	0.62	0.15	1.87	99.99	Lime (Calcite)	0.18
10	91.15	4.84	1.09	0.00	0.71	0.00	0.70	0.00	1.50	99.99	Lime (Calcite)	0.17

Figure 51: Backscatter electron (BSE) image, X-ray elemental map, and EDS elemental analyses of various points on the BSE image showing compositional variations within a residual natural cement particle (white dashed line).

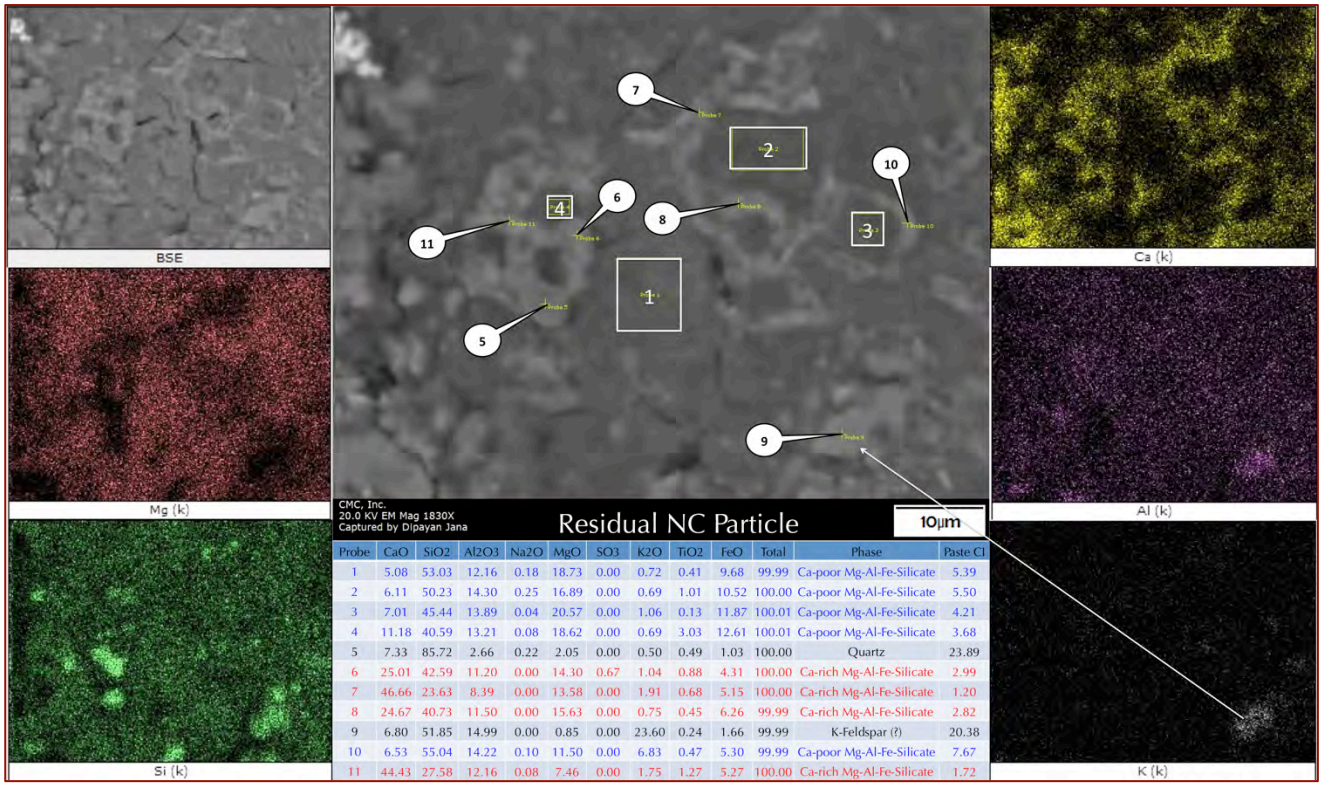

Probe	CaO	SiO2	Al2O3	Na2O	MgO	SO3	K2O	TiO2	FeO	Total	Phase	Paste Cl
1	5.08	53.03	12.16	0.18	18.73	0.00	0.72	0.41	9.68	99.99	Ca-poor Mg-Al-Fe-Silicate	5.39
2	6.11	50.23	14.30	0.25	16.89	0.00	0.69	1.01	10.52	100.00	Ca-poor Mg-Al-Fe-Silicate	5.50
3	7.01	45.44	13.89	0.04	20.57	0.00	1.06	0.13	11.87	100.01	Ca-poor Mg-Al-Fe-Silicate	4.21
4	11.18	40.59	13.21	0.08	18.62	0.00	0.69	3.03	12.61	100.01	Ca-poor Mg-Al-Fe-Silicate	3.68
5	7.33	85.72	2.66	0.22	2.05	0.00	0.50	0.49	1.03	100.00	Quartz	23.89
6	25.01	42.59	11.20	0.00	14.30	0.67	1.04	0.88	4.31	100.00	Ca-rich Mg-Al-Fe-Silicate	2.99
7	46.66	23.63	8.39	0.00	13.58	0.00	1.91	0.68	5.15	100.00	Ca-rich Mg-Al-Fe-Silicate	1.20
8	24.67	40.73	11.50	0.00	15.63	0.00	0.75	0.45	6.26	99.99	Ca-rich Mg-Al-Fe-Silicate	2.82
9	6.80	51.85	14.99	0.00	0.85	0.00	23.60	0.24	1.66	99.99	K-Feldspar (?)	20.38
10	6.53	55.04	14.22	0.10	11.50	0.00	6.83	0.47	5.30	99.99	Ca-poor Mg-Al-Fe-Silicate	7.67
11	44.43	27.58	12.16	0.08	7.46	0.00	1.75	1.27	5.27	100.00	Ca-rich Mg-Al-Fe-Silicate	1.72

Figure 52: Backscatter electron (BSE) image, X-ray elemental map, and EDS elemental analyses of various points and boxed areas on the BSE image showing compositional variations within the boxed area of the residual natural cement particle (white dashed line) shown in Figure 50.

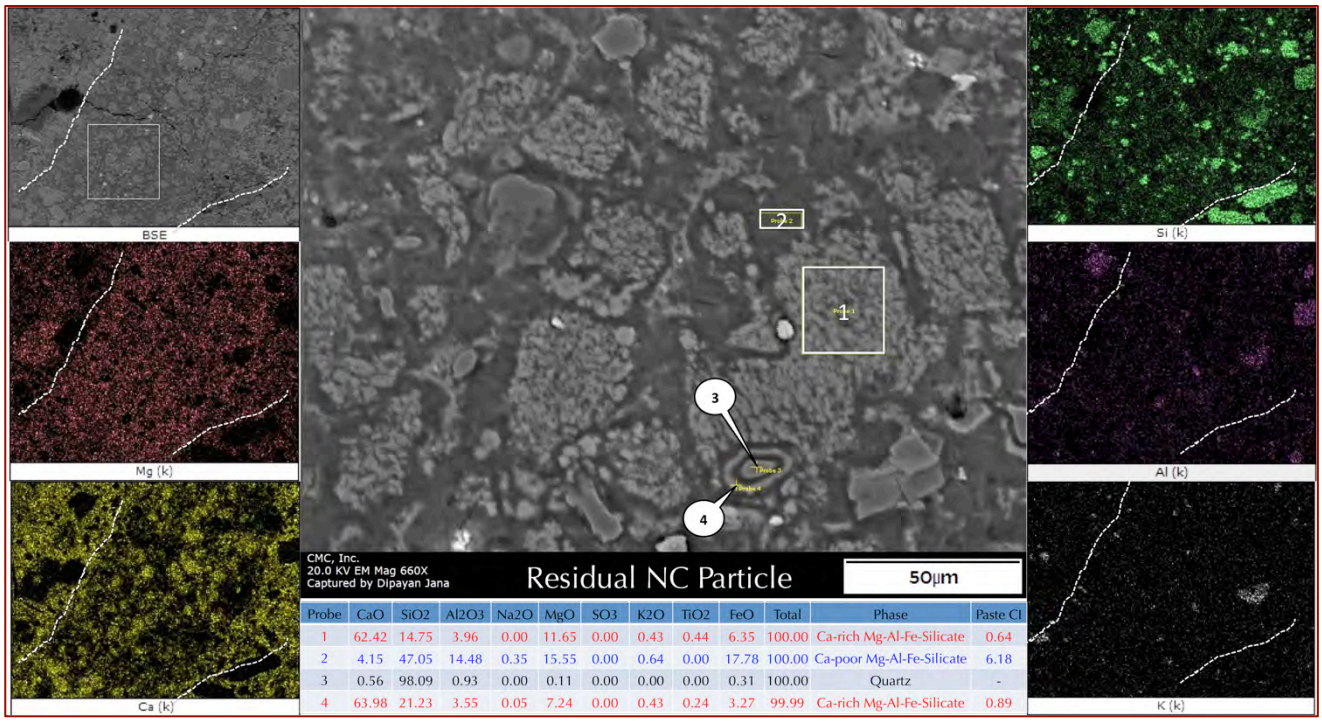

Probe	CaO	SiO2	Al2O3	Na2O	MgO	SO3	K2O	TiO2	FeO	Total	Phase	Paste Cl
1	62.42	14.75	3.96	0.00	11.65	0.00	0.43	0.44	6.35	100.00	Ca-rich Mg-Al-Fe-Silicate	0.64
2	4.15	47.05	14.48	0.35	15.55	0.00	0.64	0.00	17.78	100.00	Ca-poor Mg-Al-Fe-Silicate	6.18
3	0.56	98.09	0.93	0.00	0.11	0.00	0.00	0.00	0.31	100.00	Quartz	-
4	63.98	21.23	3.55	0.05	7.24	0.00	0.43	0.24	3.27	99.99	Ca-rich Mg-Al-Fe-Silicate	0.89

Figure 53: Backscatter electron (BSE) image, X-ray elemental map, and EDS elemental analyses of various boxed areas on the BSE image showing compositional variations within the boxed area of the residual natural cement particle (white dashed line) shown in the top left BSE image.

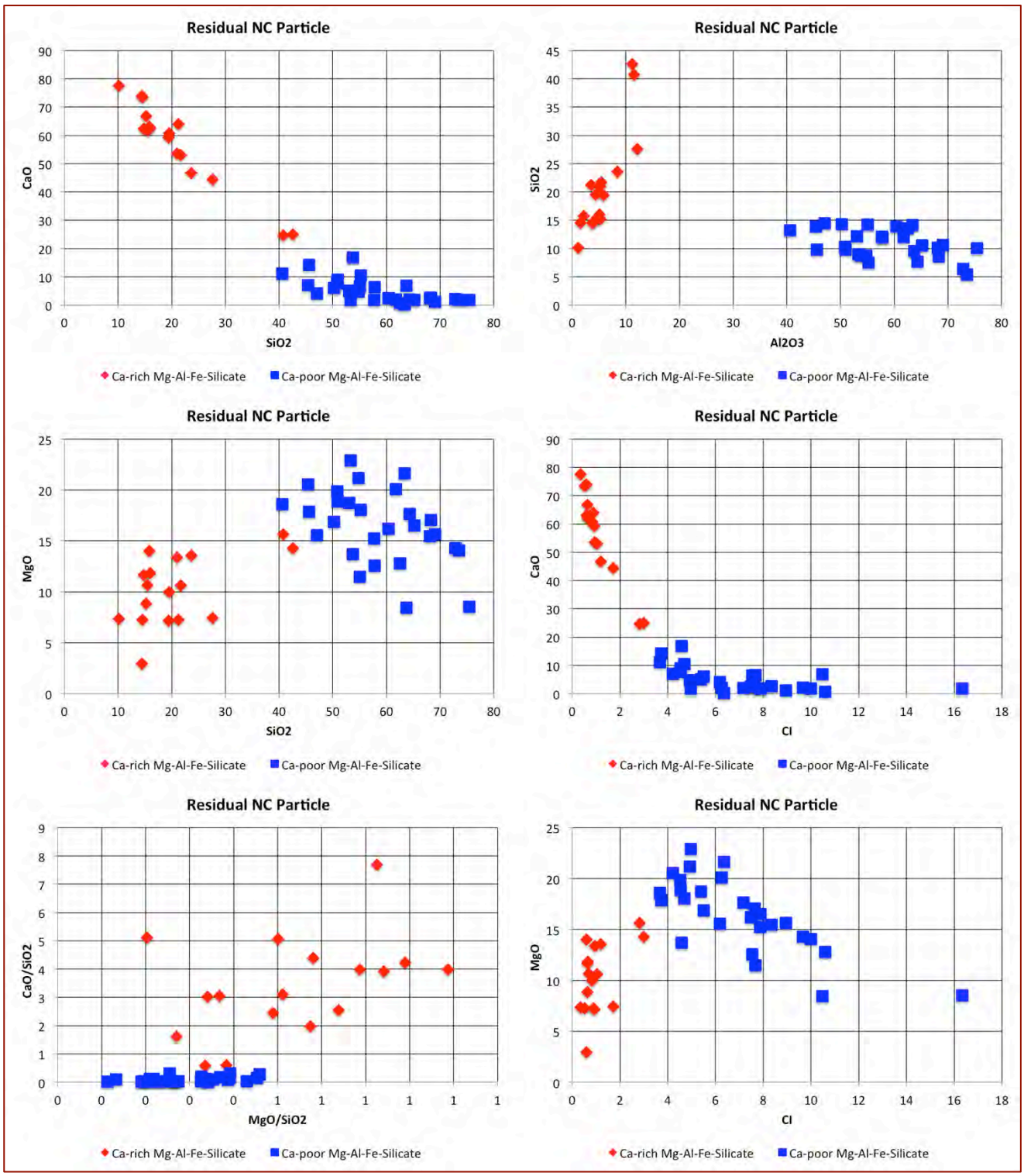

Figure 54: Compositional variations of interiors of residual natural cement particles amongst two main detectable components: (a) a calcium-rich Mg-Al-Fe-silicate (red diamonds) from the burnt lime in the raw feed, (b) a calcium-poor silica-rich Mg-Al-Fe-silicate (blue squares) from lime-silica reactions of interstitial silica-rich areas during calcination of raw feed.

Comparisons of Recycled Mortar vs. Natural Cement-Lime paste vs. Residual Natural Cement Particles

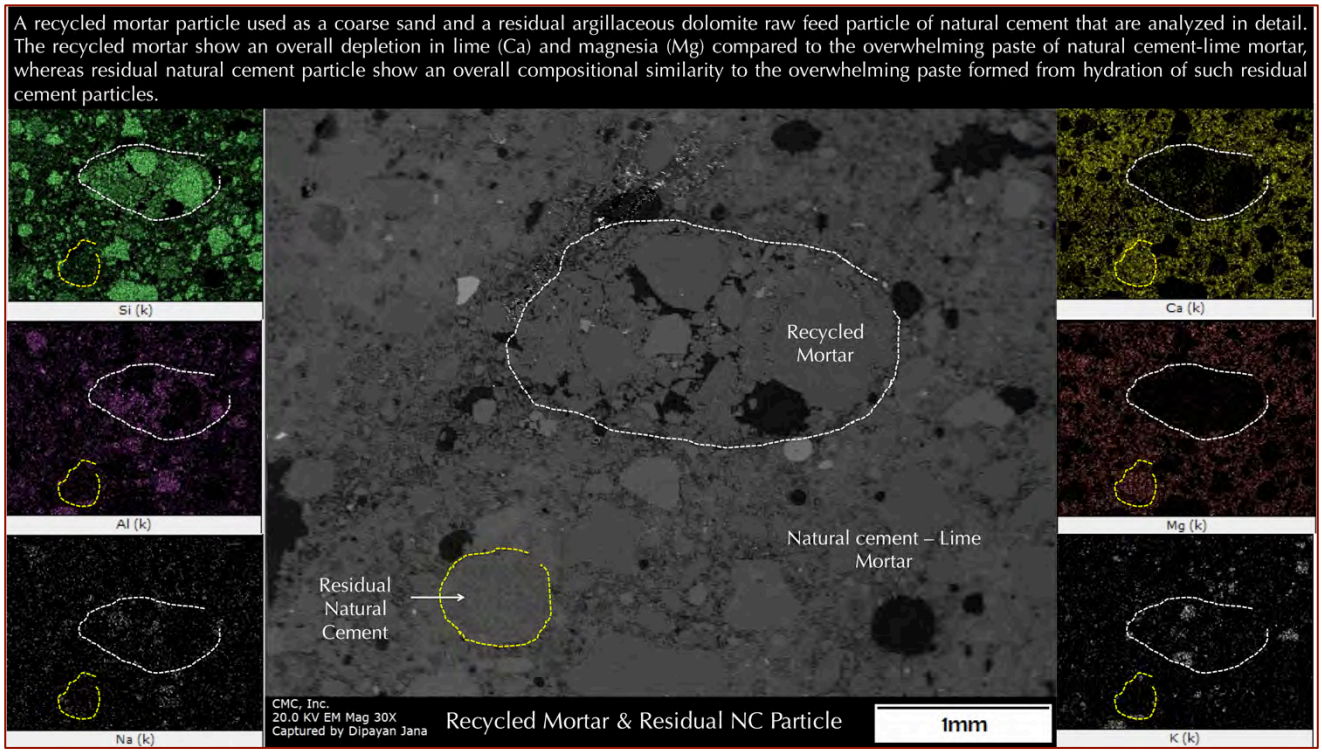

Figure 55: Backscatter electron (BSE) image, and X-ray elemental map showing compositional variations between a recycled mortar fragment at the center of BSE image marked by white dashed line, a residual natural cement particle at the bottom left marked by yellow dashed line, and overall natural cement-lime paste mixed with silica sand of the main mortar.

Notice: (a) an overall lime-poor (almost no magnesia) composition of recycled mortar compared to the main mortar, (b) an overall magnesia-rich composition of the residual natural cement particle compared to the outside paste of main mortar, (c) a potassium-rich composition of the recycled mortar compared to the main mortar, (d) a silica-rich composition of the recycled mortar compared to the main mortar (which is probably from a greater abundance of quartz sand particles in the recycled mortar in this image than the main mortar). From compositional variations of these three individual components i.e. the recycled mortar, the residual natural cement, and the overwhelming natural cement-lime paste of main mortar, it is concluded that the overwhelming main mortar was made using natural cement and lime as two components, whereas the recycled mortar was prepared with a natural hydraulic lime binder and sand where the binder could have derived from calcination of a clayey limestone raw feed.

From thin section photomicrographs it is already established that the matrix of recycled mortar is noticeably more porous, lighter colored, and finer-grained than the dense, dark brown, typical lime-iron-magnesia rich composition of natural cement-lime paste, which also indicates a natural hydraulic lime type binder for the recycled mortar as opposed to much denser natural cement-based binder of the main mortar.

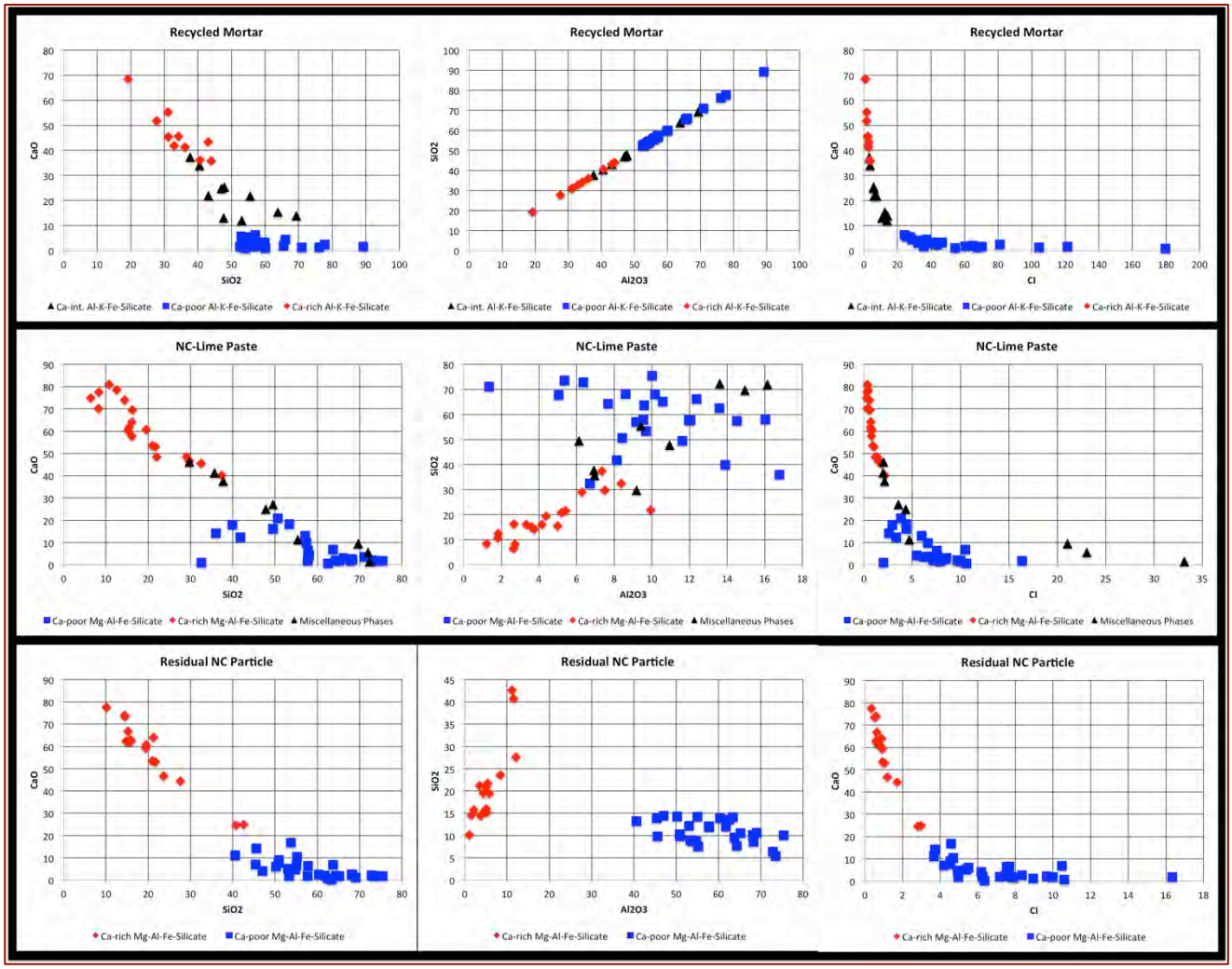

Figure 56: Similarities in compositional trends of recycled mortar, residual natural cement particle, and overall natural cement-lime paste – all three components show an overall trend between two main components.

For recycled mortar it is a trend between a lime-rich end member and a lime-poor K-Al-Si-rich end member, which is similar to many natural hydraulic lime mortars consisting of patches of lime-rich areas over a groundmass of intermediate-lime to lime-poor silica-alumina-alkali-rich areas.

For residual natural cement, it is a trend between a lime-rich silica-poor and a lime-poor magnesia-silica rich component of the calcined raw feed particle of natural cement.

For the overall natural cement-lime paste, it is a trend between the lime-rich from the added lime and relatively lower-lime to lime-poor magnesia-iron-silica-rich composition of added natural cement.

All these chemical variations are suggestive of use of natural cement and lime binders in the host mortar and hydraulic lime binder in the recycled mortar.

AIR

Both the recycled as well as the main mortars are non-air-entrained, i.e. they lack any intentionally introduced entrained air-voids that are common in many modern air-entrained cement-lime and masonry cement mortars. All void spaces in the photomicrographs of thin section of mortar in Figure 8 are interstitial voids similar to entrapped voids and do not indicate use of any air entrainment in the mortar. This finding is consistent with its historic nature.

BULK MORTARS' MINERALOGIES FROM XRD

Table 5 and Figure 57 summarize results of semi-quantitative mineralogical compositions of bulk mortar (i.e. the combined main and recycled mortar) from X-ray diffraction, and, sources of major minerals as suspected or determined from optical microscopy.

Mineralogical Components	Semi-Quantitative Estimate (%)	Possible Sources
Quartz (with minor coesite)	55.9	Sand used in recycled as well as main mortar, also some quartz from granite particles found in recycled mortar; coesite is from calcined raw feed of natural cement
Calcite	13.1	Carbonated paste of natural cement and lime, residual calcined raw feed particles of natural cement, and carbonated paste of recycled mortar
Microcline (Feldspar)	27.5	Sand
Brucite	3.5	Dolomitic lime used as the second binder component after natural cement in the main mortar

Table 5: Mineralogical composition of bulk mortar determined from XRD.

CHEMICAL ANALYSES

STRATEGY

Since optical and electron microscopy detected two different mortars intimately integrated – a recycled natural hydraulic lime mortar scattered in the main natural cement-lime mortar, it is impossible to do chemical analyses of separate mortar types since removal of recycled mortar from the main mortar without contamination is difficult. Therefore, the bulk mortar fragment was pulverized and analyzed for various chemical analyses with the assumption that since the proportion of recycled mortar component is relatively low (e.g., less than 10 percent in the piece) compared to the main mortar, composition determined for bulk mortar will be close in approximation to a natural cement-lime mortar without any recycled component.

SOLUBLE SILICA CONTENT FROM NATURAL CEMENT IN THE MORTAR

Table 6 shows results of: (a) determination of cement content in the mortar from the soluble silica content that is contributed from the cement.

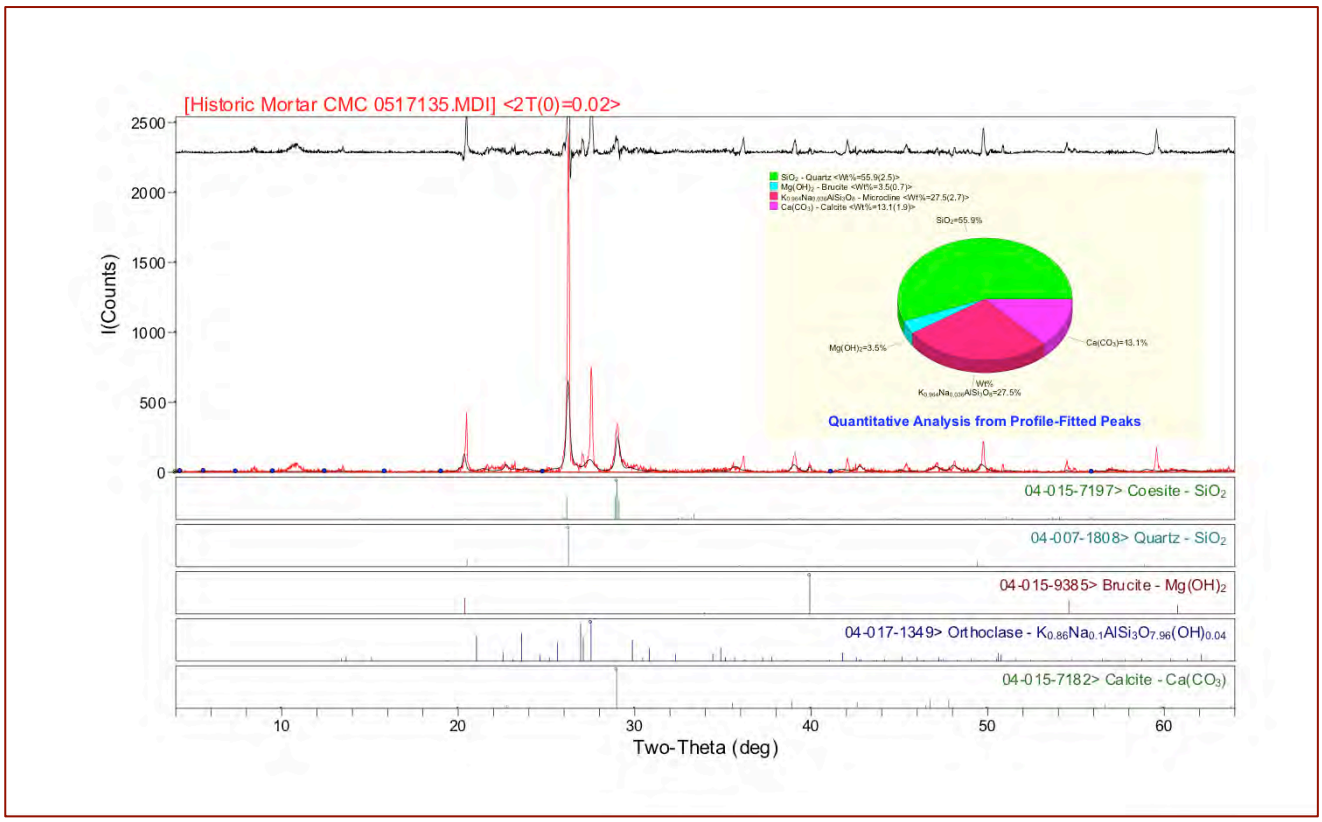

Figure 57: X-ray diffraction pattern of bulk mortar (along with the calculated pattern from the observed mineralogy in black at the top of main pattern in red) showing the dominant quartz from quartz sand, subordinate feldspar from sand, calcite and minor brucite from paste and dolomitic lime, respectively, and minor coesite from calcined raw feed particles of natural cement. Inset shows semi-quantitative estimate of phases, recalculated to 100% amongst the detectable phases.

For soluble silica determination *a la* ASTM C 1324, the combined filtrate for analysis is obtained from double filtration of (i) an original 5.00 grams of pulverized mortar i.e. after digestion in 100-mL cold (at 3 to 5°C) HCL followed by filtration (filtrate#1), (ii) then digestion of the residue left along with the filter paper in 75-mL hot (below boiling) NaOH followed by filtration (filtrate#2) and then (iii) combination of two filtrates and re-filtering of the combined filtrate for the third time to remove any suspended silica. The combined filtrate is then used for determination of soluble silica and cement content in an XRF against empirical calibration of intensities of known soluble silica and cement contents of multiple mortars (5.00 grams) prepared by the same procedure of cold HCl-digestion/filtration/hot NaOH-digestion/2nd filtration/combination of two filtrates/re-filtration. Cement contents from soluble silica contents are then calculated assuming 20.2 percent soluble silica in the Portland cement that was used for preparation of standards used in the calibrations. Cement content is calculated from the formula: Cement Content (%), CC = [ppm SiO_2 × 100] ÷ [5.00 (mortar weight used) × 0.266 (assuming a 26.6% SiO_2 content in the Natural cement used) × 4 (dilution factor of final 250 ml filtrate to 1L) × 1000 (conversation factor of g/L to mg/L or ppm)]. Cement content is calculated based on the determination of natural cement component as a cement binder used in the mortar, and the absence of Portland cement from petrographic examinations.

Component	Mortar
Cement Content from Soluble Silica Content (%)	7.05

Table 6: Cement content calculated from the soluble silica content in the mortar. Cement content is calculated based on the determination of natural cement component as a cement binder used in the mortar, and the absence of Portland cement from petrographic examinations.

BULK OXIDE COMPOSITIONS OF MORTAR FROM XRF

Table 7 and Figure 58 show results of bulk oxide composition of the mortar from XRF. Pressed pellet of pulverized (down to finer than 45 micron size) mortar is used in XRF against calibrations of various certified reference standards of cement, lime, and rock samples to get the most accurate oxide compositions.

Oxides (wt.%)	Bulk Mortar
Silica - SiO_2	48.5
Alumina - Al_2O_3	5.94
Iron - Fe_2O_3	2.3
Lime - CaO	13.1
Magnesia - MgO	7.65
Sodium - Na_2O	0.947
Potassium - K_2O	1.43
Titanium - TiO_2	0.213
Phosphorus - P_2O_5	0.088
Sulfate - SO_3	0.001
Balance	19.8
Total	100

Table 7: Bulk oxide compositon of mortar from XRF. Balance corresponds to the losses on ignition (CO_2, H_2O).

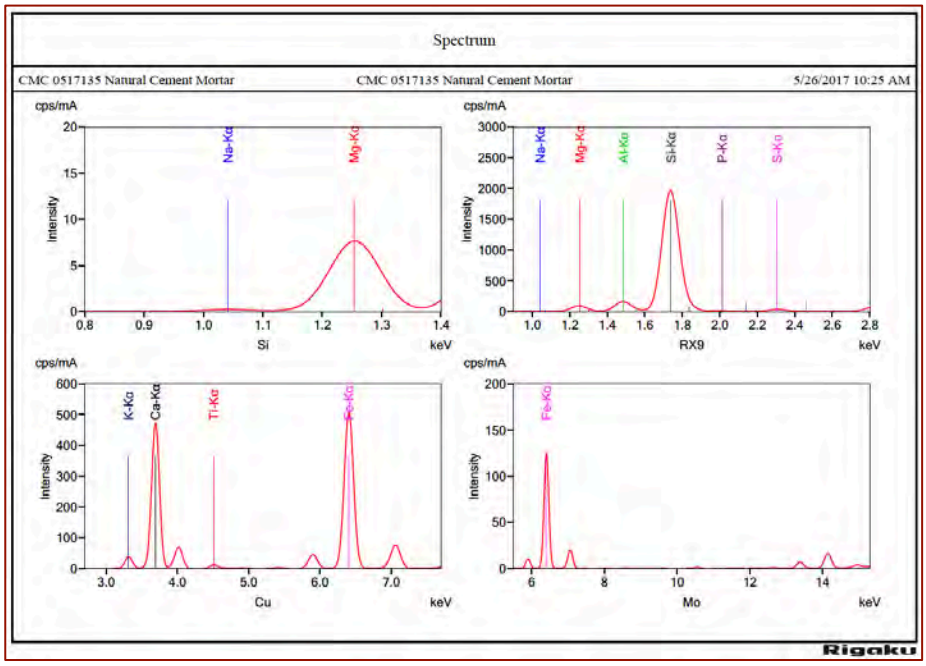

Figure 58: Elemental scan of mortar from XRF.

SAND CONTENT FROM ACID-INSOLUBLE RESIDUE, FREE PLUS COMBINED WATER CONTENTS, AND CARBONATION FROM LOSS ON IGNITION

Table 8 summarizes results of acid-insoluble residue content of mortar, after digesting a pulverized (to pass US No. 50 sieve) portion of bulk mortar in hydrochloric acid, and, loss on ignition of a separate aliquot of pulverized mortar to 110°C, 550°C, and 950°C, which correspond to free water, combined (hydrated) water, and degree of carbonation, respectively. Due to the presence of siliceous sand only (as determined from petrography) and no calcareous components in the sand, the determined acid-insoluble residue content corresponds to the sand content of the mortar.

Components	Mortar
Acid-Insoluble Residue (%)	57.3
Loss on Ignition: From 0°C to 110°C (Free Water) (%)	3.48
Loss on Ignition: From 110-550°C (Combined Water) (%)	5.53
Loss on Ignition: From 550-950°C (Carbonation, CO_2) (%)	13.37

Table 8: Hydrochloric acid-insoluble residue contents and loss on ignition to 110°C, 550°C and 950°C.

CALCITIC VS. DOLOMITIC LIME VS. NATURAL CEMENT FROM BRUCITE OR MAGNESIUM OXIDE CONTENT IN BULK MORTAR, OR, MAGNESIUM OXIDE CONTENT IN BINDER

The magnesium oxide content in the bulk mortar (7.65 percent) is indicative of use of a natural cement component in the binder, e.g., a cement similar to Rosendale natural cement, which has characteristically high magnesia composition from use of argillaceous dolomitic limestone as the raw feed. Detection of brucite in XRD indicates use of a dolomitic lime as well.

CALCULATIONS OF MIX PROPORTION OF MORTAR

Aided with the data obtained from petrography and chemical analyses of mortar, the following table first summarizes all chemical data, followed by calculations of proportions of various ingredients in the mortars from a set of assumed compositions and bulk densities of the ingredients:

Mortar Compositions & Mix Proportion	Natural Cement - Lime - Siliceous Sand Mortar
Chemical Data Relevant From Mix Calculations	
Cement Content from Soluble Silica (%)	7.05
Calcium Oxide Content (%) from XRF	13.1
Acid-Insoluble Residue (%) from Gravimetry	57.3
Assumed Compositions & Densities	
Natural Cement – From Soluble Silica (SiO_2) (%)	26.6 (Natural Cement)
Bulk Density of Natural Cement, (lbs./ft.^{3})	75

Mortar Compositions & Mix Proportion	Natural Cement - Lime - Siliceous Sand Mortar
Hydrated Lime or Lime putty	From CaO content, after assigning CaO for Natural Cement and assuming 35.6% CaO in Natural Cement, and converting the residual CaO to lime $Ca(OH)_2$ by multiplying the residual CaO with the factor 1.322 (mol. wt. of lime to CaO = 74.03/56 = 1.322)
Bulk Density of Lime, (lbs./ft.^{3})	40
Bulk Density of Sand, (lbs./ft.^{3})	80
Calculated Volumetric Proportions	
Natural Cement Content (%)	7.05
Lime Content (%), assuming 63.5% CaO in Natural cement	1.322 × [CaO content in mortar i.e. 13.1 – (cement content i.e. 7.05 × 0.356)] = 14.0%
Sand Content (%)	57.3 (from acid-insoluble residue content, entire sand is siliceous sand)
Natural Cement Volume	7.05/75 = 0.094
Hydrated Lime Volume	14.0/40 = 0.350
Sand Volume	57.3/80 = 0.716
Relative Volumes of Binder Phases: Sand	Natural Cement: Lime: Sand = 0.094:0.350:0.716 = 1: 3.7: 7.6 (1.6 times the sum of separate volumes of cement and lime)
Cement to Lime to Sand, by volume	1-part natural cement to $3^1/_2$-part lime to $7^1/_2$-part sand (1.6 times sand of the sum of separate volumes of cement and lime)

Table 9: Calculations of mix proportion of mortar, by volume, from the determined chemical compositions, and, assumed compositions and bulk densities of mortar ingredients.

Chemical composition of natural cement used in the above calculations (as well as in the soluble silica calculation in Table 6) is derived from an average composition of Rosendale cement from Eckel 1922 (average of 23 analyses of Rosendale natural cement, from Page 247, Table 121 of Eckel 1922):

Rosendale Natural Cement	SiO_2	Al_2O_3	Fe_2O_3	CaO	MgO	Alkalis	Cl
Eckel (1922)	26.66	8.02	3.98	35.60	18.30	4.05	1.42

Table 10: Average chemical composition of 23 analyses of Rosendale natural cement from Eckel 1922.

The soluble silica content of the mortar provided a natural cement content of 7.05 percent, by assuming 26.6% soluble silica in natural cement from an average chemical composition of Rosendale cement from Eckel (1922). Lime content is determined from the bulk calcium oxide content of mortar, after assigning CaO for natural cement and assuming 35.6% calcium oxide in natural cement (from Eckel 1922), and converting the residual CaO to lime i.e. $Ca(OH)_2$ by multiplying the residual CaO with the conversion factor 1.322 [ratio of mol. wt. of lime i.e. $Ca(OH)_2$ to CaO is 74.03/56 = 1.322]. Since the sand is determined to be siliceous (quartz-quartzite) sand, and contains no calcareous component, the sand content is determined from the hydrochloric acid-insoluble residue content of mortar. Assuming bulk densities of natural cement, lime, and sand as 75, 40, and 80 lbs./ft^3,

respectively, the volumetric proportion of natural cement to lime to sand is calculated to be 1-part natural cement to $3^1/_2$-part lime to $7^1/_2$-part sand. It is important here to remember that the high lime-content is a result of inclusion of natural hydraulic lime recycled mortar, which also contributed lime to the overall composition. Therefore lime content in a pointing mortar could be reduced compared to lime-to-natural cement proportion in this formulation if the pointing mortar to be used is just natural cement-lime mortar as the main mortar here without any recycled component. Sand content is 1.6 times the sum of separate volumes of cement and lime, as opposed to commonly recommended $2^1/_4$ to 3 times, thus indicating an under-sanded nature of the mortar.

CONCLUSIONS

AGGREGATES

Two different populations of sands are detected in the mortar (a) a 'coarse sand' population where majority of the particles are 1 to 3 mm in nominal size (some as much as 10 mm), which is judged to be the separate recycled mortar fragments and their finer fractions, and, (b) a 'fine sand' population of nominal 2 mm or less, which is present both in the recycled and in the host mortar. Sand in the recycled mortar consists of: (i) quartzite, (ii) biotite granitic gneiss, and (iii) fine angular siliceous sand. Sand in the main mortar consists of siliceous angular fine sand similar in composition to those in the recycled mortar, containing major amounts of quartz, along with minor feldspar (microcline, orthoclase). The fine angular quartz, feldspar sand in recycled and main mortars are compositionally similar, probably locally obtained and crushed, clean, well-graded, well-distributed, and present in sound condition with no evidence of any deleterious alkali-aggregate reaction.

ORIGINAL BINDERS

Binder in the main mortar shows the typical mineralogy and microstructure produced from the use of (i) a natural cement and (ii) lime as the two essential binders. By contrast, recycled mortar is judged to have been prepared using natural hydraulic lime binder without any natural cement or any other binder. As a result, pastes from corresponding mortars differed in color, appearance, density, and compositions of respective hydration and carbonation products.

Overwhelming composition of paste in the host mortar consisted of an intimate mixture of: (i) hydration and carbonation products of natural cement, (ii) carbonation product of lime, (iii) residual calcined raw feed argillaceous limestone/dolomite particles of natural cement, and (iv) some lime lumps from use of lime probably as lime putty. SEM-EDS studies of paste from various areas across the main mortar have detected: (a) a calcium-rich Mg-Al-Fe-silicate from lime and natural cement, (b) a calcium-poor to intermediate-calcium Mg-Al-Fe -silicate from natural cement, and, (c) a few miscellaneous minor components. Oxide compositional variations clearly showed a trend between the two end member (lime-rich and lime-poor) components, indicating use of lime and natural cement as two separate binders.

Recycled mortar showed very different binder that differed from the host in the following ways: (i) binder in the recycled mortar is noticeably lighter colored, more porous than the medium to dark brown stained and far denser paste in the main mortar, (ii) natural cement is not detected in the recycled mortar, indicating a different hydraulic binder was used in the recycled mortar; (iii) lime is the most common binder detected in the recycled mortar as opposed to natural cement and occurred as porous, fine-grained, cryptocrystalline carbonated lime matrix; and (iv) a few residual calcium silicate particles are detected in the lime-based binder of recycled mortar indicating perhaps a hydraulic lime was used in the recycled mortar, e.g., a natural hydraulic lime. SEM-EDS analyses of binder detected: (i) a calcium-rich Al-K-Fe-silicate composition, which was inherited from lime, (ii) a calcium-poor Al-K-Fe-silicate composition inherited from silica-rich (hydraulic) phases of binder, and, (iii) an intermediate calcium Al-K-Fe-silicate, which is probably the mixture of two end members of lime-rich and lime-poor components of the binder, similar in composition to a *natural (high-calcium) hydraulic lime* the raw feed of which had contained limestone as the source of lime and clay as the source of silica, alumina, potassium, and iron.

TYPES OF MORTARS

Based on detailed laboratory studies, the main mortar is determined to be a natural cement – lime – siliceous sand mortar, whereas the recycled mortar is determined to be a natural hydraulic lime mortar containing crushed biotite granite as coarse sand and fine, angular siliceous sand similar to the fine sand in the main mortar.

Due to this incorporation of a natural hydraulic lime mortar as a recycled mortar into the host natural cement-lime mortar, compositional analyses of this 'composite mortar' to get a mix proportion is not only difficult but also meaningless, unless the new pointing mortar is to be made using a natural cement-lime mortar with a natural hydraulic lime recycled mortar at similar proportions. Nevertheless, the bulk composition of this composite mortar was analyzed, and used to determine all chemical parameters, e.g., soluble silica content to get corresponding natural cement content, major oxide compositions, losses on ignitions to determine free, combined water contents and carbonation, and insoluble silica contents to get sand proportions. Chemical data obtained was then processed in mix calculations with an underlying assumption that the bulk mortar contained less than 10 percent recycled mortar at least in the sample received, and other than contributing calcium oxide and some silica from its hydraulic component of binder, the recycled mortar did not contribute a major share of the bulk chemistry of the composite mortar. With that assumption, mix proportions calculated from chemical data showed use of 1-part natural cement to $3^1/_2$-part lime to $7^1/_2$-part sand. It is important here to remember that the high lime-content is a result of inclusion of natural hydraulic lime recycled mortar, which also contributed lime to the overall composition. Therefore lime content in a pointing mortar could be reduced compared to lime-to-natural cement proportion in this formulation if the pointing mortar to be used is just natural cement-lime mortar as the main mortar here without any recycled component. Sand content is 1.6 times the sum of separate volumes of cement and lime, as opposed to commonly recommended $2^1/_4$ to 3 times, thus indicating an under-sanded nature of the mortar.

SUGGESTED TUCK POINTING MORTAR

Based on:

a. The determined natural cement and lime-based composition of the host mortar,
b. Natural siliceous sand composition of aggregate, and,
c. Its calculated volumetric proportions of 1-part natural cement to $3^1/_2$-part lime to $7^1/_2$-part sand,

A possible tuck-pointing mortar could be:

a. A natural cement-lime-sand mortar made using Rosendale natural cement, hydrated lime, and natural sand, conforming to the respective ASTM specifications of C 10, C 207, and C 144,

b. The final choice of binder and sand ingredients would depend on the match in appearance, compositions, and properties with the original mortar. Design and formulation of an appropriate tuck-pointing mortar should be based on trial and error on small test areas by the project engineer/architect.

c. Appendix A2 has provided various suggestions for formulation of tuck-pointing mortar.

REFERENCES

ASTM C 10, "Standard Specification for Natural Cement," In Annual Book of ASTM Standards, Section Four Construction, Vol. 04.01 Cement; Lime; Gypsum; ASTM Committee C01 on Cement, 2007.

ASTM C 144, "Standard Specification for Aggregate for Masonry Mortar," In Annual Book of ASTM Standards, Section Four Construction, Vol. 04.05 Chemical-Resistant Nonmetallic Materials; Vitrified Clay Pipe; Concrete Pipe; Fiber-Reinforced Cement Products; Mortars and Grouts; Masonry; Precast Concrete; ASTM Committee C12 on Mortars for Unit Masonry, 2007.

ASTM C 1324, "Standard Test Method for Examination and Analysis of Hardened Masonry Mortar," In Annual Book of ASTM Standards, Section Four Construction, Vol. 04.05 Chemical-Resistant Nonmetallic Materials; Vitrified Clay Pipe; Concrete Pipe; Fiber-Reinforced Cement Products; Mortars and Grouts; Masonry; Precast Concrete; ASTM Committee C12 on Mortars for Unit Masonry, 2007.

ASTM C 270, "Standard Specification for Mortar for Unit Masonry," In Annual Book of ASTM Standards, Section Four Construction, Vol. 04.05 Chemical-Resistant Nonmetallic Materials; Vitrified Clay Pipe; Concrete Pipe; Fiber-Reinforced Cement Products; Mortars and Grouts; Masonry; Precast Concrete; ASTM Committee C12 on Mortars and Grouts for Unit Masonry, 2007.

ASTM C 51, "Standard Terminology Relating to Lime and Limestone (as used by the Industry)'" In Annual Book of ASTM Standards, Section Four Construction, Vol. 04.01 Cement; Lime; Gypsum; ASTM Committee C07 on Lime, 2007.

ASTM C 856, "Standard Practice for Petrographic Examination of Hardened Concrete," In Annual Book of ASTM Standards, Section Four Construction, Vol. 04.02; ASTM Subcommittee C 9.65, 2010.

ASTM C 1723, "Standard Guide for Examination of Hardened Concrete Using Scanning Electron Microscopy," In Annual Book of ASTM Standards, Section Four Construction, Vol. 04.02; ASTM Subcommittee C 9.65, 2010.

Bartos, P. Groot, C., and Hughes, J.J. (eds.), *Historic Mortars: Characteristics and Tests*, Proceedings PRO12, RILEM Publications, France, 2000.

Boynton, R., *Chemistry and Technology of Lime and Limestone, 2nd edition*, John Wiley & Sons, Inc. 1980.

Charloa, A.E., "Mortar Analysis: A Comparison of European Procedures." *US/ICOMOS Scientific Journal: Historic Mortars & Acidic Deposition on Stone*, 3 (1), pp. 2-5, 2001.

Chiari, G., Torraca, G., and Santarelli, M.L., "Recommendations for Systematic Instrumental Analysis of Ancient Mortars: The Italian Experience", *Standards for Preservation and Rehabilitation*, ASTM STP 1258, S.J. Kelley, ed., American Society for Testing and Materials, pp. 275-284, 1996.

Doebley, C.E., and Spitzer, D., "Guidelines and Standards for Testing Historic Mortars", *Standards for Preservation and Rehabilitation*, ASTM STP 1258, S.J. Kelley, ed., American Society for Testing and Materials, pp. 285-293, 1996.

Eckel, Edwin, C., *Cements, Limes, and Plasters*, John Wiley & Sons, Inc. 655pp, 1922.

Edison, M.P. (Editor), *Natural Cement*, ASTM STP 1494, American Society for Testing and Materials, 2008.

Elsen, J., "Microscopy of Historic Mortars – A Review", *Cement and Concrete Research 36*, 1416-1424, 2006.

Erlin, B., and Hime, W.G., "Evaluating Mortar Deterioration", *APT Bulletin*, Vol. 19, No. 4, pp. 8-10+54, 1987.

Goins E.S., "Standard Practice for Determining the Components of Historic Cementitious Materials," *National Center for Preservation Technology and Training, Materials Research Series*, NCPTT 2004.

Hughes, D.C., Jaglin, D., Kozlowski, R., Mayr, N., Mucha, D., and Weber, J., "Calcination of Marls to Produce Roman Cement", pp. 84-95, In, Edison, M.P. (Editor), *Natural Cement*, ASTM STP 1494, American Society for Testing and Materials, 2007.

Hughes, J.J., Cuthbert, S., and, Bartos, P., "Alteration Textures in Historic Scottish Lime Mortars and the Implications for Practical Mortar Analysis", *Proceedings of the 7th Euroseminar on Microscopy Applied to Building Materials*, Delft, pp. 417-426, 1999.

Jana, D., "Application of Petrography In Restoration of Historic Masonry Structures", In: Hughes, J.J., Lesie, A.B. and Walsh, J.A., eds. *Proceedings of 10th Euroseminar on Microscopy Applied to Building Materials*, Paisley, 2005.

Jana, D., "Sample Preparation Techniques in Petrographic Examinations of Construction Materials: A State-of-the-art Review", *Proceedings of the 28th Conference on Cement Microscopy*, International Cement Microcopy Association, Denver, Colorado, pp. 23-70, 2006.

Leslie, A.B., and Hughes, J.J., "Binder Microstructure in Lime Mortars: Implications for the Interpretation of Analysis Results", *Quarterly Journal of Engineering Geology & Hydrogeology*, V. 35, No. 3, pp. 257-263, 2001.

Mack, Robert, and Speweik, John P., *Preservation Briefs 2*, U.S. Department of the Interior, National Park Service Cultural Resources, Heritage Preservation Services, pp. 1-16, 1998.

Middendorf, B., Hughes, J.J., Callebaut, K., Baronio, G., and Papayanni, I., "Investigative Methods for the Characterization of Historic Mortars – Part 2: Chemical Characterization," *Materials and Structures*, Vol. 38, pp 771-780, 2005a.

Middendorf, B., Hughes, J.J., Callebaut, K., Baronio, G., and Papayanni, I., "Investigative Methods for the Characterization of Historic Mortars – Part 1: Mineralogical Characterization," *Materials and Structures*, Vol. 38, 2005b.

Speweik, J.P., *The History of Masonry Mortar in America 1720-1995*, 2010.

Valek, J., Hughes, J.J., and Groot, C. (eds.), *Historic Mortars: Characterization, Assessment and Repair*, Springer, RILEM Book series Vol. 7, p. 464, 2012.

✪ ✪ ✪ END OF TEXT ✪ ✪ ✪

APPENDIX A1 –
METHODOLOGIES FOR LABORATORY TESTING OF MASONRY MORTARS

METHODOLOGIES

The mortar sample was tested by following the methods of ASTM C 1324 "Standard Test Method for Examination and Analysis of Hardened Masonry Mortar," along with various analytical methods to test masonry mortars as described in various literatures, e.g., Erlin and Hime 1987, Doebley and Spitzer 1996, Chiari et al. 1996, Middendorf et al. 2005 a and b, Elsen 2006, Bartos et al. 2000, Valek et al. 2012, Jana 2005, 2006, and Goins 2001 and 2004.

For laboratory testing of masonry mortars, CMC provides two packages – a *basic package*, and, a *comprehensive package*. Tests followed in both packages are shown in Figure 5. Basic package is suitable for modern masonry mortars, formulated by following the specifications of ASTM C 270, whereas comprehensive package is more informative for historic mortars, or mortars that are not formulated according to the specifications of ASTM C 270, or have components outside the Portland cement, hydrated lime (or lime putty), masonry cement, and mortar cement components recommended in formulations of ASTM C 270 mortars. Both packages provide volumetric proportions of various binder and sand components that are useful for formulation of a tuck-pointing mortar to be used as a replacement of the examined mortar.

The present mortar was requested to be analyzed by the *basic package*. Therefore Test Nos. 1, 3, 4, 5, and 7 in Figure A1-1 were followed to determine the composition of the mortar and assess appropriate formulation for a tuck-pointing mortar that could be suitable for replacement of the examined mortar.

SAMPLE SELECTION & SAMPLE PREPARATION

From the mortar fragment received, 'representative' subset fragment(s) were selected for various laboratory techniques, e.g., visual examinations, digital and flatbed scanner photography, optical microscopy using a Stereozoom and a petrographic microscope both equipped with reflected, transmitted, polarizing-light facilities, scanning electron microscopy and energy-dispersive X-ray fluorescence spectroscopy (SEM-EDS), X-ray fluorescence of bulk mortar, X-ray diffraction (of bulk mortar, sand extract, or binder extract), various chemical analyses (e.g., gravimetric), and thermal analysis (e.g., DTA, TGA, DSC). As shown in the flowchart, original mortar was first examined visually and with the help of a Stereozoom microscope at low magnifications. Any piece that appeared 'unusual' in visual examinations from the rest i.e. in having markedly different appearance was not included, since the piece may represent a different mortar accidentally mixed up with the mortar to be analyzed during the retrieval process (e.g., in masonries that have received multiple episodes of renovations and repointing in the past). From the pieces representative of the mortar to be analyzed, two broad groups were separated, one for microscopy (optical microscopy and SEM-EDS), and, the other group for chemical analysis, XRD-XRF, thermal analysis, sand extraction and sieve analyses, etc. Information obtained from microscopy is used to devise appropriate procedure to be followed in subsequent chemical analyses.

Laboratory Examinations of Masonry Mortar

Initial Mortar (50+ grams) [Photographed with digital camera & flat-bed scanner, As-received condition, total weight, and dimensions of largest piece are documented]

Intact Pieces (20+ g)

1. Optical Microscopy

i. Take digital and flat bed scanner photos of intact piece(s) as received,
ii. Encapsulate a representative piece in a mold with a low-viscosity colored dye-mixed epoxy to highlight voids, pores, cracks, etc.,
iii. Prepare thin section and polish the thin section for SEM-EDS analyses,
iv. Scan the thin section on a flat-bed scanner with the thin section residue,
v. Take transmitted light stereo-zoom photomicrographs of thin sections from different areas to determine volumes of pore spaces and sand by Image J,
vi. Take plane and crossed polarized-light photomicrographs of sand and binder fractions in thin section from a petrographic microscope and determine areas for further studies by SEM-EDS,
vii. Do detailed petrographic examinations in Stereozoom and Petrographic microscopes.

2. SEM-EDS

i. Gold-coat only the portion of polished thin section or a solid polished piece intended for SEM-EDS studies,
ii. Take backscatter and/or secondary electron images, and if needed x-ray elemental maps,
iii. Select multiple areas on paste by point and/or raster modes to determine elemental compositions and cementation indices
iv. Tabulate compositional variations of paste across the backscatter/secondary electron image.

Lightly hand-ground in a Mortar & Pestle (30+ g)

3. Chemical Analysis – Soluble Silica (5 g)

i. Grind 10 g of lightly ground fraction from mortar & pestle in a WC pulverizer for 30 sec.
ii. Sieve thru. No. 50 sieve, collect the fraction passing the sieve,
iii. Re-grind the residue retained on sieve for 15 sec. and mix thoroughly with the previous fraction;
iv. Use 5.00 g of thus prepared powder (passing No. 50 sieve) for digestion in 100 ml cold (3-5°C/ 38-41°F) HCl (1+4) in a 250 ml beaker for 15 min. on a magnetic stirrer,
v. Filter thru. two 2.5 micron filter paper and keep the filtrate# 1,
vi. Digest the residue with filter paper in 75 ml hot NaOH (below boiling) on hot plate for 15 min. on magnetic stirrer,
vii. Cool down to room temp. and filter thru. two 2.5 micron filter paper and collect filtrate# 2,
viii. Combine these two filtrates, filter the combined filtrates thru. two 2.5 micron filter paper to remove any suspended silica (especially for sand-rich mortars, or if mortar is grounded too long); then dilute to 250 ml in a volumetric flask with dist. water, an aliquot (about 10 ml) is then used soluble silica determination (e.g., in AAS/XRF against calibrations with standard PC mortars of known soluble silica and cement contents prepared in the exact same ways).

4. Chemical Analysis – Acid-Insoluble Residue (2 g)

i. Take 1-2 g of prepared mortar powder from Step 3 iii (passing No. 50 sieve) and digest in 50 ml HCl (1+3) in a 250 ml beaker (covered) on a hot pate rapidly near boiling, then 15 min. at a temp. below boiling, then cool down to room temperatures,
ii. Filter thru. two pre-weighed 2.5 micron filter papers, washing the beaker, paper, and residue thoroughly with hot water,
iii. Dry the filter paper at 110C for 10 min, cool in a desiccator to room temp. and measure the weight.
iv. Subtract from mass of dry filter paper to determine acid-insoluble residue content.
v. Take digital/optical photomicrographs of acid-insoluble residue (e.g., siliceous sand).

5. Chemical Analysis – Loss On Ignition (2 g)

i. Take 1-2 g (W_1) of prepared mortar powder from Step 3 iii (passing No. 50 sieve) in a tarred porcelain crucible (keep a record of mass of the empty crucible),
ii. Dry at 110°C for 15 min in a muffle furnace pre-set to 110°C, cool in a desiccator to room temp. and measure the mass (W_2) by subtracting the empty crucible mass from the total mass,
iii. Ignite at 550°C for 15 min. in the muffle furnace pre-set to 550°C, cool in a desiccator to room temp. and measure the mass (W_3) by subtracting the empty crucible mass from the total mass,
iv. Ignite at 950°C for 15 min. in the muffle furnace pre-set to 950°C, cool in a desiccator to room temp. and measure the mass (W_4) by subtracting the empty crucible mass from the total mass,
v. Calculate the losses on ignition at 110°C, 550°C, and 950°C for free water, combined water, and carbonation, respectively.

6. Sand Color & Size Distribution (10 g)

i. Take 10 g. of mortar lightly ground in mortar & pestle and digest in HCl (1+3) in a 250 ml beaker on a magnetic stirrer until all sand separates and settles at the bottom of beaker,
ii. Filter all through two 2.5 micron filter paper, wash the beaker, filter paper, and all sand residue with dist. water,
iii. Dry the residue at 110°C in an oven for 10 min., gently brush out from the filter paper and collect, then sieve the entire sand residue through No. 4 through 200 sieves,
iv. Determine the mass retained on each sieve, and on the pan (finer than No. 200 sieve),
v. Take photomicrographs of sand particles retained on each sieve for sand color variations.
vi. Provide plots of grain-size variations of sand against ASTM C 144 limits for masonry sands.

7. Bulk Mortar Composition from XRF (8 g)

i. Weigh 8.00 g of mortar lightly ground in mortar & pestle, add three grinding/pelletizing aid tablets and re-grind in a WC mill for 3 min. with anhydrous alcohol to get <45 micron size (passing No. 325 sieve),
ii. Take 6.8 to 7.0 g. of ground <45 micron prepared mass in an aluminum sample holder inside a die to prepare a 32 mm pellet with 25 ton pressure for 1 min,
iii. Use the prepared pellet for XRF and then use same the same pellet for XRD.

8. Bulk Mortar Mineralogy from XRD

i. Use the XRF pellet to run in Siemens D5000 theta/two-theta powder diffractometer (Cu Kα radiation, 40 kV, 30mA) with MDI's Datascan, Jade Search/Match, & Rietveld modules to determine mineralogical composition of bulk mortar.

9. Thermal Analyses (1 g), e.g., for dolomitic lime mortar to obtain the brucite content.

Figure A1-1: Flowchart of laboratory testing of masonry mortar followed in the CMC laboratories. For our 'comprehensive package' all above tests are done. For 'basic package', Nos. 1, 3, 4, 5, and 7 are done. Both packages provide volumetric proportions of various binder components and sand that are helpful for formulation of a suitable pointing mortar. Comprehensive package is more useful for historic mortars that are not similar to modern ASTM C 270 cement-lime or masonry/mortar cement mortars. Basic package is suitable for modern mortars that are formulated following the specification of ASTM C 270.

OPTICAL MICROSCOPY

Along with ASTM C 1324, procedures for optical microscopical examinations of construction materials are also described in ASTM C 856. Fragment(s) selected for microscopical examinations are examined and photographed with a digital camera, a flatbed scanner, and, a low-power stereomicroscope. After preliminary visual examinations and photographing, subsequent sample preparation steps are followed for optical microscopy. Figure A1-2 shows the equipments used during preparation of thin section and examination by using various optical microscopes.

For thin section preparation, representative fragments are placed in a flexible (molded silicone) sample holder, and encapsulated with a colored (blue or fluorescent) dye-mixed low-viscosity epoxy resin under vacuum to impregnate the pore spaces of mortar and improve the overall integrity by the cured epoxy. The epoxy-encapsulated cured solid block of sample is then de-molded and processed through coarse to fine grinding, lapping, attachment of the lapped surface to a frosted large-area (50 × 75 mm) glass slide, precision sectioning and precision grinding in a thin-sectioning machine (Figure A1-2), and final polishing steps to prepare a final polished thin section of 30 micron thickness suitable for examinations in a petrographic microscope and in SEM-EDS. Sample preparation steps are described in detail in Jana 2005, 2006.

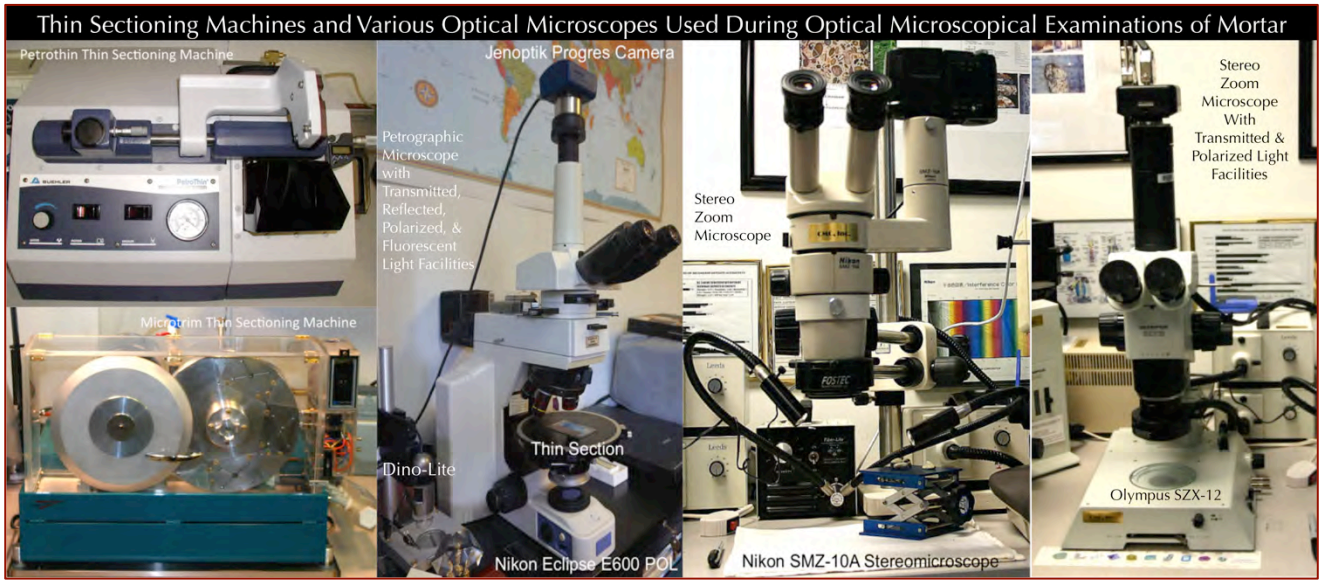

Figure A1-2: Buehler (top, left) and Microtrim (bottom left) thin-sectioning machines used for production of less than 30-micron thin sections of mortars. Four 50 × 75 mm size thin sections can be simultaneously prepared by the Microtrim unit. Nikon Eclipse E600 POL petrographic microscope with Jenoptik Progres Camera (left), Nikon SMZ-10A Stereozoom reflected-light microscope with Omax camera (middle), and Olympus SZX-12 Stereozoom microscope with reflected, transmitted, and polarized light facilities and Progres camera used for examinations of mortar

Steps followed during light optical microscopical examinations of a mortar sample include:

a) Visual examinations of mortar fragments, as received, to select fragments for detailed optical microscopy; initial digital and flatbed scanner photography of mortar as received;

b) Low-power stereomicroscopic (e.g., by using Nikon Stereozoom microscope shown in Figure A1-2) examinations of saw-cut and freshly fractured sections of mortar for evaluation of textures, compositions, and appearances;

c) Examinations of oil immersion mounts for special features and materials from mortar in a petrographic microscope (e.g., Nikon Eclipse E600 POL shown in Figure A1-2);

d) Examinations of colored (blue or fluorescent) dye-mixed epoxy-impregnated polished thin sections of mortar fragments in a transmitted-light Stereozoom microscope (e.g., Olympus SZX-12 microscope shown in Figure A1-2) for determination of size, shape, angularity, and distribution of sand, as well as abundance and distribution of void and pore spaces that are highlighted by the colored dye-mixed epoxy;

e) Image analyses of photomicrographs of blue dye-mixed epoxy-impregnated thin sections of mortar fragments for estimations of pores, voids, intergranular open spaces, and shrinkage microcracks (i.e. areas that were impregnated by blue dye-mixed epoxy and highlighted in image analysis) by using Image J, a Java-based image processing program developed by National Institutes of Health. Large-area thin section photomicrographs are collected in plane and crossed polarized light modes by using a high-resolution Stereozoom microscope equipped with transmitted and polarizing light facilities (e.g., Olympus SZX-12 microscope shown in Figure A1-2);

f) Examinations of colored (blue or fluorescent) dye-mixed epoxy-impregnated polished thin sections of mortar fragments in a petrographic microscope (Figure A1-2) for detailed compositional, mineralogical, textural, and microstructural analyses of aggregates and binders in mortars, along with diagnoses of evidence of any deleterious processes. The purpose of using a colored dye-mixed epoxy is to highlight the overall variations in density/porosity of mortars as well as highlighting any void spaces and cracks in the samples;

g) Examinations of any physical or chemical deterioration of mortar or signs of improper construction practices from microstructural evidences; and,

h) Optical microscopical examinations of size, shape, and color variations of sand extracted after hydrochloric acid digestion from determination of acid-insoluble residue content.

SCANNING ELECTRON MICROSCOPY AND ENERGY-DISPERSIVE X-RAY SPECTROSCOPY (SEM-EDS)

For comprehensive package, a portion of the thin section used for optical microscopy is subsequently coated with a thin conductive gold film for detailed SEM-EDS studies.

Procedures for SEM examinations are described in ASTM C 1723. Polished and coated thin section (or polished solid encapsulated block) of mortar is examined in a CamScan SEM equipped with backscatter detector, secondary electron detector, and x-ray fluorescence spectrometer (Figure A1-3) to observe:

a) The morphology and microstructure of various phases; and,

b) Determine the chemical compositions of the binders, including the original components of the binders, and the hydration and/or carbonation/alteration products.

Figure A1-3: Cambridge CamScan Series II Scanning Electron Microscope and 4Pi Revolution software, backscatter detector, secondary electron detector, and energy-dispersive X-ray fluorescence spectrometer used for microstructural and microchemical analyses of mortar.

Due to characteristic difference in compositions of pastes made using various binders, e.g., non-hydraulic lime (CaO dominants over all other oxides), variably hydraulic lime (CaO with variable SiO_2 contents depending on hydraulicity), dolomitic lime (high CaO and MgO), natural cement (CaO, SiO_2, and MgO contents are high, high MgO and FeO contents are characteristic), and Portland cement (CaO and SiO_2 contents are higher than all other oxides), SEM-EDS analysis of paste is a powerful method for detection of the original binder components) in the mortar. Effects of chemical alterations and various chemical deteriorations of a mortar can also be detected by SEM-EDS.

X-RAY DIFFRACTION

X-ray diffraction is a powerful laboratory technique during investigation of masonry mortars, for various reasons, such as:

a) Determination of bulk mineralogical composition of mortar, including its aggregate and binder mineralogies; e.g., quartz in sand from major diffraction peaks at 26.65º, 20.85º, 50.14º 2θ, or calcite in sand or carbonated lime binder from major peaks at 29.41º, 39.40º, 43.15º 2θ, or Portlandite in binder from major peaks at 34.09º, 18.09º, 47.12º 2θ;
b) Individual primary mineralogy and alteration products of aggregate at various size fractions, and binder phases;
c) Detection of dolomitic lime binder from brucite in the mortar from major peaks at 38.02º, 18.59º, 50.86º 2θ;
d) Detection of use of lime (Portlandite), gypsum (11.59º, 20.72º, 29.11º 2θ), or cement binders from their characteristic mineralogies;
e) Detection of any potentially deleterious constituents, e.g., deleterious salts, or efflorescence deposits;
f) Detection of a mineral oxide-based pigmenting component in the mortar; and,
g) Detection of components that are difficult to detect by microscopical methods.

X-ray diffraction can be done on (see Figure A1-5): (i) pulverized (to finer than 45 micron) portion of bulk mortar, or (ii) on the sand extracted from the mortar by acid digestion, if sand has a complex mineralogy, or requested for additional examination, or also (iii) on the binder-fraction by separating the sand from the binder from a lightly ground mortar (in a mortar and pestle) and passing the ground mass through US 325 sieve (44 micron) to collect the fraction rich in binder.

Figure A1-4: Siemens D5000 X-ray diffractometer and MDI Jade search/match software used for determination of mineralogical composition of mortar.

X-ray diffraction is carried out in a Siemens D5000 Powder diffractometer (Figure A1-4) employing a long line focus Cu X-ray tube, divergent and anti-scatter slits fixed at 1 mm, a receiving slit (0.6 mm), diffracted and incident beam Soller slits (0.04 rad), a curved graphite diffracted beam monochromator, and a sealed proportional counter. Generator settings used are 45 kV and 30mA. A dry, finely ground sample pulverized to pass US 325 sieve (44-μm) is placed in a 1-in. diameter circular sample holder and excited with the copper radiation of 1.54 angstroms. Tests are performed at a 2-theta range from 4° to 64° with a step of 0.02° and a dwell time of one second.

The resulting diffraction patterns are collected by using DataScan 4 software of Materials Data, Inc. (MDI), analyzed by using Jade 9.0 software of MDI with ICDD PDF-4 (Minerals 2017) diffraction data, and, phase identification, and quantitative analyses were carried out with MDI's Search/Match and Easy Quant modules, respectively. Steps followed during

sample preparation for XRD are provided in Figure A1-5. For the present mortar, pulverized (to minus US 325 sieve) portions of representative fragments of bulk mortar sample (Step 2 in Figure A1-5) are analyzed.

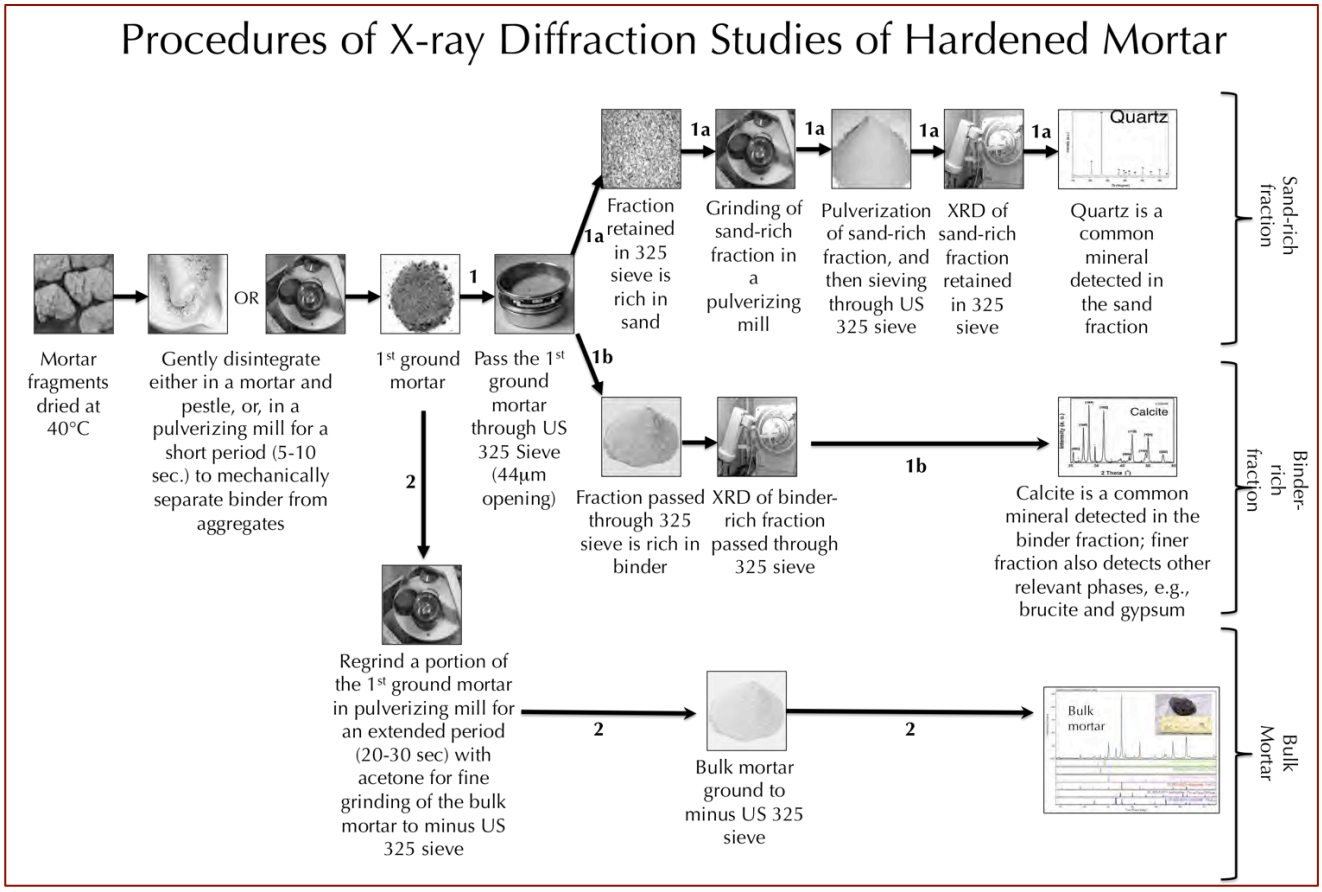

Figure A1-5: Steps followed during sample preparation for X-ray diffraction studies.

ENERGY-DISPERSIVE X-RAY FLUORESCENCE SPECTROSCOPY (ED-XRF)

An energy-dispersive bench-top x-ray fluorescence unit from Rigaku Americas Corporation (NEX-CG, Figure A1-6) is used for determination of bulk chemical (oxide) composition of mortar. The instrument is calibrated by using various certified reference standards of cements and rocks.

Figure A1-6: Rigaku NEX-CG bench-top ED-XRF unit used for bulk chemical composition of mortar.

A representative portion of mortar (about 8 grams) is pulverized down to minus US 325 sieve (finer than 45 microns size) in a Rocklab pulverizer with a grinding

aid/binder (7.5% binder by weight of sample), and then pelletized (approximately 7 grams) to a 31-mm diameter pellet in a 25-ton press.

The instrument is powerful enough to determine ppm-level silica in solutions suitable for determination of soluble silica content in an acid-digested mortar from calibration of laboratory-prepared standard mortar samples of known cement and soluble silica contents.

CHEMICAL ANALYSES (GRAVIMETRY & INSTRUMENTAL ANALYSES)

Following petrographic examinations, chemical analyses of the mortar are done to determine the:

a) Hydrochloric acid-insoluble residue content,
b) Loss on ignition,
c) Soluble silica content,
d) Calcium and magnesium oxide contents, and
e) The presence of magnesium hydroxide, if any (e.g. to determine if dolomitic lime was used).

Chemical analyses are done by using various methods outlined in ASTM C 1324 and Middendorf et al. 2005a, e.g., by wet chemistry, atomic absorption spectroscopy (AAS), inductively-coupled plasma atomic emission spectroscopy (ICP-AES), energy-dispersive X-ray fluorescence spectroscopy (EDS), thermal analysis (DTA, TGA, DSC), and X-ray diffraction (XRD). Steps followed during chemical analyses of mortars are described in ASTM C 1324, which are summarized in Figure A1-7.

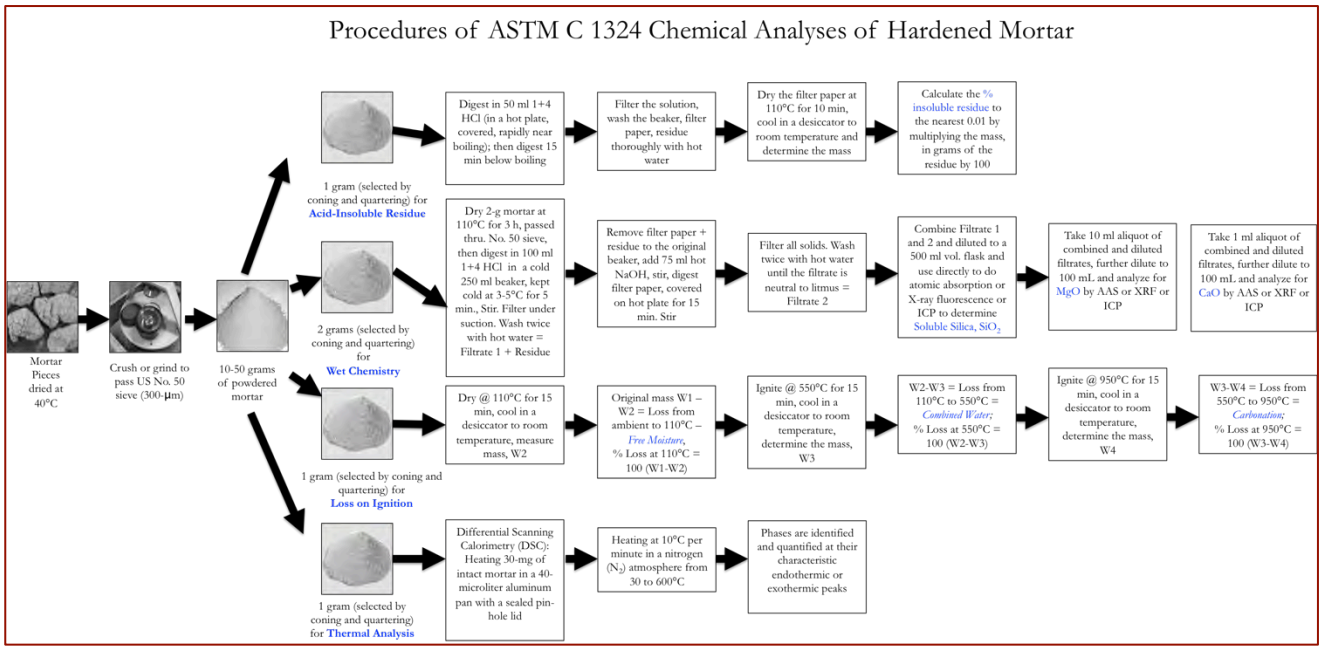

Figure A1-7: Steps followed during various chemical analyses of mortars according to ASTM C 1324.

The hydrochloric acid-insoluble residue content provides the siliceous (non-soluble) content of mortar, which corresponds to the siliceous components of sand. The soluble silica content corresponds to the silica mostly contributed from the binder components (and a minor amount from any soluble silica component in the aggregates). The loss in weight by ignition of a pulverized portion of bulk mortar in a muffle furnace from ambient temperature to 110°C corresponds to the free water content of mortar, whereas, further weight loss from 110°C to 550°C corresponds to the structurally bound hydrate water content, which is proportionate to the amount of hydrated component in the mortar. Finally, the loss of weight by calcination to 950°C corresponds to the degree of carbonation of lime binder of mortar. Oxide compositions determined from wet chemistry, or, other instrumental techniques (e.g., AAS, XRF, ICP) provide compositions of binder, and, bulk mortar.

THERMAL ANALYSES

Thermal analyses (DTA, TGA, and DSC) of mortar are done to determine the presence and amounts of:

a) Hydrates (e.g., detection of brucite by its decomposition at 300-400ºC to check the presence of dolomitic lime, or from soluble magnesium in the paste from use of natural cement),
b) Sulfates (gypsum from decompositions at 125ºC, and 185-200ºC, ettringite at 120-130ºC, thaumasite at 150ºC),
c) Hydrate water, e.g., calcium silicate hydrate from decomposition at 180-190ºC, Portlandite from decomposition at 400-600ºC,
d) High-temperature transformations of silica polymorphs (α to β form) at 573ºC,
e) Cryptocrystalline calcite in the carbonated lime matrix from decomposition at 620-690ºC, or
f) Coarsely crystalline calcite e.g., in limestone by decomposition at 680-800ºC or
g) Dolomite at 740-800ºC and 925ºC, etc.
h) Phases are determined from their characteristic decomposition temperatures occurring mostly as endothermic peaks.

Figure A1-8 shows the four main steps followed during laboratory investigation of masonry mortars, e.g.,

a) From preliminary visual examinations to petrographic examinations of mortars to determine the types of aggregates used and the binders present, based on which
b) Subsequent chemical analyses were done to determine the chemical compositions of binders and proportions of sand, water, and degree of carbonation. Information obtained from petrographic examinations is useful and form the very guidelines to devise the appropriate chemical methods to follow, and to properly interpret the results of chemical analyses.
c) For example, detection of siliceous versus calcareous versus argillaceous natures of aggregates in mortar, or the presence of any pozzolan in the binder (slag, fly ash, ceramic dusts, etc.) from petrography restricts which chemical method to follow, and how to interpret the results of such analyses, e.g., acid-insoluble residue contents.

d) Therefore, a direct chemical analysis e.g., acid digestion of a mortar without doing a prior petrographic examination to determine the types of aggregates and binder used could lead to highly erroneous results and interpretation.

e) Armed with petrographic and chemical data, and based on assumed compositions and bulk densities of the sand and the binder(s) similar to the ones detected from petrographic examinations volumetric proportions of sand and various binders present in the examined mortar can be calculated.

f) The estimated mix proportions from such calculations can provide at least a rough guideline to use as a starting mix during formulation of a tuck pointing mortar to match with the existing (examined) mortar.

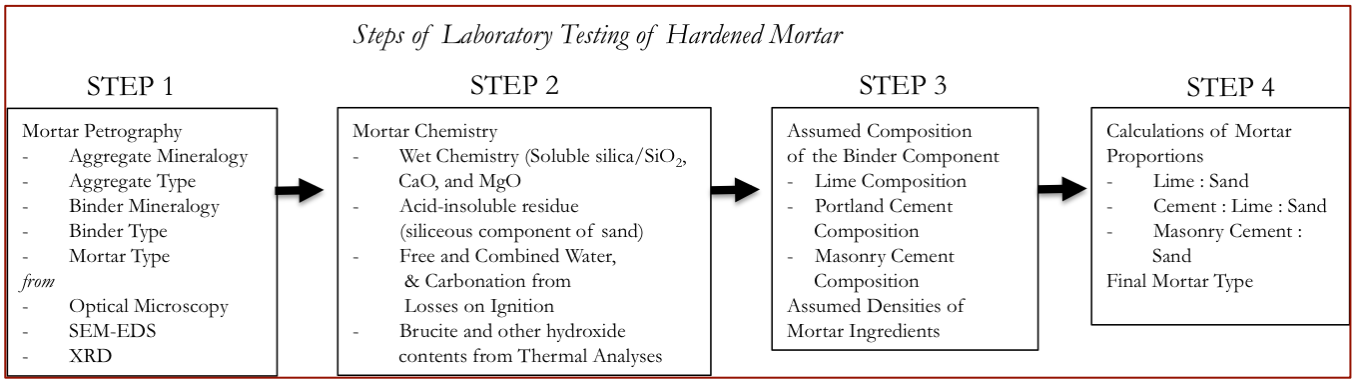

Figure A1-8: Steps followed during laboratory investigation of mortars.

APPENDIX A2 – SUGGESTIONS FOR TUCK-POINTING MORTAR

SUGGESTIONS ON FORMULATION OF TUCK-POINTING MORTARS

The following two Tables provide various tuck pointing mortar formulations many of which are commonly suggested for historic as well as modern masonry renovation projects where the choice depends on: (a) the type of the masonry units present, (b) the exposure condition during service, and (c) the type of the original mortar present. The following suggestions from various references are for general guideline purposes only and provide no guarantee to the overall match in appearance and properties to the existing mortars, which must be determined by trial and error by the project architect/engineer.

Masonry Units	Mortar Type		
	Sheltered	Moderate	Severe
Very hard and durable (e.g., granite, hard-cored brick, etc.)	O (1-2-9)	N (1-1-6)	S (1-0.5-4.5)
Moderately hard and durable (e.g., limestone, durable stone, molded brick)	K (1-3-11)	O (1-2-9)	N (1-1-6)
Minimally durable, soft (soft hand-made brick)	L (0-1-3)	K (1-3-11)	O (1-2-9)

Table A2-1: Various possibilities of tuck pointing mortars made using cement, lime, and sand for various masonry units and exposure conditions (Mack and Speweik, 1998), where the mix proportions by volume within parentheses indicate cement-to-lime-to-sand proportions for various formulations. Type 'L' is a straight lime mortar containing no cement.

Location	Mortar Type	
	Recommended	Alternative
Interior	O	K or N
Exterior - Above Grade, Exposed on one side, unlikely to be frozen when saturated, not subject to high wind or other significant lateral load	O	N or K
Exterior – Other than above	N	O

Table A2-2: ASTM C 270 Guide for selection of tuck-pointing mortar. Mix formulations for different suggestions are as follows: Type K: 1 part Portland cement and $2^1/_2$ to 4 parts hydrated lime; Type O: 1 part Portland cement and $2^1/_2$ parts hydrated lime or lime putty; Type N: 1 part Portland cement to over $1^1/_4$ to $2^1/_2$ parts hydrated lime or lime putty. Aggregate ratio of $2^1/_4$ to 3 times sum of volume of cement and lime for all formulations.

Finally, the following section provides some additional information to consider during selection of an appropriate tuck-pointing mortar for a renovation project (many of which may not be applicable for the present project):

a) It is more important for a tuck pointing mortar to be as close in physical, chemical, and mechanical properties to the existing mortar as possible than to conform to the ASTM C 270 specification for cement-

lime or masonry/mortar cement mortars for unit masonry, which are for modern mortars to use for modern structural applications, and not necessarily applicable to renovation of historic lime mortars. As a general rule, tuck-pointing mortar should be of same strength or softer than the original mortar.

b) Aggregate to use in the tuck-pointing mortar should be similar in color, gradation, appearance, mineralogy, and composition to the sand used in the existing mortar. Sand should be clean, free of any debris, unsound, or clay particles. Masonry sands should conform to the grading requirements of ASTM C 144. Avoid using sand that contains appreciable amounts of potentially alkali-silica reactive particles (e.g., strained quartz, quartzite, chert).

c) Binder for tuck-pointing mortar should be as close to the binder of the existing mortar in composition and properties as possible. For historic lime mortars, possible choices of binders are many:

   (i) Non-hydraulic high-calcium lime, or magnesian lime, or dolomitic lime (ASTM C 51) either in dry hydrate (hydrated lime) form, or as slurry or putty form;

   (ii) Hydraulic lime;

   (iii) Natural hydraulic lime (i.e. NHL 2, NHL 3.5, and NHL 5 with increasing strengths; feebly, moderately and eminently hydraulic natural hydraulic limes with increasing hydraulicity and 28-day compressive strengths from >2 to <7 MPa, to >3.5 to <10 MPa, to >5 to <15 MPa, respectively, produced from calcination of impure limestones having up to 10% clay, 11-20% clay, and 21-30% clay, respectively);

   (iv) Natural cements (conforming to specifications of ASTM C 10); or,

   (v) A combination of these,

   (vi) With or without a pozzolan (fly ash, slag, etc. if added strength and durability are needed).

   (vii) Portland cement, if used must be added at lesser proportions than lime, having proportions tested to find the best match in properties to the existing mortar.

   (viii) For breathability of the masonry wall, least stress to the exiting mortar, accommodation of building movements, and good bond to masonry units, the binder of choice should be durable and similar in properties and performance to the existing binder having a good service record.

d) During applications of modern masonry mortars: (i) a job-mixed cement-lime mortar is commonly preferred by the architects than a masonry cement mortar, due to the better quality control of the former mortar; (ii) a masonry cement mortar is characteristically air-entrained, which may interfere with the bond to the adjacent masonry units, whereas, a non-air-entrained cement-lime mortar provides a better bond to the adjacent masonry units than an air-entrained masonry cement mortar, (iii) air entrainment usually provides better workability and freeze-thaw durability to a mortar, however, as mentioned, it reduces the bond to the adjacent masonry units (depending on air content); (iv) for Portland cement-lime mortars, a Type M or S mortar (i.e. having a higher cement content than lime and hence a higher strength) is preferred for load-bearing applications than a Type N mortar (having a higher lime content than cement, hence provides better workability and water retention than a Type S or M mortar); (v) Portland cement to

use in a mortar should conform to the specification of ASTM C 150; hydrated lime should conform to ASTM C 207; masonry/mortar cement, if used, should conform to ASTM C 91/C 1329; blended hydraulic cement, if used, should conform to ASTM C 595; (vi) relative proportions of Portland cement and lime will control the overall strength, workability, and bond properties of the repointing mortar.

e) Mineral oxides or carbon-based pigments, if used and positively detected in an examined mortar, should be carefully replicated in the tuck pointing process to reproduce the color, texture, and appearance similar to the existing mortar (including the effects of atmospheric weathering on pigments). Dosage of pigment in the tuck-pointing mortars should be estimated from trial mixes of various dosages.

f) If the original mortar contains a polymer component as suspected from microscopy, characterization of polymer could be done by FTIR-spectroscopy.

g) A mortar strong in compressive strength might be desirable for a hard stone (such as granite), whereas a softer, more permeable lime mortar would be preferable for a historic wall of soft brick. Masonry deterioration caused by salt deposition results when the mortar is less permeable than the masonry unit. A strong mortar is still more permeable than hard, dense stone. However, in a wall constructed of soft bricks where the masonry unit itself has a relatively high permeability or vapor transmission rate, a soft, high lime mortar is necessary to retain sufficient permeability; using a strong mortar with a soft brick will result in spalling of bricks.

h) To have an optimum bond of a mortar to the adjacent masonry unit, relative proportions of cementitious materials and lime contents in the mortar should be carefully controlled. Lime provides the necessary workability and water retention, which are important in a mortar when used with a masonry unit of high suction). Therefore, the initial rate of absorption (or suction property) of the adjacent masonry units should also be carefully determined to match with the appropriate lime content in the mortar.

i) The final tuck pointing mortar should match in color and appearance to the existing mortars, and the closest match should be determined by trial and error on small test areas of the masonry wall to be tuck-pointed.

END OF REPORT[1]

[1] The CMC logo is made using a lapped polished section of a 1930's concrete from an underground tunnel in the U.S. Capitol.